FUNDAMENTAL STUDY ON PRODUCING A FAVORABLE IONIC MOBILITY OF PVA BLENDS IN CELLULOSE-BASED POLYMER ELECTROLYTES VIA ELECTROCHEMICAL ANALYSIS

(KAJIAN ASAS MENGENAI PENGHASILAN MOBILITI IONIK BERSESUAIAN DARIPADA PVA CAMPURAN DALAM SELULOSA BERBASIS ELEKTROLIT POLYMER MELALUI ELEKTROKIMIA ANALYSIS)

AHMAD SALIHIN BIN SAMSUDIN
IZAN IZWAN MISNON
SAIFFUL KAMALUDDIN BIN MUZAKIR
MOHD IKMAR NIZAM MOHAMAD ISA
MOHD FAKHRUL ZAMANI ABDUL KADIR

FRGS 2017-2019 FINAL REPORT

RESEARCH VOTE NO:
RDU 170115

FACULTY INDUSTRIAL SCIENCE & TECHNOLOGY
UNIVERSITI MALAYSIA PAHANG

2019

ACKNOWLEDGEMENTS

In the name of almighty **ALLAH S.W.T.**, most compassionate, most Merciful. Alhamdulillah, for giving me the strength, patience and health to complete this research work that have taken of my time for about 2 years.

First of all, I would like to thanks to **MINISTRY OF HIGHER EDUCATION (MOHE) MALAYSIA** for the research financial given via FRGS grant with vote number **RDU 1700115** with entitled "FUNDAMENTAL STUDY ON PRODUCING A FAVORABLE IONIC MOBILITY OF PVA BLENDS IN CELLULOSE-BASED POLYMER ELECTROLYTES VIA ELECTROCHEMICAL ANALYSIS" in order to complete the research work within 2 years. I am grateful to express my sincere gratitude and appreciation to my co-reasearher **Dr. Izan Izwan Misnon, Dr. Saifful Kamaluddin Muzakir, Professor Mohd Ikmar Nizam, Ass. Prof. Mohd Fakhrul Zamani, Nur Khalidah Zainuddin** and **Nur Fatihah Mazuki** for their encouragement and support for completing this work

My sincere gratitude is also conveyed to Faculty Industrial Science & Technology, Universiti Malaysia Pahang and FIST laboratory technical staff members for all the help and friendship given to me.

ABSTRAK

Dalam penyelidikan ini, polimer campuran campuran karboksimetil selulosa (CMC) - polyvinyl alcohol (PVA) berasaskan elektrolit biopolimer yang diperbadankan dengan pelbagai ammonium bromida (NH_4Br) pada suhu bilik dilaporkan. Filem elektrolit terdiri daripada CMC-PVA yang berfungsi sebagai polimer hos dan NH_4Br sebagai penyedia proton telah berjaya disediakan melalui teknik pemutus. Interaksi antara polimer tuan rumah dan garam dopan telah disahkan melalui analisa Infra Spektroskopi Inframerah Fourier Transform (FTIR) di mana terdapat pergeseran dan intensiti puncak yang diperhatikan. Analisis Densim sinar-X telah membuktikan amorfus sampel ketika lebih banyak NH_4Br hingga AB20 diperkenalkan ke dalam sistem. Sifat-sifat terma elektrolit biopolimer pepejal (SBEs) telah dikaji menggunakan Analisis Thermo Gravimetric (TGA) dan Calorimetri Pengimbasan Berbeza (DSC). Ia diperhatikan dalam TGA bahawa suhu penguraian (T_d) meningkat yang menunjukkan peningkatan dalam kestabilan haba elektrolit biopolimer. Semasa dalam analisis DCS, suhu peralihan kaca (T_g) menurun dan kepekatan NH_4Br meningkat. Kekonduksian ionik suhu bilik optimum 3.21 x 10^{-4} S cm^{-1} dicapai apabila 20 wt. % NH_4Br diperkenalkan ke dalam sistem. Ketergantungan suhu semua SBEs ditemui mematuhi tingkah laku Arrhenius di mana nilai regresi hampir kesatuan (R^2 ~ 1). Penambahan NH_4Br memimpin tenaga pengaktifan sistem CMC-PVA-NH_4Br untuk mengurangkan. Tingkah laku dielektrik telah dilakukan dengan menggunakan kepelbagaian dielektrik dan spektrum modulus elektrik. Sifat-sifat pengangkutan SBEs disiasat melalui pendekatan analitik pemasangan FTIR dan Spectroscopy Impedansi Elektrik (EIS). Kedua-dua kaedah tersebut menunjukkan kekonduksian ionik elektrolit biopolimer berasaskan CMC-PVA-NH_4Br dipengaruhi terutamanya oleh pekali penyebaran ioniti mobiliti dan ion. Pengukuran Nombor Pengalihan Transmisi (TNM) ion mudah alih telah dianggarkan oleh kaedah polarisasi dc dan telah menemui masa untuk 0.99 untuk sampel dengan kekonduksian ionik tertinggi. Elektroda boleh terbalik yang tidak tersekat telah digunakan dalam kerja semasa untuk mengenal pasti nombor pemindahan (H^+) proton (H^+) yang diamati nilai t_{H^+} 0.31. kemudiannya, menunjukkan bahawa spesies mengendalikan kebanyakannya disebabkan oleh konduksi kationik. Tingkap elektrokimia yang paling menjalankan

elektrolit biopolimer adalah sehingga 1.55 V. Kapasitansian khusus (Csp) CMC-PVA-20 wt. % NH_4Br Elektrolit biopolimer dikira dari lengkung Voltammetry (CV) Cyclic dan hasilnya menunjukkan persetujuan yang baik dengan Csp diperolehi dari Galvanostatic Charge-Discharge (GCD). Nilai purata ketumpatan kuasa dan ketumpatan tenaga diperhatikan pada ~ 1.94 kW kg^{-1} dan ~ 3.05 Wh kg^{-1}, masing-masing. Penemuan kerja pada sistem elektrolit biopolimer berasaskan CMC-PVA-NH_4Br dianggap mempunyai potensi untuk digunakan dalam peranti storan tenaga.

ABSTRACT

In present work, polymer blend carboxymethyl cellulose (CMC)-polyvinyl alcohol (PVA) based biopolymer electrolyte incorporated with various amount of ammonium bromide (NH_4Br) at room temperature is reported. The electrolyte films comprise CMC-PVA which acts as host polymer and NH_4Br as proton provider were successfully prepared via casting technique. The interaction between host polymer and dopant salt were confirmed via Fourier Transform Infrared Spectroscopy (FTIR) analysis where there is shifting and intensity of the peak observed. The X-ray Diffraction analysis has proved the amorphousness of the sample when more NH_4Br up to AB20 was introduced into the system. The thermal properties of solid biopolymer electrolytes (SBEs) were studied using Thermo Gravimetric Analysis (TGA) and Differential Scanning Calorimetry (DSC). It was observed in TGA that the decomposition temperature (T_d) increased which indicates the improvement in thermal stability of biopolymer electrolytes. While in DCS analysis, the glass transition temperature (T_g) decreased as well as NH_4Br concentration increased. The optimum room temperature ionic conductivity of 3.21×10^{-4} S cm^{-1} was achieved when 20 wt. % of NH_4Br was introduced into the system. The temperature dependence of all the SBEs were discovered obeys to Arrhenius behavior where the regression value almost unity ($R^2 \sim 1$). The increment of NH_4Br leads activation energy of CMC-PVA-NH_4Br system to decrease. The dielectric behavior has been carried out using dielectric permittivity and electrical modulus spectra. The transport properties of SBEs was investigated via deconvoluted FTIR and Electrical Impedance Spectroscopy (EIS) fitting analysis approach. Both of the method revealed the ionic conductivity of CMC-PVA-NH_4Br based biopolymer electrolyte is primarily influenced by the ionic mobility and ions diffusion coefficient. The dc polarization method has been used to estimate the Transference Number Measurement (TNM) of mobile ions and has found the t_{ion} to be 0.99 for sample with highest ionic conductivity. The non-blocking reversible electrode was used in present work to identify the proton (H^+) transference number which is observed the t_{H^+} value of 0.31. subsequently, indicates that the conducting species are predominantly due to cationic conduction. The electrochemical potential window of the most conducting biopolymer electrolyte is up to

1.55 V. The specific capacitance (C_{sp}) of CMC-PVA-20 wt. % NH_4Br biopolymer electrolyte was calculated from Cyclic Voltammetry (CV) curve and the results shows good agreement with C_{sp} obtained from Galvanostatic Charge-Discharge (GCD). The average value of power density and energy density was observed to be at ~1.94 kW kg^{-1} and ~3.05 Wh kg^{-1}, respectively. The work finding on biopolymer electrolyte-based CMC-PVA-NH_4Br system is considered has potential to be applied in energy storage devices.

TABLE OF CONTENT

LIST OF TABLES

LIST OF FIGURES

LIST OF SYMBOLS

ml	Mililiter
℃	Degree Celcius
g	Grams
º	Degree
σ	Ionic Conductivity
%	Percentage
π	Pi
θ	Theta
A	Area
cm	Centimetre
cm^{-1}	Per Centimetre
cm^2	Square Centimetre
f	Frequency
Hz	Hertz
MHz	Mega Hertz
Z_i	Imaginary Parts of Modulus
Z_r	Real Parts of Modulus
R_b	Bulk Resistance
E_a	Activation Energy
eV	Electron Voltage
T_d	Temperature Decomposition
T_g	Glass Transition Temperature
~	Approximately
a.u	Arbitrary Unit
η	Number of Ions
D	Diffusion Coefficient
μ	Ionic Mobility
t_{ion}	Ionic Transference Number
I	Normalized polarization current

t	Time
t_{H^+}	Cation Transference Number
V	Voltage
M_r	Real Modulus
M_i	Imaginary Modulus
ε_r	Dielectric Constant
ε_i	Dielectric Loss
ε_o	Free Space Permittivity
K_b	Boltzman Constant
e	Electric Charge Constant
N_A	Avogadro Constant
T	Temperature in Kelvin
H^+	Proton Ion

LIST OF ABBREVIATIONS

CMC	Carboxymethyl Cellulose
CV	Cyclic Voltammetry
DSC	Differential Scanning Calorimetry
EDLC	Electrical Double Layer Capacitor
EIS	Electrical Impedance Spectroscopy
FTIR	Fourier Transform Infrared Spectroscopy
GCD	Galvanostatic Charge Discharge
GPE	Gel Polymer Electolyte
ILPE	Ionic Liquid Polymer Electrolyte
LSV	Linear Sweep Voltammetry
NH_4Br	Ammonium Bromide
NH_4Cl	Ammonium Chloride
NH_4NO_3	Ammonium Nitrate
PEs	Polymer Electrolytes
PVA	Polyvinyl Alcohol
SBEs	Solid Biopolymer Electrolytes
TGA	Thermogravimetric Analysis
TNM	Transference Number Measurement
XRD	X-ray Diffraction
PVDF-HFP	Poly(vinylidene fluoride-co-hexafluoropropylene)
PMMA	Poly(methyl methacrylate)
PNIPAM	Poly(N-isopropylacrylamide)
PEO	Poly-ethylene oxide
PAN	Polyacrylonitrile
P(AN-MAH)	Poly(acrylonitrile-maleic anhydride)

CHAPTER 1

INTRODUCTION

1.1 Background of Research

Currently, solid waste has become an issue in wide world due to its hazardousness to environment, especially electronic waste. Batteries is one of the examples of electronic waste that are nonbiodegradable. Wright and co-worker have found the ionic conduction in Polyethylene based electrolyte (Wright, 1975). Since then, solid biopolymer electrolytes (SBEs) become quiet famous among chemist and physicist due to their possible potential in application in electrochemical devices such as solar cell, fuel cell, supercapacitor and battery (Nik Aziz, Idris, & Isa, 2010; Rajendran, Sivakumar, & Subadevi, 2003). Besides that, SBEs are a type of electrolyte that has been targeted to be widely used in batteries because of the low-cost production, biodegradable properties, and natural based product compared to commercial batteries that hazardous and non-biodegradable. In recent years, biodegradable biopolymers have attracted the global attention due to their various advantageous properties. Therefore, researchers are now focusing on developing biopolymer electrolytes from natural polymers that exhibit good ionic conductivity.

Cellulose-based solid biopolymer electrolytes have become quiet famous among researcher over the past few years for many applications in electrochemical devices. In present work, carboxymethyl cellulose (CMC) from natural polymer has chosen as host polymer due to non-toxic, biodegradable and suitable to form into thin film (N. H. Ahmad & M. I. N. Isa, 2015a; Ahmad & Isa, 2012; Chai & Isa, 2013). CMC contains hydrophobic backbone and many hydrophilic carboxyl groups and hence shows water-soluble features (N. H. Ahmad & M. I. N. Isa, 2016b). However, cellulose-based biopolymer electrolyte

faced an inherent problem of low ionic conductivity due to its high degree of crystalline that limits the application of this type of biopolymer electrolytes (Chai & Isa, 2016). (Kamarudin & Isa, 2013) and (M. A. Ramlli & M. I. N. Isa, 2015) have reported pure CMC possess low conductivity of ~10^{-8} S cm^{-1} at room temperature (303K). Another one of the promising materials which are biodegradable is polyvinyl alcohol (PVA). PVA is a potential material having a very high dielectric strength of >1000 kV/mm and it is also hydrophilicity properties which can give advantage in the application of composite films (M. A. Saadiah & A. S. Samsudin, 2018; Sivadevi et al., 2015). In addition, PVA is a semi-crystalline polymer studied widely due to its many interesting physical properties which improve from the presence of OH groups and the hydrogen bond formation, making it to be the source of intermolecular attraction forces which is suitable to form polymer blends (Rajeswari et al., 2011). Pure PVA gave lower conductivity of 1.9 x 10^{-6} Scm^{-1} (Hema, Selvasekarapandian, Arunkumar, Sakunthala, & Nithya, 2009). Since PVA give good tensile strength and abrasion resistance, the polymer can be used as binder, in double layer capacitors and electrochemical windows (Michael M Coleman & Painter, 1995). The enhancement of conductivity can be improved via blending PVA with another polymer. Since PVA give good tensile strength and abrasion resistance, the polymer can be used as binder, in double layer capacitors and electrochemical windows (Michael M Coleman & Painter, 1995).

There are several methods to improve the conductivity such as polymer blending, adding plasticizer/ceramic and polymer grafting (Vieira, da Silva, dos Santos, & Beppu, 2011; N. A. Zakaria, S. Y. S. Yahya, M. I. N. Isa, M. Nor Sabirin, & R. H. Y. Subban, 2010). In present work, polymer blending method were used due to its well-used method whenever modification of the properties is required. It is because of its uses conventional technology at low cost and can promising good conductivity. In order to enhance the conductivity, CMC is blended with some biodegradable polymer. Polyvinyl alcohol (PVA) is chosen as binder in present work to be blended with CMC. PVA is water soluble polymer which contain of hydroxyl group (-OH). The interaction between CMC and PVA is expected occur via formation of hydrogen bonding. Rajendran and co-worker

(Rajendran et al., 2003) have agreed that OH group from PVA can be source of hydrogen bonding, thus can assist in the formation of polymer blend.

In present work, CMC and PVA is used as host polymer due to the superior characteristics such as non-toxic, biocompatible, renewable and biodegradable capabilities. In order to enhance the ionic conductivity, ammonium bromide (NH_4Br) was selected as proton donor to be doped into the polymer blend matrix. The blending of carboxymethyl cellulose with PVA doped with NH_4Br were prepared by using casting method. The biopolymer–salt complex formation will be analysed through Electrical Impedance Spectroscopy (EIS), Fourier Transform Infrared (FTIR) spectroscopy, X-Ray Diffraction (XRD), transference number measurement (TNM), Differential Scanning Calorimetry (DSC) and Thermo Gravimetric Analysis (TGA).

Further analysis has been made into the most conducting sample via electrical double layer capacitor (EDLC) in order to study the performance of the sample to be apply as energy storage. Recently, EDLC already is widely used in solid polymer-based electrolytes. This is due to its numerous properties in electrochemical devices such as fast energy storage, ability to be charged and discharged continuously without degrading, free maintenance and toxic materials, high power density and long lifetime cycle of charge and discharge (Burke, 2000; Francis, Liew, Ramesh, & Ramesh, 2016; Kibi, Saito, Kurata, Tabuchi, & Ochi, 1996) EDLC have been characterized using linear sweep voltammetry (LSV), cyclic voltammetry (CV) and galvanostatic charge-discharge (GDC).

1.2 Problem Statement

Solid biopolymer electrolytes (SBEs) have become a centre of interest to researchers for the past few decades due to potential applications in batteries, fuel cells, sensors and super capacitors. In present system, CMC was blend with PVA and doped with various amount of NH_4Br based SBEs. However, pure CMC and PVA possess low conductivity of ~10^{-8} and ~10^{-10} S cm^{-1}, respectively (A. A. Mohamad et al., 2003; M. A. Ramlli & M. I. N. Isa, 2015). Several methods were used in present

system in order to enhance the ionic conductivity such as polymer blending and addition of dopant salt using casting technique.

In addition, there also some obstacle need to faced during running the present work. At first project, ammonium chloride (NH_4Cl) was choosen to be doped with polymer blend CMC-PVA but the results shows an irregularities behaviour. The ionic conductivity decrease when NH_4Cl was introduced into the system which might be due to several factors as discussed in (N F Mazuki, Fuzlin, Saadiah, & Samsudin, 2018). To develop successful biopolymer electrolytes, NH_4Br was choosen to be replaced NH_4Cl as proton provider in present work. However, the results get at the first place does not very satisfied. Therefore, the characterization on the sample need to repeat several times to get the ideal results following samples or materials behaviour as reported in previous work with same fields. Further, the broken instrument also contributes the research work to be slow down. In order to overcome these shortcoming, the samples was sent in other faculty and instituation for characterization.

1.3 Significant of Research

The findings of this study will redound to the benefits of society considering that solid biopolymer plays an important role in science and technologies today. The use of 'eco-friendly' materials as conducting biopolymer electrolyte (BE) can certainly contribute to the sustainability of the planet. BE has advantages over liquid electrolyte such as light weight, improve leakage problem, mechanically stable and flexible for packaging design. Ionically conductive BE has become the key object of academic and industrial interests. They also offer numerous advantages, for example, eliminate corrosive solvent and harmful gas formation, wider electrochemical and thermal stability range as well as low volatility with easy handling. Data produced from this study will be used to show the comparison and provide insight into the issue of furthering responsible environment practice in manufacturing.

1.4 Objectives

1) To formulate CMC blended with PVA doped NH_4Br that can be applied as solid biopolymer electrolytes.

2) To determine the structural and thermal properties of CMC-PVA- NH_4Br biopolymer electrolytes system by using Fourier Transform Infrared (FTIR) Spectroscopy, X-ray diffraction (XRD), Differential Scanning Calorimetry (DSC) and Thermo Gravimetric Analysis (TGA).

3) To determine the ionic conduction properties of the CMC-PVA- NH_4Br biopolymer electrolytes system by using Electrical Impedance Spectroscopy (EIS) and Transference Number Measurement (TNM).

4) To investigate the performance of solid biopolymer electrolytes system in electrical double layer capacitor (EDLC) via Linear Sweep Voltammetry (LSV), Cyclic Voltammetry (CV) and Galvanostatic Charge-Discharge (GDC).

1.5 Thesis Outline

Chapter 1 discuss about the research background of the project, problem statement from the previous research that give signification for this work in order to improve the earlier study. Also discusses about research objective and scope of study which explain generally about the methodology of the research.

Chapter 2 explains about literature review which included electrolytes, type of polymer electrolytes, blending and dopant method and utilization of solid biopolymer electrolyte in electrical double layer capacitor (EDLC) that use in the research and the latest research of this research.

Chapter 3 describes about the methodology part which included preparation of the sample procedure, the equipment and materials that were used for the research. It also contains the precaution during the research in working so that the sample not damaged.

Chapter 4 explains about result obtained from characterization that were used for the research and discuss the result in detail based on theory and support the result from previous research.

Chapter 5 concludes all the results that collected from the project based on the objectives are drawn in this chapter whether it achieve or not. It also consists overall of conclusions for the entire work. Several suggestions were also given out for the future works to improve this research.

CHAPTER 2

LITERATURE REVIEW

2.1 Electrolytes

Basically, an electrolytes is a substance that can conducts electricity when dissolve in solvent or water. They generally consists of free ions which acts as an electrically conductive medium which interacts at cathode and anode, thus make electrolyte possible to work (N. N. Aziz, Idris, & Isa, 2010). Electrolytes also known as medium which responsible for ionic transport espeacially for H^+ ion transport in SBEs and thus controls the power density. One of the most important properties for an electrolyte is ionic conductivity. To avoid short circuit, ionic conductivity should have negligible electronic conductivity. Electrolytes also is the main component in electrochemical devices such as batteries, fuel cells, supercapacitor and solar cells (J. Chen, Asano, Maekawa, & Yoshida, 2008; C.-H. Park, Park, Yoo, & Joo, 2006). (S. Majid & Arof, 2005) has identifies that dopant salt were needed to be added into solvent in order to form an electrolyte. The individual atomic component are separated by the force applied upon the solute molecule, in a process known as chemical dissociation in which the solution applies force to hold the ions apart.

The study of polymer electrolyte (PE) was discovered by (Fenton, 1973) and according to (Ramesh & Wen, 2010) reported in the early 1970s, electrolytes based solid state materials such as crystalline, ceramic, glass and polymer electrolytes have revealed. The science of PE is a highly specialized interdisciplinary field which encompasses the disciplines of electrochemistry, polymer science, organic chemistry and inorganic chemistry (Samsudin, Khairul, & Isa, 2012). The new development of new electrolyte materials for PEs based hybrid composite materials polymer,

amorphous polymer and crystalline polymers and their properties is creating new opportunity for new types of electrochemical devices (Samsudin et al., 2012; Vashishta, Mundy, & Shenoy, 1979). These creation may themselves, in turn revolutionize many areas of industrial. Ionically, PEs is a membrane which made from salts dissolution in a polymer matrix with high molecular weight (Ramesh & Lu, 2012).

Recently, the natural resources prevention and recycling has become huge discussion and have attracted attention among reseacher to concerning biomaterials with focus on renewable raw materials. This is because of environmental consciousness on solid waste especially electric waste has been highlighted around the world. Batteries is one example that contribute increasing of solid waste that can harm the environment and living organism due to the chemical used in commercial batteries are hazardous and non-biodegradable (N. H. Ahmad & M. I. N. Isa, 2015a). Generally, PE system owns ionic conduction properties and extensively used in electrochemical devices like solid state batteries and rechargeable batteries, especially lithium-ion batteries. Lithium-ion batteries have been reported to possess a myriad of desirable properties and hence have been extensively utilized in most portable electronic devices (Choudhary & Sengwa, 2013). However, the lithium-ion batteries are exposed to high rish as they use liquid electrolytes with organic solvents. Like the use of any technology, batteries based lithium-ion has their own disadvantages such as low protection, limited in ships transportation and costly. To overcome this problem, an alternative solution based green materials can be applied into the battery system. It is more safe to be used which are not harmful to the environment since it was made using natural materials and consequently have gained due attention among both academia and industry owing to their unique properties namely high ionic conductivity, good electrode/electrolytes contact apart from their inherent advantage over liquid or gel-based electrolytes such as low self-discharge in batteries and no

leakage (Ning, Xingxiang, Haihui, & Benqiao, 2009; Mohd Saiful Asmal Rani, Rudhziah, Ahmad, & Mohamed, 2014).

2.2 Previous Study of Gel and Liquid based Polymer Electrolytes

Generally, there were three type of polymer electrolytes (PEs) that have been extensively studied by numerous researchers knowing as gel polymer electrolytes (GPEs), Ionic Liquid Polymer Electrolytes (ILPEs) and solid polymer electrolytes (SPEs). The electrolytic properties has been improved using different approaces in order to achieve a better polymer, resulting into different types of PEs.

2.2.1 Gel Polymer Electrolytes (GPEs)

The GPEs systems has been studied over the latest few decades because of their ability in showed good elasticity, high mechanical strength which able to keep ionic conductivity after being contructed as an integrated flexible supercapacitor (K. Wang et al., 2015). Generally, GPEs also often known as a plasticized based polymer elecytrolyte due their appearent neither liquid nor solid or conversely both liquid and solid. However, in 1975, as stated by (Appetecchi et al., 1994) that GPEs was famous as gelionics and has been introduced from work done by (Feuillade & Perche, 1975). In gel, there were solid skeleton of polymer or long-chain molecules cross-linked intermolecularly or intermolecularly, which entrapped an uninterrupted liquid phase (Y N, Kumar, & Bhat, 2018). The GPEs incorporates both the diffusive property of liquid and the cohesive propery of solids which balance the high conductivity of organic liquid electrolytes and the dimensional stability of SPEs (Samsudin, 2014).

The past decade has seen the rapid development of GPEs in many application industrial, especially in energy storage devices. There were many literature have reported the usage of GPE in their system with different host polymer including poly(vinylidene fluoride-co-hexafluoropropylene) (PVDF-HFP)/poly(methyl methacrylate) (PMMA)/poly(N-isopropylacrylamide) (PNIPAM) (Aishova et al., 2018), poly-ethylene oxide (PEO) (Siyal et al., 2019), polyacrylonitrile (PAN) (Xiuli

Wang et al., 2019) and poly(acrylonitrile-maleic anhydride) (P(AN-MAH)) (Huang et al., 2018). Most of the research on GPEs were solid state GPEs for application to flexible supercapacitors (Yong, Park, Jung, & Jung, 2019). GPEs owing its own ability such as can enhanced the conductivity, low reactivity, low volatility, good in mechanical and chemical and can promise good electrochemical performances (Ramesh, Liew, & Ramesh, 2011; Ramesh & Wen, 2010). In addition, GPEs can exibit high ionic conductivity at room temperature with ~10^{-3} to 10^{-2} S cm^{-1} (Zhu et al., 2018).

However, among these excellent advantages of GPEs, there were several shortcoming which can effect their utility in wider practical applications. Based on findings by (Zhang et al., 2011) and (J.-K. Kim et al., 2008), they have claimed that the impregnation with liquid or aqueous electrolytes solution contributed to the poor mechanical strength. A sufficient mechanical strength is needed in polymer electrolyte in order to withstand the stress between the electrodes (H.-S. Kim, Kum, Cho, Cho, & Rhee, 2003). Other than that, the presence of water phase in the GPEs limits their temperature range of stable performance, thus possible to leads to the explosions due to uncontrolled preasure build up (Armand, Endres, MacFarlane, Ohno, & Scrosati, 2011; Quartarone & Mustarelli, 2011).

2.2.2 Ionic Liquid Polymer Electrolytes (ILPEs)

Ionic liquids (ILs) is a salt in fluids shape which can participate in a variety of attractive interractions ranging from weak to strong (Hayes, Warr, & Atkin, 2015). ILs often known as designer solvent due to its can be synthesized from different types of ionic species (Tsuchida, Matsumiya, & Tsunashima, 2019). The polymer electrolyte based ionic liquid are generally electrochemically and thermally stable, low volatility, good solvents for a wide range of both organic and inorganic materials and good in conductivity (Seddon & Holbrey, 1999; Welton, 1999; Wilkes, 2002) which can give advantages in fabrication of electrochemical devices. Moreover, the

polymer electrolytes can afford mechanical integrity while maintaining the ILs advantages (Kokubo, Sano, Murai, Ishii, & Watanabe, 2018).

In recent years, there has been an increasing amount of literature on ILs usage in industrial application especially in ion battery (Bose, Deb, & Bhattacharya, 2019; Koduru, Marinov, Hadjichristov, & Scaramuzza, 2019; Lu et al., 2019; Polu & Rhee, 2017). However, safely issues has become serious crisis in ILPEs usage nowaday due combustible organic solvents in traditional non-aqueous liquid electrolytes (Zhou, Shanmukaraj, Tkacheva, Armand, & Wang, 2019). These drawback thus leads to the leakage of electrolyte, easy to explode and easy to burn which restricts their performance in batteries for future development (Mindemark, Lacey, Bowden, & Brandell, 2018).

2.3 Solid Biopolymer Electrolytes (SBEs)

In the past three decades, the development of new polymer electrolyte system has been an important part in research due to the need to search new types of electrolyte for applications in various electrochemical devices. By compared to liquid and gel polymer electrolytes, solid biopolymer electrolyte (SBE) possess individual properties such as good compatibility with electrodes, no leakage, low self-discharge in batteries, flexibility and easy to fabricate (Yahya et al., 2006). Biopolymer electrolytes have been divided into two types based on their sources and origins: (a) natural and (b) synthetic. Some of the natural sources have been studied widely to achieve the development of SBEs system such as poly (vinyl chloride) (PVC) (N. Zakaria, S. Yahya, M. Isa, M. Nor Sabirin, & R. H. Y. Subban, 2010), polypropylene oxide (PPO), polyethylene imine (PEI) (Samsudin, Isa, & Mohamad, 2011) and carboxymethyl cellulose (CMC) (N. A. M. Noor & M. Isa, 2015). While polyvinyl alcohol (PVA) (El Sayed & El-Gamal, 2015; J. Wang, Song, Muchakayala, Hu, & Liu, 2017), polyethylene oxide (PEO) and polyvinyledene fluoride (PVdF) (Muthuvinayagam & Gopinathan, 2015) were classified as synthetic polymer which are favourable in the preparation of polymer electrolytes.

Commonly, biopolymers are biodegradable polymer which are a newly in emerging field. Three major areas of application that biopolymer focuses to such as medical, agricultural and consumer goods packaging (Y N et al., 2018). These applications have been developed interest in biopolymer to increase as well. The use of portable electronic devices like mobile phones, power banks and laptops recently has been increasing, subsequently made biopolymer research as important insights in power sources, thus promoting more interest among researcher. Besides that, SBEs also have unique properties namely high ionic conductivity, ease of fabrication into thin film with large surface area to give high energy density, good electrode-electrolytes contact and their ability to accommodate a wide range of doping salt concentrations which good enough to play important role in solid state ionic due to their potential application in capacitors, fuel cells and batteries (M. Ramlli, K. Kamarudin, & M. Isa, 2015; Mohd Saiful Asmal Rani et al., 2014; Wiers, 2015; Wright, 1975).

In recent decades, the explosive advancement of modern technology is bringing revolutionary changes to the human society. However, it also leads to a more and more serious environmental issue on electronic and plastic wastes (Xudong Wang, Yao, Wang, & Li, 2017). Selecting biopolymer with a high mechanical strength to act as the matrix of SBEs may serve as a viable approach to compensate for their insufficient mechanical strength. The crystallinity of biopolymers nearest to zero or are transparent (Rajantharan, 2011). Thus, choosing biopolymer electrolyte-based plant material like cellulose derivative as semi-crystalline nature were agreed for many researchers due to it can make our technology evolution more sustainable (Kuutti et al., 2011; Nawaz, Casarano, & El Seoud, 2012).

An environmentally friendly material, cellulose is the most abundant natural polymer in the earth in terms of biomass. It is also can provides a sustainable green resource that is renewable, degradable, biocompatible and effective in cost (Gale et al., 2016; Liu, Tao, Bai, & Liu, 2012; Moon, Martini, Nairn, Simonsen, & Youngblood, 2011; Zeng, Li, Liu, & Zhang, 2011). Moreover, the cellulose derivative have become widely used among researcher in electrolytes due to their excellent properties which

include biodegradable materials, high specific strength, low density and ability to form film (Debeaufort, Voilley, & Meares, 1994; Samad, Asghar, & Hashaikeh, 2013; Samir et al., 2005; Sit, Samsudin, & Isa, 2012; Yue, McEwen, & Cowie, 2003). The biopolymer electrolytes based cellulose derivative has been studied by (Zainuddin, Saadiah, Abdul Majeed, & Samsudin, 2018) and (Saadiah, Zhang, Nagao, Muzakir, & Samsudin, 2019) in their works of carboxymethyl cellulose (CMC) as host polymer electrolytes.

CMC was reported to be synthesized from diverse plant biomasses, which contain 40 – 50 % cellulose, 25 – 40 % hemicellulose and 15 – 35 % lignin on a dry basis (R. K. Singh & Singh, 2013). The synthesis of CMC from various agricultural waste cellulose sources such as sugar beet pulp, cavendish banana pseudo stem, cashew tree gum, sago waste, orange peel, papaya peel and Mimosa pigra peel have been reported by many researchers (Koh, 2013). The present work use CMC from Acros Organic Co. with average molecular weight of 90000. Besides that, CMC also one of the hydrophilic carboxyl groups where CMC consists of hydrophobic polysaccharide backbone and thus shows that water soluble features (Chai & Isa, 2011). A distinctive structural feature of these cellulose materials is heterogeneity owing to its fiber structure. In addition, it is a biodegradable material, low-cost material to be produced, non-toxic to environment, semi-crystalline material and exhibit excellent film forming ability but lack of strength and low in ionic conductivity (N. H. Ahmad & M. I. N. Isa, 2015a; Chai & Isa, 2012; M. Ramlli et al., 2015). There have been several studies in the literature reporting CMC as single host polymer can enhanced the nature of insulating biopolymer cellulose towards ionic conductivity and potential to be applied in energy storage when ionic dopant was incorporated into the system (N. H. Ahmad & M. I. N. Isa, 2015b; Ahmad & Isa, 2012; El-Gamal, El Sayed, & Abdel-Hady, 2017; N. A. M. Noor & M. I. N. Isa, 2015; A. S. Samsudin, H. M. Lai, & M. I. N. Isa, 2014). Table 2.1 listed previous study using CMC as single polymer.

Table 2 1 CMC as host polymer.

Sample	Conductivity (S cm^{-1})	References

CMC – AA	6.12×10^{-7}	(Rozali & ISA, 2014)
CMC – NH_4SCN	6.48×10^{-5}	(M. Ramlli & M. Isa, 2015)
CMC - DTAB	7.72×10^{-4}	(A. Samsudin & M. Isa, 2012a)
CMC – NH_4Cl	1.43×10^{-3}	(N. Ahmad & M. Isa, 2016)

Another potential candidate is polyvinyl alcohol (PVA) which can promise the advantages in composite films application since it has hydrophilicity properties. PVA is essentially made from polyvinyl acetate through hydrolysis. It is also easily degradable by biological organisms and in water is a solubilized crystalline structure polymer (Razzak & Darwis, 2001). During the first half of the 20th century, PVA has been used worldwide in many application including industrial, commercial, medical, and food sectors (DeMerlis & Schoneker, 2003). PVA is a biodegradable imitation of natural polymers used in paper coating, textile sizing and electrolytes. This polymer is widely used by blending with other polymer compounds, such as biopolymers and other polymers with hydrophilic properties; it is utilized for various industrial applications to enhance the mechanical properties of films because of its compatible structure and hydrophilic properties (Gaaz et al., 2015). The complete dissolution of PVA in water is bound by its intrinsic properties, which require the water temperature to be at ~100 °C with a holding time of 30 min (Albdiry & Yousif, 2013). All PVA grades are hydrophilic and depend on certain factors, such as molecular weight, element dimensions of distribution, and particle crystal structure. Moreover, in 2015, Sivadevi explained PVA is a potential material which having a very high dielectric strength up to >1,000 kV mm^{-1}, thus have bright future to be used in electrochemical application (Sivadevi et al., 2015). (Saadiah et al., 2019) also agreed that PVA is a non-toxic material with high tensile strength and flexibility. Literature has found the used of PVA as single polymer can possess high in ionic conductivity when doped with dopant salt as recorded in Table 2.2.

Table 2 2 Previous study on PVA as single host polymer.

Sample	**Conductivity (S cm^{-1})**	**References**
PVA – KOH	8.5×10^{-4}	(Mokhtar et al., 2016)

PVA – NH_4NO_3	7.5 x 10^{-3}	(Hema, Selvasekarapandian, Nithya, Sakunthala, & Arunkumar, 2009)
PVA – NH_4SCN	2.58 x 10^{-3}	(Abdelgawad, Hudson, & Rojas, 2014)
PVA-NH_4Br	5.70 x 10^{-4}	(Hema, Selvasekerapandian, & Hirankumar, 2007)

2.4 Blended Polymer

Back to 1975, Wright and co-worker has found the electrical conductivity in ionic polymers in polyethylene-based electrolyte (Wright, 1975). Since the initial finding on ionic conduction, many works has been done in order to enhance the ionic conductivity of SBE for application in high energy density batteries approach (Nik Aziz et al., 2010). In 2011, (Khiar & Arof, 2011) published a paper in which they described the ideal ionic conductivity for solid polymer electrolyte is at range of 10^{-3} to 10^{-2} S cm^{-1}. In order to enhance the ionic conductivity, many methods have been pursued including polymer blending, use different polymers for polymer blend, copolymer grafting, addition of dopant salt or plasticizer and varying the ratios of polymers, salts or plasticizer in order to modify the degree of crystallinity (Hema, Selvasekarapandian, Nithya, et al., 2009; M. F. Z. Kadir, S. R. Majid, & A. K. Arof, 2010; M. F. Shukur, R. Ithnin, & M. F. Z. Kadir, 2014b).

Polymer blend is a mixture of at least two macromolecular substances (polymers or copolymers). Polymer blending technique were applied in present system due to its well-used technique whenever modification of the properties is required because its uses conventional technology at low cost and can promising good conductivity (Khiar & Arof, 2011; Ramly, Isa, & Khiar, 2011). Nevertheless, the SBE system properties depend on the miscibility of blend. The conductivity will increase when the miscibility blend does not show any phase separation between both of the polymer. The blending method has growth attention among researcher due to it can provides a set of properties required for specific application in lower cost (Sivadevi et al., 2015). Polymer blends are also easy to prepare and the physical properties of the films can be controlled (M. Kadir, S. Majid,

& A. Arof, 2010; M. Shukur, R. Ithnin, & M. Kadir, 2014). Interactions between the two blended polymers can greatly influence the conductivity and physical properties of the films.

Further, CMC often blended with other polymer such as starch and PVA in order to improve the quality and stability of product, provide desirable texture and to control the mobility of water and moisture since it is water soluble heteropoly saccharides with high molecular weight properties (Bertuzzi, Vidaurre, Armada, & Gottifredi, 2007; M. A. Saadiah & A. S. Samsudin, 2018). In addition, the incorporation of PVA into CMC is believed that polymer blending can enhance the conductivity through formation of hydrogen bonding (Varnell & Coleman, 1981; Varnell, Runt, & Coleman, 1983). When these two polymers are blend together, the interactions between CMC and PVA are predicted to happen via inter-chain H-bonding between the carbonyl group of CMC and the hydroxyl group of PVA. CMC-PVA is flexible blend, semi-transparent and permits the observation of the healing process so it can be used as a dressing material (El-Gamal et al., 2017; Wei, Fu, Zhang, Wang, & Ren, 2014). The application of polymer blending in polymer electrolyte field has received much attention as tabulated in Table 2.3.

Table 2 3 Previous research on polymer blending based electrolytes.

Sample	Conductivity (S cm^{-1})	References
CMC/PVA	9.12 x 10^{-6}	(M. A. Saadiah & A. S. Samsudin, 2018)
CMC/KC	3.91 x 10^{-7}	(Zainuddin et al., 2018)
MC/Potato starch	1.04 x 10^{-11}	(M. Hamsan, M. Shukur, & M. Kadir, 2017)
CMC/chitosan	3.15 x 10^{-9}	(Bakar, Muhamaruesa, Aniskari, & Isa, 2015)
PVA/PVP	1.58 x 10^{-6}	(Rajeswari et al., 2011)

2.5 Doping System

Another promising method to enhanced the ionic conductivity is by doping system using ionic dopant. There were different kinds of proton conductor that are widely used recent decaded such as acid base (Chai & Isa, 2012; Kalaiselvimary, Pradeepa, Sowmya, Edwinraj, & Prabhu, 2016; Rozali & ISA, 2014), lithium salt (Dhatarwal, Choudhary, & Sengwa, 2018; Jiang et al., 2018; Ramesh & Chai, 2007) and ammonium salt (Fuzlin, Rasali, & Samsudin, 2018; Kadir et al., 2018; N. F. Mazuki, A. F. Fuzlin, et al., 2018; Y. M. Yusof, H. A. Illias, & M. F. Z. Kadir, 2014). Dopant salt based biopolymer complex is a multicomponent system. The salt can provide the conduction pathways which the conducting species migrate through the polymer material when electric field was applied.

In 1990, Hashmi claimed that ammonium salt can possess excellent proton donor in polymer electrolyte (S. A. Hashmi, Kumar, Maurya, & Chandra, 1990). Therefore, ionic dopant materials acts as sources of charge carrier in polymer electrolyte, assuming it play an important role as proton conductor. It is also can effect the miscibility of polymer pairs and the morphology of the electrolytes through interaction between ions and polymer backbone (Chew, Ng, & How, 2013; A. S. Samsudin et al., 2014). (M. F. Shukur et al., 2014b) reported that blended polymer electrolyte based starch/chitosan possess conductivity of 4.00 x 10^{-10} Scm^{-1} and when incorporate NH_4Cl, the ionic conductivity increase up to 6.51 x 10^{-9} S cm^{-1} for sample containing 5 wt. % NH_4Cl.

On the other hand, ammonium salt is claimed as good proton donor to the matrix ion for membrane develop with highest proton conducting (N. H. Ahmad & M. I. N. M. Isa, 2015; Nik Aziz et al., 2010; Sikkanthar et al., 2015). According to (C. S. Ramya, S. Selvasekarapandian, G. Hirankumar, T. Savitha, & P. C. Angelo, 2008), proton or NH_4^+ cations from ammonium salt can acts as mobile species which is believed to be responsible for the ionic conduction in electrolyte. A considerable

amount of literature has been publised on ammonium bromide (NH_4Br) as a dopant salt in bio/polymer electrolytes which can provide in increment of ionic conductivity (Bakar et al., 2015; M N Hafiza, Bashirah, Bakar, & Isa, 2014; Nor fatihah Mazuki, Nagao, & Samsudin, 2019; Mejenom, Hafiza, & Mohamad Isa, 2018; Sikkanthar et al., 2015). Another literature based polymer blend from biodegradable materials doped with ammonium salt as mention in Table 2.4.

Table 2 4 Previous study of polymer blend-salt complexes electrolytes

Sample	Conductivity (S cm^{-1})	References
PVA/Chitosan – NH_4Br	7.68×10^{-4}	(Y. Yusof, H. Illias, & M. Kadir, 2014)
Chitosan/PVA – NH_4I	1.77×10^{-6}	(Buraidah & Arof, 2011b)
Starch/Chitosan-NH_4NO_3	3.89×10^{-5}	(Khiar & Arof, 2011)
Starch/PEO-NH_4NO_3	2.81×10^{-7}	(Ramly et al., 2011)
MC/potato starch-NH_4NO_3	4.37×10^{-5}	(M. Hamsan et al., 2017)

Futhermore, proton (H^+) can provide benefits for developing a proton battery such as low cost of fabrication on electrode and electrolyte materials (A. S. Samsudin et al., 2014). Due of that, there were widely studied on proton conducting polymer for their potential applications in low devices (Ng & Mohamad, 2008).

2.6 Utilization of Solid Biopolymer Electrolyte in Electrical Double Layer Capacitor (EDLC)

Generally, polymer electrolyte (PE) is one of the important component in solid state energy devices and has been extensively studied. According to (Bhargav, Mohan, Sharma, & Rao, 2009) and (Hatta et al., 2009), they have stated that ionic conductivity must be sufficient to be applied in electrochemical devices. The basic principle of

charge storage is related to the formation of double layer as a result of electrostatic charge accumulation between electrode/electrolyte without any chemical reaction. Electrochemical capacitors also known as supercapacitor cells are commonly consists of electrolyte and one electrodes pair. (Numan et al., 2016) and (Nadiah et al., 2017) claimed that supercapacitor has potential to replace batteries in industrial application due its ability in high power density, excellent cyclic retention, fast charging and can store high energy density. Other than that, supercapacitor is one type of electrochemical devices which divided into three main categories namely hybrid capacitors EDLCs and pseudocapacitors (Liew, Ramesh, & Arof, 2016a). Further, there were differences between pseudocapacitor and EDLC. Where in pseudocapacitor, energy is stored through a faradaic process while in EDLCs, energy is stored in the double layer at electrode/electrolytes interface without going through faradiac process (Liew, Ramesh, & Arof, 2014b; Omar et al., 2016).

Ionically, EDLCs have attracted enormous attention worldwide as alternative energy storage systems (Varzi & Passerini, 2015). In addition, EDLC is widely used among researcher due to they offer relatively wide potential window including free maintenance, free toxic materials, higher power density, large capacitance and longer cycle life compared with batteries (Burke, 2000; Kibi et al., 1996; Zubieta & Bonert, 2000). Furthermore, EDLC consist of two electrodes and one electrolyte where electrode can be derived from many materials such as graphite (Faraji & Abedini, 2019), activated carbon (Liew et al., 2016a), carbon black (S. A. Hashmi, Latham, Linford, & Schlindwein, 1997) and carbon aerogel (Abbas, Mirzaeian, Ogwu, Mazur, & Gibson, 2018). This storage mechanism has contributed these devices can be charged and discharged within seconds as they feature high power up to 10 kW kg^{-1} and an extremely high cycle life with more than 500,000 (Böckenfeld, Jeong, Winter, Passerini, & Balducci, 2013; Brandt & Balducci, 2014). EDLC based solid and gel polymer electrolytes has advantage overcome the leakage and safety issue compared with liquid electrolytes (Teoh, Lim, Liew, & Ramesh, 2015). However, the performance of EDLC also depends on electrode, electrolytes and device configuration (H. Yang, Liu, Kong, Kang, & Ran, 2019).

CHAPTER 3

METHODOLOGY

In this chapter, there were two system applied in research work which is carboxymethyl cellulose (CMC)-polyvinyl alcohol (PVA) based polymer blend electrolytes system and polymer blend CMC-PVA doped with ammonium bromide (NH_4Br) as biopolymer electrolytes system. These both systems were prepared via casting method. The study on electrical and structural properties of polymer blend CMC-PVA is to find the suitable ratio as host polymer to be doped with NH_4Br. Afterwards, the electron donor atoms from polymer blend complex will interact with proton (H^+) ions from NH_4Br through salt dissociation, resulting to the ionic conductivity of solid biopolymer electrolytes system.

3.1 Preparation of Solid Biopolymer Electrolytes

3.1.1 Polymer Blend CMC-PVA

CMC and PVA (~85 % hydrolysis) were obtained from Acros Organic Co. (M.W. 90000) and Merck Co. (M.W. 70000), respectively. The polymer blend based electrolytes were established using different ratio of weight percentage for CMC and PVA as tabulated in Table 3.1. The polymer blend CMC-PVA was prepared by a solution casting technique. Various percentage of CMC-PVA concentration was dissolved in distilled water. The mixed solution was casting into glass petri dishes followed by oven drying for about 300 minutes at 60 °C and accompanied by further drying in desiccator to ensure all solvent has been evaporated.

Table 3 1 List of samples with their compositions respectively.

Designation	CMC/PVA Ratio
E0	100 : 0
E1	90 : 10
E2	80 : 20
E3	70 : 30
E4	60 : 40
E5	50 : 50
E6	40 : 60

3.1.2 CMC-PVA-NH_4Br based electrolytes system

. The 80/20 ratio of CMC/PVA was used as biopolymer blended host and dissolved in distilled water. Then, a varied amount of NH_4Br from the range of 5 wt. % to 35 wt. % was added into the CMC-PVA blended solution and stirred continuously until a homogenous solution was attained. The solution was cast into several petri dishes and left to be dried further at room temperature until the film was formed. The various amount of NH_4Br and designation of SBE systems is tabulated in Table 3.2.

Table 3 2 Designation of CMC-PVA-NH_4Br based SBEs system.

Design	**Concentration of SBEs system**				
	Weight (g)		Weight percent (wt. %)	Weight (g) NH_4Br	Weight percent (wt. %)
	CMC	PVA			
AB0	1.6	0.4	80:20	-	0
AB5				0.1054	5
AB10				0.2222	10

AB15	0.3529	15
AB20	0.5	20
AB25	0.6667	25
AB30	0.8571	30
AB35	1.0769	35

3.2 Characterization of SBEs system

3.2.1 Fourier Transform Infrared Spectroscopy (FTIR)

Infrared Spectroscopy is one of the techniques used to study the salt complexation and free ions transport property of biopolymer-salt complexes. In present work, the complexation of CMC-PVA-NH_4Br SBEs system was characterized using infrared spectra and recorded using Perkin Elmer Spectrum 100. The spectrometer was equipped with an Attenuated Total Reflection (ATR) accessory with a germanium crystal. The FTIR spectra for pure NH_4Br was carried out using potassium bromide (KBr) in pellets shape. The sample was put on germanium crystal and infrared light was passed through the sample with the frequency ranging from 700 to 4000 cm^{-1} with spectra resolution of 2 cm^{-1}. The FTIR spectra and peak deconvolution were analyzed by using OriginPro 8 software which is provided by OriginLab Corporation. Baseline correction and curve fitting were accomplished to analyze the deconvolution process of the FTIR spectra. The curve fitting was done by applying the gaussian and lorentzian mode.

The intra- and inter- molecular interactions between the CMC and PVA were studied via density functional theory (DFT) calculations which executed by Gaussian G09W software. The simulation was performed based on gradient corrected DFT (Hohenberg & Kohn, 1964) using the Becke three-parameter hybrid functional (B3) (Becke, 1993) which is for exchange component and the Lee-Yang-Parr (LYP) correlation function (Lee, Yang, & Parr, 1988). Chemical structures of pure CMC, PVA, and CMC-PVA complexes were built and arranged based on their internal coordinates (bond length, bond angle, and dihedral angle) using GaussView 5.0 software. The internal

coordinates of the models were then optimized to the lowest energy structure using B3LYP functional and 6-31g (d, p) basis set (Xianlong Wang, Wang, & Zhao, 2012). The modeled structures were then examined using the harmonic frequency calculations using the same functional and basis set. The calculated mode of vibration of the optimized structures presented positive frequencies, which indicate minimum energy structures (Lee et al., 1988); evaluated as realistic models. The stage of validation and establishment of the realistic models is crucial; would yield trustworthy information to be compared with that of the experimental observations.

3.2.2 X-ray Diffraction (XRD)

XRD analysis is useful tool in the determination of degree of crystallinity and amorphousness. The XRD measurements were performed using XRD-Rigaku MiniFlex II outfitted with nickel-filtered C_u K_α (λ= 0.154 nm) radiation (30 kV, 15 mA) and scanned at angle 2θ between 5° to 80°. Meanwhile, the XRD deconvolution analysis was performed using Origin Lab 8.0 software was used to deconvolute specific region (crystal or amorphous peaks). The crystalline and amorphous peaks were deconvolute based on the assumption of Gaussian function in order to ensure all peaks are fit with original spectrum. The percentage of crystallinity was determined by using equation (1) (N. Zainuddin & A. Samsudin, 2018) as follows:

$$X_c = \frac{A_c}{A_T} x\ 100\% \qquad (3.1)$$

where A_c is an area of crystalline region, A_a is an area of amorphous region, A_T is the total area under the peak representing the area of crystalline region and area of amorphous region and X_c is the degree of crystalline in percentage.

Further analysis on the crystallite size (D) was done using full width at half maximum (FWHM) information. The calculation is based on Debye-Scherrer equation shown in equation (2).

$$D = \frac{K\lambda}{FWHM \cos\theta} \tag{3.2}$$

where K is 0.94, λ is the X-ray wavelength used which is 0.154 nm and θ is the peak location.

3.2.3 Thermogravimetric Analysis (TGA)

The thermal stability of solid biopolymer electrolytes system was measured with a TGA instrument via Mettle Toledo TGA DSC 1. The measurements were recorded in a nitrogen gas atmosphere at a flow rate of 20 ml min^{-1}. The sample from vary salt concentration was heated from 5 to 800 ºC at a heating rate of 20 ºC min^{-1}.

3.2.4 Differential Scanning Calorimetry (DSC)

Thermal properties such as glass transition temperature, melting temperature and crystallization temperature can be measured by using DSC. The thermal properties of the SBE system are determined by DSC analysis which was conducted using DSC TA Q500 model where the electrolyte was sealed in a pan of aluminum. An empty pan was used as reference. The SBE system was heated at an elevated temperature to erase previous thermal history, and then cooled at a linear rate before heating again. The glass transition temperature (T_g) of SBE system was analyzed using TA Universal analysis at a heating rate of 10 °C min^{-1} from 25 to 280 °C. A nitrogen flow (50 mL min^{-1}) was applied during the experiment.

3.2.5 Electrical Impedance Spectroscopy (EIS)

The ionic conductivity of the polymer blend CMC-PVA system and CMC-PVA doped with various amount of NH_4Br based solid polymer electrolytes were analyzed by using HIOKI 3532-50 LCR Hi-TESTER at a frequency range of 50 Hz to 1 MHz. The samples were tested at different temperature from 303 K to 373 K. The prepared samples were subsequently cut into suitable size and flanked between two

stainless steel electrodes. From the imaginary impedance (Z_i) versus real impedance (Z_r) of Cole-Cole plot, the bulk resistance (R_b) value is obtained and the ionic conductivity, σ was determined using the following equation:

$$\sigma = \frac{y}{R_b A} \tag{3}$$

where y is the thickness of the sample and A (cm^2) the cross-sectional area of the sample.

3.2.6 Transference Number Measurement (TNM)

TNM was conducted in order to determine the mechanism of conducting species of the biopolymer electrolytes system-based CMC-PVA-NH_4Br, indicating the sample's conductivity of either being more cationic than anionic or otherwise by using UNI-T UT803. The sample was sandwich between two stainless steel blocking electrodes and the current through the circuit was monitored with the time until it saturates with dc voltage of 0.8 V. For the evaluation of H^+ transference number, the Watanabe technique was used by using MnO_2 as a blocking electrode (Sukeshini, Nishimoto, & Watanabe, 1996; H. J. Woo, Majid, & Arof, 2011). The H^+ transference number for the highest conducting sample was recorded with a dc voltage and the impedance analyser (PGSTAT M101 with FRA32M module Autolab) at a frequency between 0.01 Hz to 100 kHz with an amplitude of 0.5 mV.

3.2.7 Linear Sweep Voltammetry (LSV)

Electrochemical stability window of the electrolyte was determined using linear sweep voltammetry (LSV). The EDLC cell of biopolymer electrolyte-based polymer blend CMC-PVA doped with 20 wt. % NH_4Br has been done via Autolab PGSTAT M101 with FRA32M module autolab system (Metrohm Autolab B.V., the Netherlends),

operated by Nova 1.9 sofware. from 0 to 3 V. LSV measurement was conducted with sandwiched the biopolymer electrolyte between two stainless steel at a scan rate of 5 mV s^{-1} under room temperature.

3.3 Preparation of Electrodes

EDLC electrodes were prepared by ratio 80:10:10 of activated carbon (AC BP20) : black carbon or super P : poly(vinylidene fluoride) (PVdF) in 2.8 ml acetone. Stir the mixture until slurry was formed via treatment in ultrasonic bath for 30 minutes and then continues stirring on hot plate for additional 36 hours. Afterwards, the homogenous slurry was then spread on the graphite sheet via dropping technique. The spread slurry was heated in an vacuum oven until slurry dried. The casted electrodes were kept in the drying cabinet filled with silica gel for further drying.

3.4 Preparation of Electrical Double Layer Capacitor (EDLC)

EDLC was assembled by sandwiching the polymer electrolyte with two activated carbon electrodes as displayed in Figure 3.1. The electrodes were cut using electrode cutter with area of 1.77 cm^2 and the mass is ~0.0085 g. The assembled EDLC coin cells were then pressed under pressure to ensure electrodes and biopolymer electrolyte-based CMC-PVA-NH_4Br in good contact.

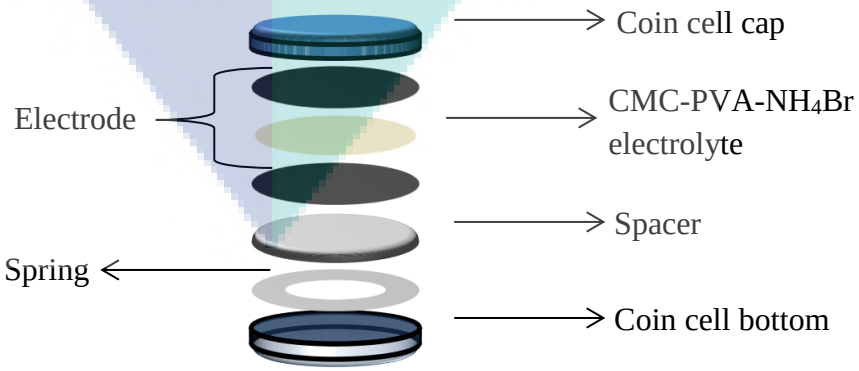

Figure 3 1 Arrangement of EDLC for sample with highest conductance.

3.5 Electrical Double Layer Capacitor Characterization

3.5.1 Cycle Voltammetry (CV)

The formation of the EDLC coin cell was characterized via cyclic voltammetry (CV) and galvanostatic charge-discharge studies. CV was carried out using Autolab PGSTAT M101 with FRA32M module autolab system (Metrohm Autolab B.V., the Netherlends), operated by Nova 1.9 sofware from 0 to 1 V with vary scan rate of 2, 4, 6, 8, 10, 20, 30, 40 and 0 mV s^{-1}. Figure 3.2 exhibits the one of the example CV curve work done by (Shukur, Ithnin, Illias, & Kadir, 2013) based plasticized chitosan-poly(ethylene oxide) (PEO) doped with ammonium nitrate (NH_4NO_3) polymer electrolyte. It can be seen from Figure 3.2, the CV curve is in leaf shape and become smaller as decrease the scan rate. This can be concluded that EDLC cell revealed the characteristic of cells of capacitor.

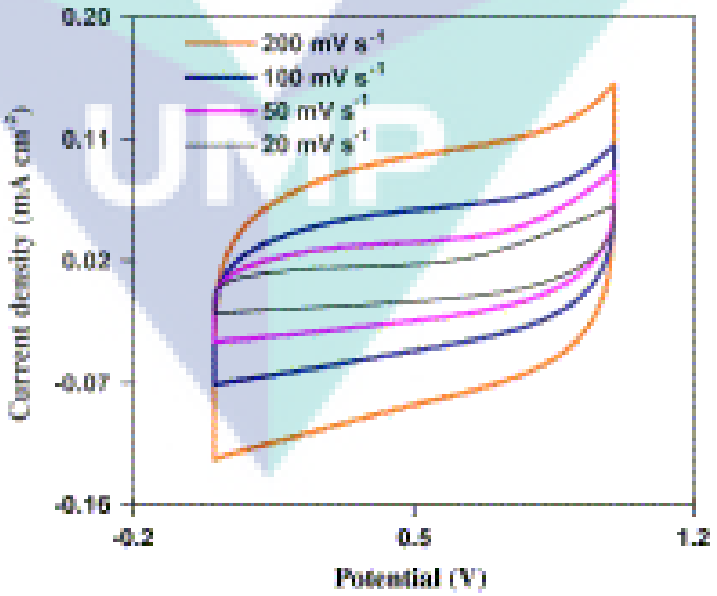

Figure 3 2 Cyclic voltammetry plots of EDLC coin cell at different scan rate (Shukur et al., 2013).

3.5.2 Galvanostatic Charge-Discharge (GCD)

The galvanostatic charge-discharge characteristics of the EDLC were carried out via Neware battery testing system in a voltage of 1 V at a different current density of 0.5, 0.4, 0.3 and 0.1 mA g^{-1}. Using selected charge-discharged cycle, the specific capacitance were calculated as well as power density and enrgy density in order to evaluate the performance of the most conducting biopolymer electrolyte-based CMC-PVA-NH_4Br in EDLC coin cell. The GCD curve of EDLC cell from previous work has shown in Figure 3.3. As observed in that figure, there were abrupt jump in voltage at discharge curve and according to (Arof et al., 2012), they have discussed that these phenomenon is attributed to the existence of the internal resistance and equivalent series resistance in the electrode and electrolyte.

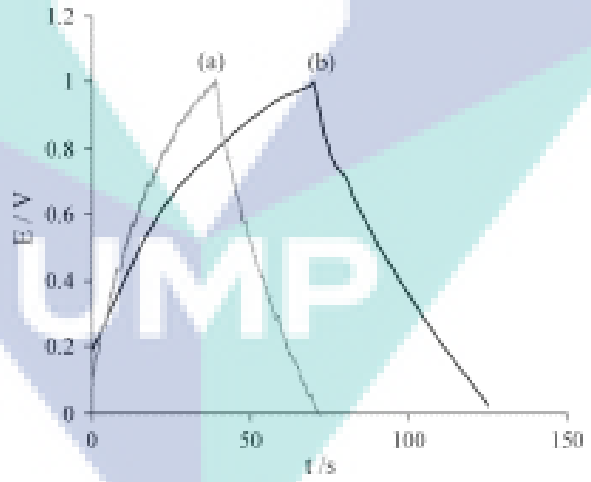

Figure 3 3 GCD curve of two EDLCs cell (a) CAC/GPE/CAC and (b) MKS/GPE/MKS EDLC at first cycle (Arof et al., 2012).

CHAPTER 4

RESULTS AND DISCUSSION OF POLYMER BLEND

This chapter discussed results obtained from all the characterization used in this work including the structural and thermal properties of polymer blend CMC-PVA biopolymer electrolytes system using Fourier Transform Infrared (FTIR) Spectroscopy, X-ray diffraction (XRD), Differential Scanning Calorimetry (DSC) and Thermo Gravimetric Analysis (TGA). The ionic conduction properties of biopolymer electrolytes system measured via Electrical Impedance Spectroscopy (EIS)

4.1 Physical Appearance of the CMC-PVA

This research was established with the host polymer consisting of carboxymethyl cellulose (CMC) and polyvinyl alcohol (PVA) and known as blend polymer electrolyte (BPe). The BPe was prepared via economical method with various composition of the CMC and PVA. The resulting BPe has are transparent, clear, flexible, self-standing thin films with good mechanical properties. Figure 4.1 shows the free standing film of CMC-PVA which has fully dried prior to the characterization.

Figure 4 1 A transparent thin film of CMC-PVA of the BPe system

4.2 Attenuated Total Reflection-Fourier Transforms Infrared Spectroscopy (ATR-FTIR)

4.2.1 ATR-FTIR Spectra of Pure CMC and Pure PVA

The prominence of IR spectroscopy is to characterize the configuration and conformation structure of polymers to explain the complexation between the bio-polymer blends. The most common complexation in polymer is the hydrogen bonding (H-bonding) which become literally important to change the crystallinity nature of wide range materials. The IR spectra of pure CMC and pure PVA is presented in Figure 4.2. Meanwhile, detail list of ATR-FTIR vibrational modes of pure CMC and pure PVA is tabulated in Table 4.1.

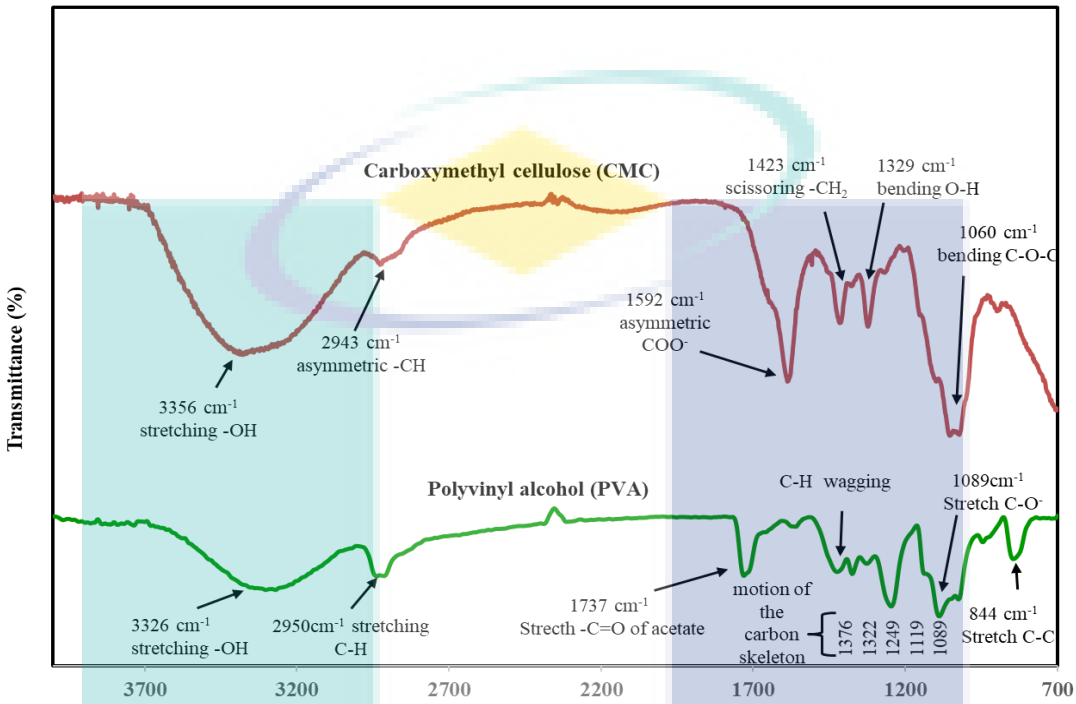

Figure 4 2 Experimental FTIR spectra of pure CMC and pure PVA of the BPe system

There are five absorption bands which appeared in the region 1060 cm^{-1}, 1329 cm^{-1}, 1423 cm^{-1}, 1592 cm^{-1} and 3356 cm^{-1} correspond to bending C-O-C, bending –OH, scissoring $–CH_2$, asymmetric $–COO^-$ and stretching –OH respectively which are considered as the signature peaks of the CMC. (A. Samsudin & M. Isa, 2012b) reported the similar signature bands of the CMC at 1056 cm^{-1}, 1334 cm^{-1}, 1421 cm^{-1} and 1581 cm^{-1}. These are the characteristic peaks of carbohydrate and confirmed the carboxymethyl substituent at the CMC backbone. The pure PVA showed absorption bands at 844 cm^{-1}, 1089 cm^{-1}, 1376 cm^{-1}, 1737 cm^{-1} and 3326 cm^{-1}, attributed to the stretching C-C, stretching $–CO^-$, wagging –CH, stretching C=O and stretching –OH respectively. The main features of PVA given by the appearance of vibration carbon skeleton motion at the range 1089 to 1376 cm^{-1}.

Table 4 1 List of ATR-FTIR vibrational modes of pure CMC and pure PVA.

Sample	Wavenumber (cm^{-1})	Assignment	References
Carboxymethyl cellulose (CMC)	1060	Bending C-O-C Ether linkage or 1,4-beta-d glucoside	El sawy et al. 2010 Kuanova et al. 2017
	1329	Bending -OH	Biswal & Singh, 2004
	1423	Scissoring $–CH_2$	Biswal & Singh, 2004; Liew & Ramesh, 2015
	1592	Asymmetrical COO^-	Biswal & Singh, 2004; Liew & Ramesh, 2015; Zhu et al. 2015
	2943	Aliphatic -CH	Kuanova et al. 2017; Zhu et al. 2015
	3356	Stretching -OH	Biswal & Singh, 2004; Zhu et al. 2015
Polyvinyl alcohol (PVA)	844	Stretch C-C	El sawy et al. 2010
	1089	Stretching $C-O^-$	El sawy et al. 2010
	1246-1376	Peaks correspond to motion of the carbon skeleton	Kuanova et al. 2017
	1376	Wagging -CH	Singh et al. 2013
	1737	Stretching C=O and C-O from acetate group remaining from PVA	Kuanova et al. 2017; Mansur et al. 2008
	2950	Stretching -CH	[33]

3326	Stretching -OH	[34, 35]

4.2.2 ATR-FTIR Spectra of CMC-PVA

The study on the complexation of the polymer blend electrolyte process can be explained through different types of interaction such as H-bonding and configuration which help to predict the thermal and electrical properties of the BPe system. H-bonding interaction is well known with its diversity and strength (Guo, Sato, Hashimoto, & Ozaki, 2010). (Xing, Dong, Feng, & Feng, 1998) reported that polymers contain the hydroxyl group can be mixed with polyester because of the intermolecular H-bonding resulting in completely or partially miscible system. The ATR-FTIR spectrum for the CMC-PVA at different composition is shown in Figure 4.3.

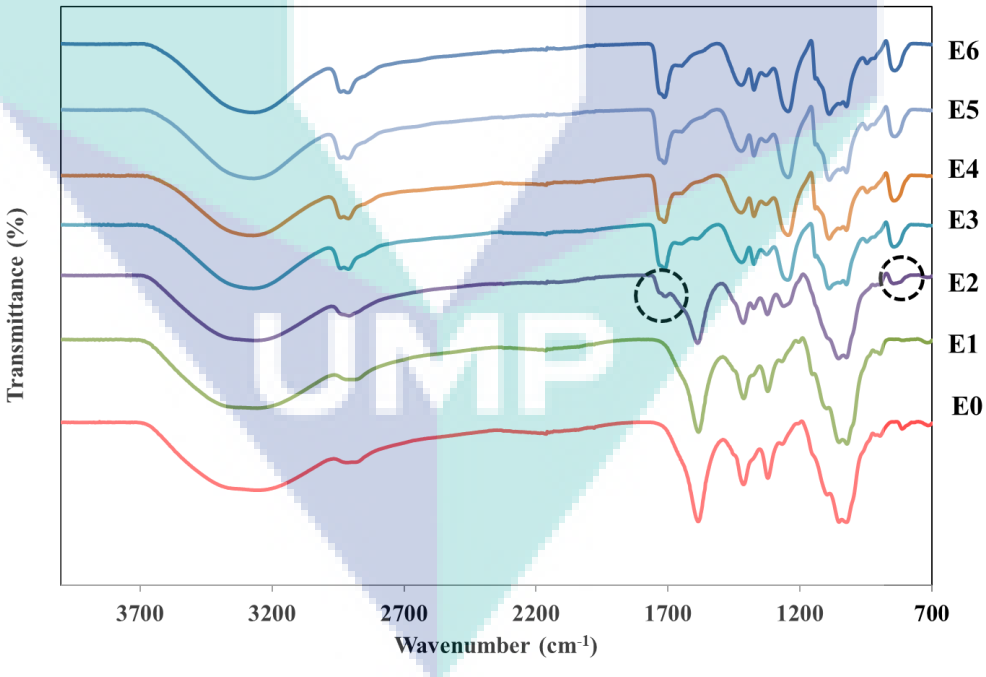

Figure 4 3 FTIR spectrum for CMC-PVA BPes system

The evaluation of the complexation between CMC and PVA BPe is done based on changes to position, shift in absorption and change in peak intensity attributed to the

disappearance/appearance of peak at specific region (Sim, Majid, & Arof, 2012). Based on the figure, two new shoulder peaks start to appear for E2 sample at 844 cm^{-1} and 1737 cm^{-1} which is referring to vibration of stretching C-C and C=O of PVA respectively. The transmittance of the shoulder peak has increased compare to that of the original band with increasing PVA content which gives reflection that complexation has occurred. Though, the functional group of interest, $-COO^-$ for the CMC begins to disappear from sample E3 until E6, suggesting the substitution of PVA into the CMC

(Riaz & Ashraf, 2014) mentioned that the physical properties of polymer blend are influenced by the molecular chain of the polymer. Meanwhile in this present work, the peak intensity of the C-O-C, –COO- and –OH found at 1060 cm^{-1}, 1329 cm^{-1}, 1592 cm^{-1} and 3356 cm^{-1} has reduced in comparison to other peaks suggesting the occurrence of intermolecular H-bonding during the complexation in the blend polymer system. A study conducted by Coleman et al. (Michael M. Coleman, Skrovanek, Hu, & Painter, 1988) revealed that the process to blended two polymers require favorable interaction at active sites such as oxygen and nitrogen which has capability to exert strong forces of attraction (H-bonding).

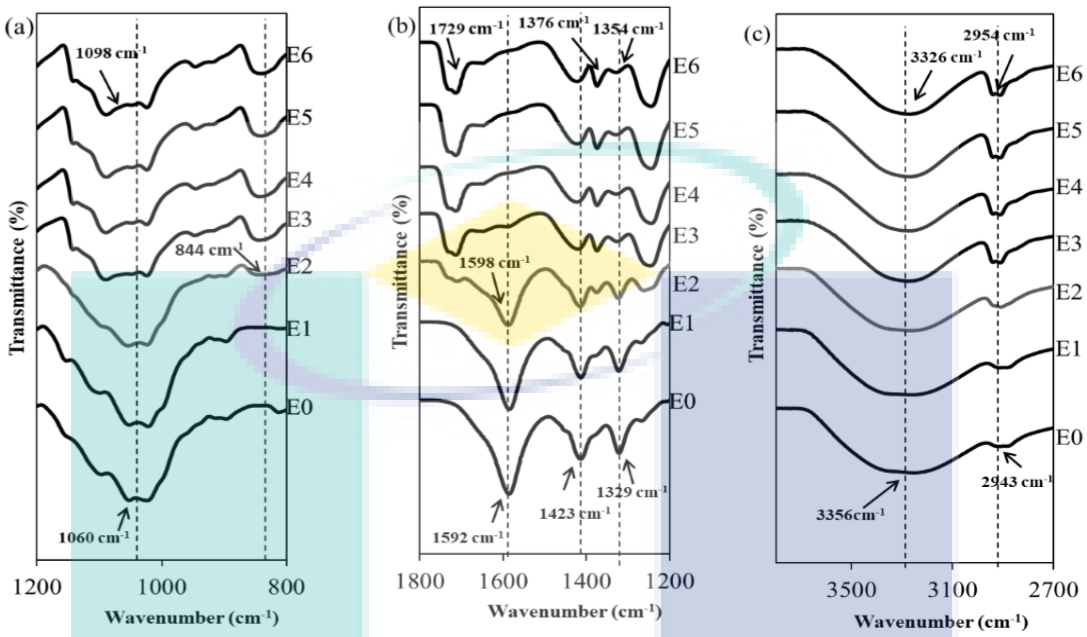

Figure 4 4 FTIR spectrum for CMC-PVA of BPe system in the wavenumbers of (a) 800-1200 cm^{-1}, (b) 1200-1800 cm^{-1} and (b) 2700-3500 cm^{-1}

The ATR-FTIR spectrum is analysed based on three potential regions in Figure 4.4 which are at the following wavenumber (a) 800 to 1200 cm^{-1} (b) 1200-1800 cm^{-1} and (c) 2700 to 3500 cm^{-1} in order to have more apparent evaluation. Figure 4.4(a) reveals the complexation for blend polymer with dual polymer host of CMC and PVA. The most intensive spectrum is found at 1060 cm^{-1} due to ether linkage (C-O-C) which does contain the oxygen site that is capable to form the inter-molecular H-bonding with another molecule such as PVA (Michael M. Coleman et al., 1988). This is supported by an obvious shifting to higher wavenumber, 1060 cm^{-1} to 1098 cm^{-1} and thus, confirmed the interaction between CMC and PVA. Two bands located at 1329 cm^{-1} and 1592 cm^{-1} shown in Figure 4.4(b) correspond to intramolecular forces of the hydroxyl and carboxylate group. Band intensity for both peaks are gradually decreased until E2 and eventually disappear when content of PVA exceeds the 20 percentage composition. The intermolecular forces of H-bonding predominated between the CMC and PVA of the BPe system, where the formation are expected to take place at the region assigned to the bending –OH and asymmetric $–COO^-$ functional group as they are the major indicative bands for the complexation (Cuevas, Heurich, Pauly, Wenzel, & Schön, 2003). (El-Sawy,

El-Arnaouty, & Ghaffar, 2010) has also discovered the complexation to occur within these two regions. Apparently, the absorption band of bending –OH of CMC has shifted from wavenumber 1329 cm^{-1} to 1354 cm^{-1} confirmed the complexation between CMC and PVA.

Beyond sample E3 the peak at wavenumber 1329 cm^{-1} and 1423 cm^{-1} begin to be substituted by wagging –CH of PVA. Another obvious complexation which appears at 1592 cm^{-1} assigned to free carboxylate anion ($-COO^-$) and shifted to 1598 cm^{-1}ascribed by H-bonded carboxylate ($-COO^-$) (W. Wang, Liang, Bai, Dong, & Liu, 2018). We can speculate that the optimum number of hydrogen bond between CMC and PVA has occurred until E2 sample since the pattern was observed from sample E0 until E2 (Durán-Guerrero et al., 2018). Conversely, this carboxylate peaks disappeared when PVA was added progressively beginning from E3 until E6 suggesting the substitution of PVA into the CMC (N. Zainuddin & A. Samsudin, 2018). The appearance of new peak corresponds to C=O stretching at 1740 cm^{-1} was attributable to PVA used in this work which is partially hydrolyzed (~ 85 %). Thus, the carbonyl band was expected to appear around that region (Buraidah & Arof, 2011a; Rajendran, Sivakumar, & Subadevi, 2004). Figure 4.4(c) represents a broad absorption band at the region 3356 cm^{-1} corresponds to free hydroxyl group of CMC. The addition of PVA leads to the formation of hydrogen-bonded hydroxyl groups in the BPe system and causes the band getting narrow and shifted to lower wavenumber, 3326 cm^{-1}. There is a small hump observed at 2943 cm^{-1} due to stretching –CH which experience a shifting to higher wavenumber, 2954 cm^{-1}.

Based on Figure. 4.4(a) and (b), two new shoulder peaks start to appear for E2 sample at 844 cm^{-1} and 1737 cm^{-1} which is referring to vibration of stretching C-C and C=O of PVA with increasing PVA content. The transmittance of the shoulder peak has increased compare to that of the original band with increasing PVA content which gives reflection that complexation has occurred. Based on the analysis, sample E2 showed significant changes through blending method. This explain that composition of 80:20, CMC-PVA BPe system has been complexed with the finest interaction due to the appearance of new peak while retaining the original features of polymers used in this

work. This is expected would lead to improve in the amorphousness and thermal stability of the sample. However, this hypothesis requires further investigation in order to achieve a parallel explanation.

4.2.3 Theoretical Modelling of CMC-PVA

The prominence of IR spectroscopy is to characterize the configuration and conformation structural of polymers to explain the complexation between the bio-polymer blends. The most common complexation in polymer is the hydrogen bonding (H-bonding) which become literally important to change the crystallinity nature of wide range materials. Figure 4.5 presents the calculated IR spectra of CMC and PVA and optimized structure for both compounds and were compared with the experimental ATR-FTIR spectra.

Optimization of the molecular structure is very crucial in most theoretical studies in order to perform further computational analysis (Orio, Pantazis, & Neese, 2009). The DFT calculations could provide structural information of a set of molecule such as polymer with a relatively higher precision of 1-2 % (Cuevas et al., 2003). According to (Scott & Radom, 1996), the DFT able to provide important prediction concerning on the vibrational frequencies of a broad range of molecules with percentage of accuracy of 5-10% which can eventually correlate the ATR-FTIR characterization of the SBE system in this present work. The vibrational frequency of CMC and PVA were determined using single scaling factor, 0.95 (Andersson & Uvdal, 2005). It is worthy to note that the wavenumber measured by the DFT analysis of CMC, PVA and CMC-PVA BPe system are about the same with the ATR-FTIR analysis. This work supports the observations made by previous studies (Andersson & Uvdal, 2005; Awada & Daneault, 2015; Orio et al., 2009; Stratmann, Burant, Scuseria, & Frisch, 1997). The result explicates that DFT calculation may give significant input for comparative studies and the results obtained reflect the overall trend which was observed in FTIR analysis.

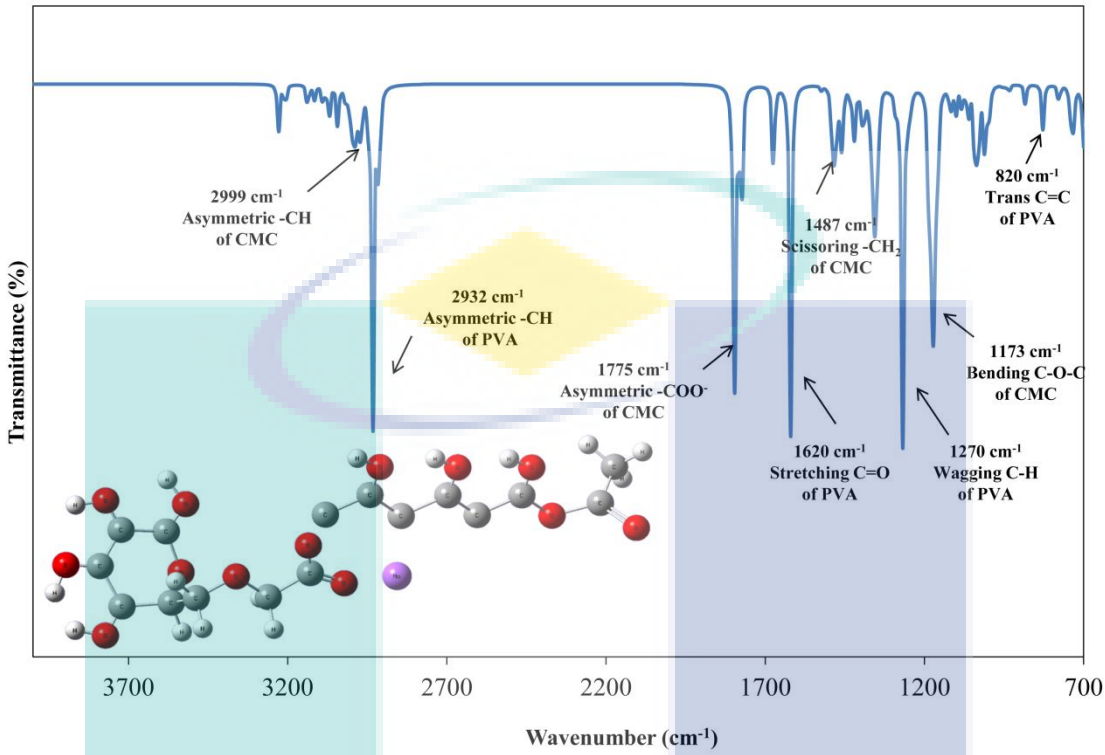

Figure 4 5 Calculated spectra of pure CMC and pure PVA of the BPe system. Inset shows the optimized structure of the CMC and PVA.

(Riaz & Ashraf, 2014) mentioned that the physical properties of polymer blend are influenced by the molecular chain of the polymer. The study on the complexation of the polymer blend electrolyte process can be explained through different types of interaction such as H-bonding and configuration which help to predict the thermal and electrical properties of the SBE system (Daniliuc & David, 1996; Kubo & Kadla, 2003). H-bonding interaction is well known with its diversity and strength (Guo et al., 2010). Xing et al. (Xing et al., 1998) reported that polymers contains the hydroxyl group can be mixed with polyester because of the intermolecular H-bonding resulting in completely or partially miscible system. The finding for the theoretical spectra of the CMC blend with PVA presented in Figure 4.6 shows a similarity in terms of vibrational frequency and modes as reported by previous researchers via experimental works [35, 36, 40, 41]. However, the C-O-C, –COO- and –OH peaks intensity has reduced in comparison to other peaks might suggest the occurrence of complexation in the blend polymer system.

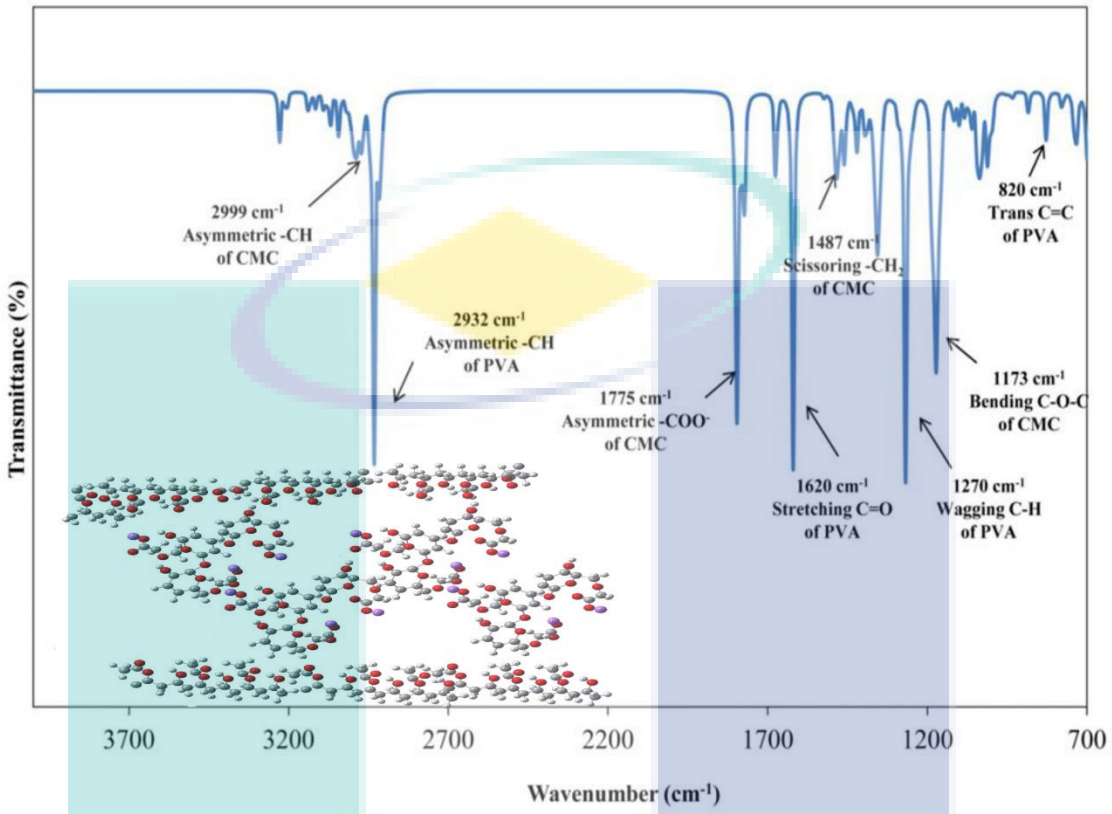

Figure 4 6 Theoretical FTIR spectra of CMC blended with PVA. Inset shows the optimized structure of the CMC-PVA BPe system.

A study conducted by (Michael M. Coleman et al., 1988) revealed that blending two polymers require favorable interaction at active sites such as oxygen and nitrogen which has capability to exert strong forces of attraction (H-bonding). The evaluation of the complexation between CMC and PVA is done based on shift in absorption and change in peak intensity attributed to the disappearance/appearance of peak at specific region.

4.3 X-ray Diffraction (XRD) Spectroscopy

4.3.1 XRD Spectra of Pure CMC and Pure PVA

The understanding about the nature of the host polymer in terms of amorphous or crystalline nature could be revealed by the XRD analysis. Figure 4.7 shows the XRD spectrum of pure CMC and pure PVA at ambient room temperature from 2° to 80°. Three

diffraction peaks for the pure CMC appeared at 2θ, 20.7°, 34.4° and 44.7°. On the other hand, pure PVA has two sharp diffraction peaks at 19.9° and 34.7° correspond to an orthorhombic lattice (110) reflection (Alakanandana, Subrahmanyam, & Siva Kumar, 2016). As observed in the figure, the two polymers applied in this study is generally semi-crystalline materials because of the occurrence both crystalline and amorphous region (Krumova, Lopez, Benavente, Mijangos, & Perena, 2000; Kuutti et al., 2011; Nawaz et al., 2012).

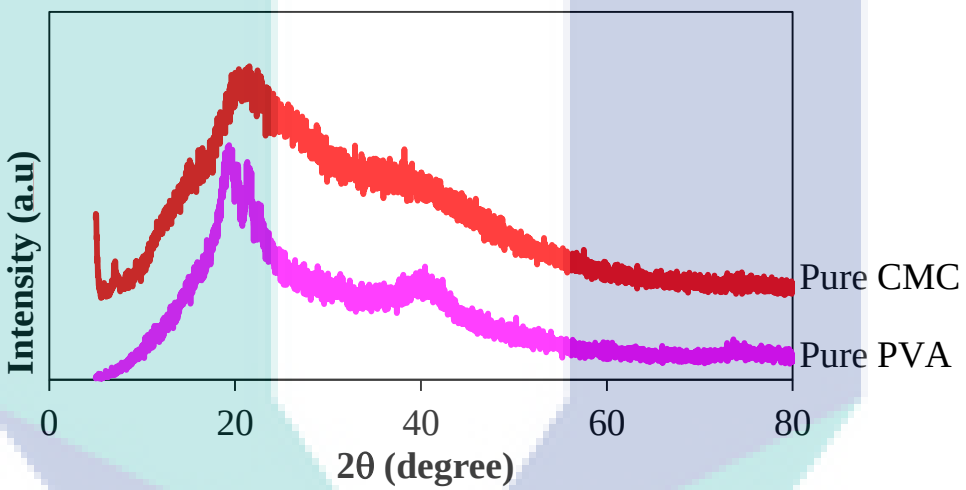

Figure 4 7 XRD spectrum pure CMC and pure PVA

4.3.2 XRD Spectra of CMC-PVA

Molecular modification of the polymer blend into the amorphous character is very essential as it can promote the capability of the ionic motion and allow good complex formation between the polymer blend structure. Figure 4.8 presents the XRD spectra for CMC-PVA polymer blend electrolyte based on various composition. Based on the analysis, the change in amorphousness of CMC (E0) can be seen after the introduction of PVA into the CMC as the diffraction peak becomes less intense. It can be inferred that complexation has taken place between CMC and PVA. On top of that, crystalline peaks correspond to PVA was not present in the sample up to E2 sample and indicating complete dissociation or success of miscibility which suggests greater diffusion and conductance ability (A. Mohamad et al., 2003).Thus, blending method revealed the

success in terms of miscibility and compatibility within the polymer blend based on the change in the intensity and area under the peaks which becomes broadened (C. Ramya, S. Selvasekarapandian, G. Hirankumar, T. Savitha, & P. Angelo, 2008).

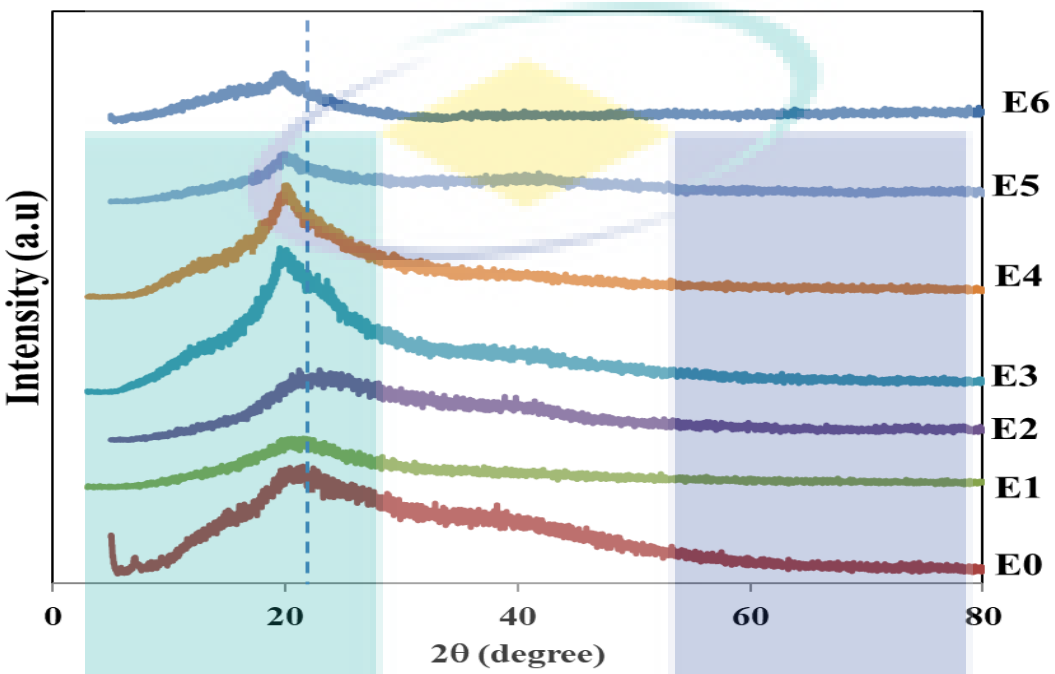

Figure 4 8 XRD spectrum for CMC/PVA SBE system

As discussed in FTIR analysis, the carboxylate anion of CMC has interacted with hydroxyl group of PVA resulting in ion-dipolar complexes which can lessen the polymer chain rigidity and hence decreasing the degree of crystallinity (Stephan & Nahm, 2006). The complexation in CMC/PVA BPe system was expected to occur via intra- or inter-chain hopping between polar functional group of the two host polymer. Consequently, the polymer chain become lack in orderly structure and become more amorphous which could facilitate for higher conductivity. However, the crystallinity of the blend polymer was increased progressively with an increase amount of PVA from E3 until E6 samples which influenced by the nature of PVA since it is more crystalline and affect the interaction between the CMC and PVA.

4.3.3 XRD Deconvolution of CMC-PVA

The extension of XRD analysis is on further investigation of the degree of crystallinity that present in the PBe system. Therefore, deconvolution approach was adopted using Origin Lab 8.0. The baseline function was applied to the specified region. By assuming a Gaussian function, the amorphous and crystalline peaks were deconvoluted, and all peaks were confirmed to fit the original spectrum. After extracting the peak, the area under the peaks was determined, and the percentage of crystallinity and crystallite size were calculated using equations 3.1.

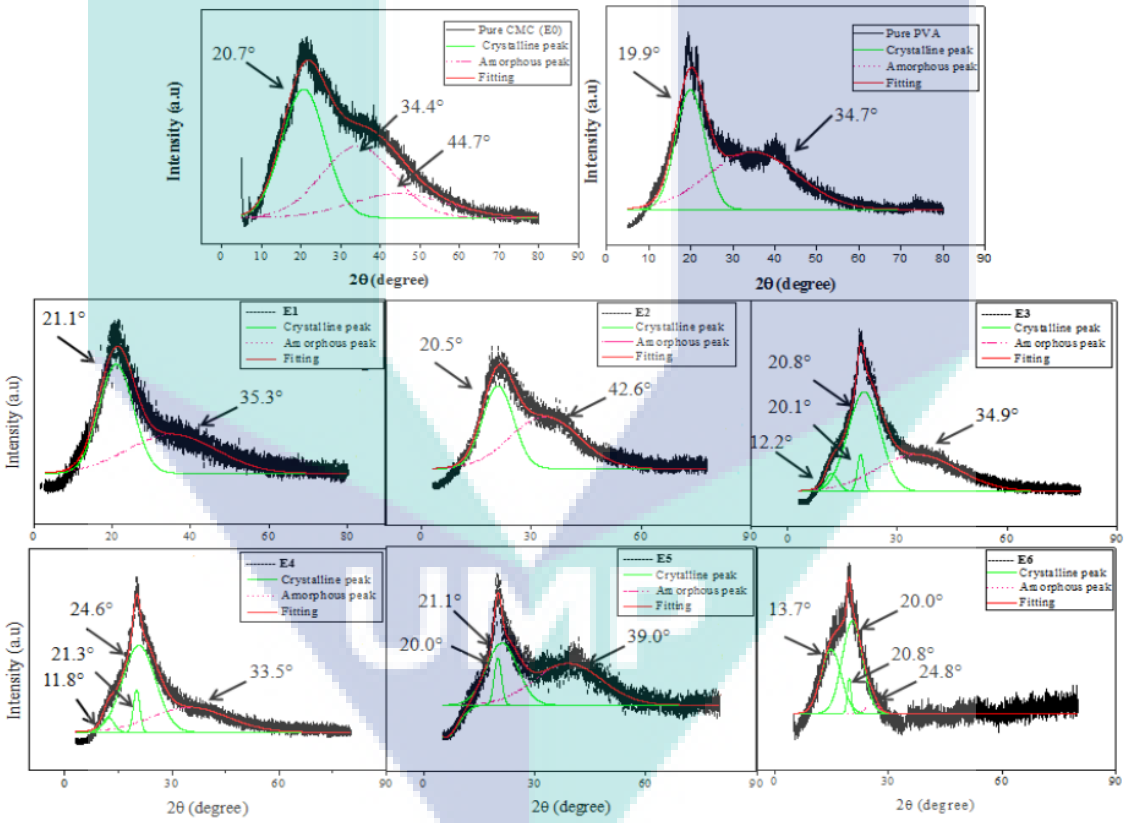

Figure 4 9 Fitting XRD deconvolution for pure CMC, pure PVA and CMC-PVA PBe system

Figure 4.9 demonstrates the XRD deconvolution for BPe system. The figure disclosed two distinct regions of crystalline and amorphous and shown in Table 4.2. Upon the blended of CMC and PVA, we could notice the changes in both regions due to the complexation that has taken place between the two polymers. Based on the calculated

value; sample E2 gives the lowest percentage of crystallinity (more amorphous) which is 16.02 %. The extension study of crystallite size was done using the information of full width half maximum (FWHM) and calculated by using Scherrer equation which further supports the nature of the BPe system studied in this work. The calculated value of crystallite size shown a value of 16.80 ± 0.06 Å, 8.24 ± 0.06 Å, 7.37 ± 0.06 Å and 38.21 ± 0.06 Å for sample E0, E1, E2 and E3, respectively. The incorporation of PVA managed to alter the crystallite size of the BPe system. The calculated value obtained from the deconvolution was in line with the Debye Scherrer relation where the lowest percentage of crystallinity sample possesses the smallest crystallite size which is shown by E2 sample. The increased in amorphous region in the polymer electrolyte ascribed by delocalized complex system that affects the flexibility of the CMC backbone (N. Rasali & A. Samsudin, 2017). Nonetheless, it is obvious that the intensity of E3 increases as more PVA added suggesting that E3 until E6 sample possessed higher degree of crystallinity and larger crystallite size.

Table 4 2 Percentage of crystallinity of CMC-PVA BPe system.

Sample	A_c	A_a	X_c **(%)**
E0	5248.78	7091.87	42.53
E1	5690.20	25532.73	18.22
E2	7044.07	36940.58	16.015
E3	5580.90	4517.37	55.27
E4	4202.45	2420.32	63.45
E5	2642.87	1492.55	63.91
E6	1560.67	217.53	87.77

However, the deconvolution technique offers semi-quantitative evaluation for the amount of crystalline and amorphous of the BPe system which is useful for comparison with experimental result in the XRD analysis (Jenkins & Snyder, 2012; Klug & Alexander, 1974).

4.4 Thermogravimetric Analysis (TGA)

TGA thermogram of CMC-PVA BPe system is shown in Figure 4.10 and the inset was referring to thermogram of pure CMC. The curves elucidate thermal stability of the BPe system which the degradation has completed in three stages. TGA curve of E1 and E2 showed similar pattern to that of pure CMC and had a slower slope. Based on pure CMC curve, the first stage in the range of 25 to 200 °C is associated to loss of water. This first decomposition involved a small weight loss (10-15 %) which is due to the decomposition of hydroxyl group. This result was in agreement with study performed by (El-Sayed, Mahmoud, Fatah, & Hassen, 2011) Pure CMC is hygroscopic (high moisture sensitivity), blending CMC with other polymer able to improve this problem which is clearly shown at the first region.

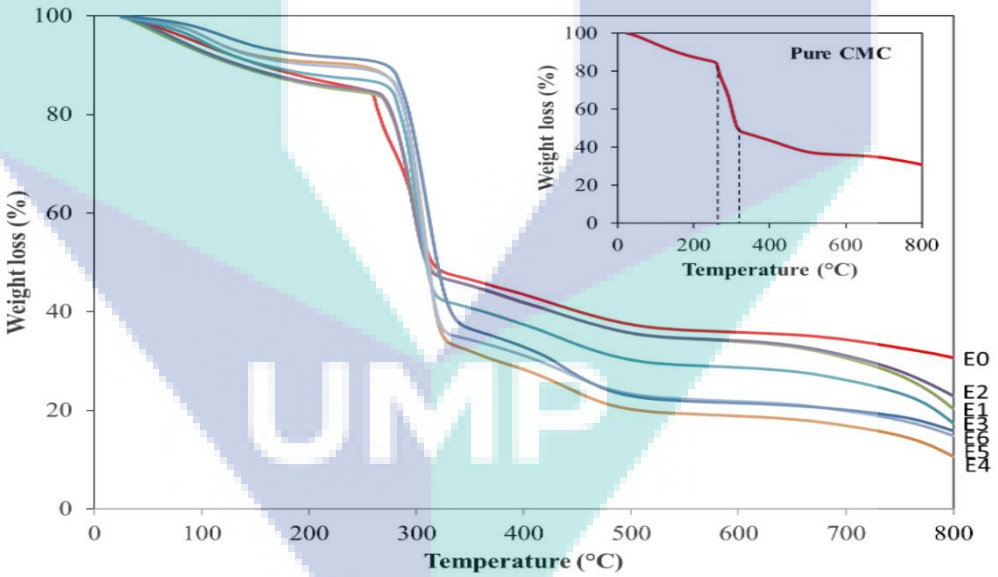

Figure 4 10 TGA thermogram of various CMC-PVA PBe system

The second decomposition showed more significant weight loss in the temperature range 250 to 325 °C. This decrease is because of the degradation of the characteristic structure of CMC which is the carboxylate group that occupies about 20 % of each BPe system (Ibrahim, Adel, El–Wahab, & Al–Shemy, 2011). TGA curve of E0 until E2 showed a slower slope demonstrating high thermal stability whereas E3 until E6

BPe system experience a rapid weight loss which become unfavourable in polymer electrolyte system because of low thermal stability.

According to (Mahdavinia, Massoudi, Baghban, & Shokri, 2014) the decomposition of bond scission in PVA backbone can be found in the range of 318 to 450 °C. Obvious gap in the weight loss has been monitored at this region which is an indication of lower thermal stability with increasing PVA content. The observation reveals that at higher temperature, the disruption of H-bonding in the BPe system has happened for the system containing more than 20 weight percentage (M. Shukur et al., 2014).

Table 4 3 Maximum decomposition temperature of various composition CMC-PVA BPe system

Sample	**Maximum decomposition temperature, T_d (°C)**	**Weight loss (%)**
E0	311.16	48.40
E1	306.83	47.16
E2	305.00	47.09
E3	309.83	50.67
E4	316.67	58.43
E5	318.33	59.82
E6	327.33	57.24

It was noted the final stage which is the plateau region was due to the decomposition of the remaining carbonaceous material and ash formation (Meena et al., 2014). The weight loss of E0, E1 and E2 occurred with slower slope and more plateau compared to E3 until E6 again confirming the thermal stability of BPe system with less

than 20 weight percentage of PVA. Table 4.3 shows the maximum decomposition temperature (T_d) for all BPe system study in this work. The data revealed that E2 sample showed the least weight loss could be attributed to the enhancement of interaction and amorphous phase of the CMC-PVA as explained by FTIR and XRD analysis and led to enhance the thermal stability. Based on the observations, it shows the present sample is a promising to be act as polymer host in electrolyte system where can stand at higher temperature above 90 °C.

4.5 Differential Scanning Calorimetry (DSC)

Thermogram of DSC shows heating run for various composition CMC-PVA BPe system up to 300 °C and presented in Figure 4.11. Based on the thermogram, there are two endothermic peaks observed which correspond to glass transition and melting phase transition.

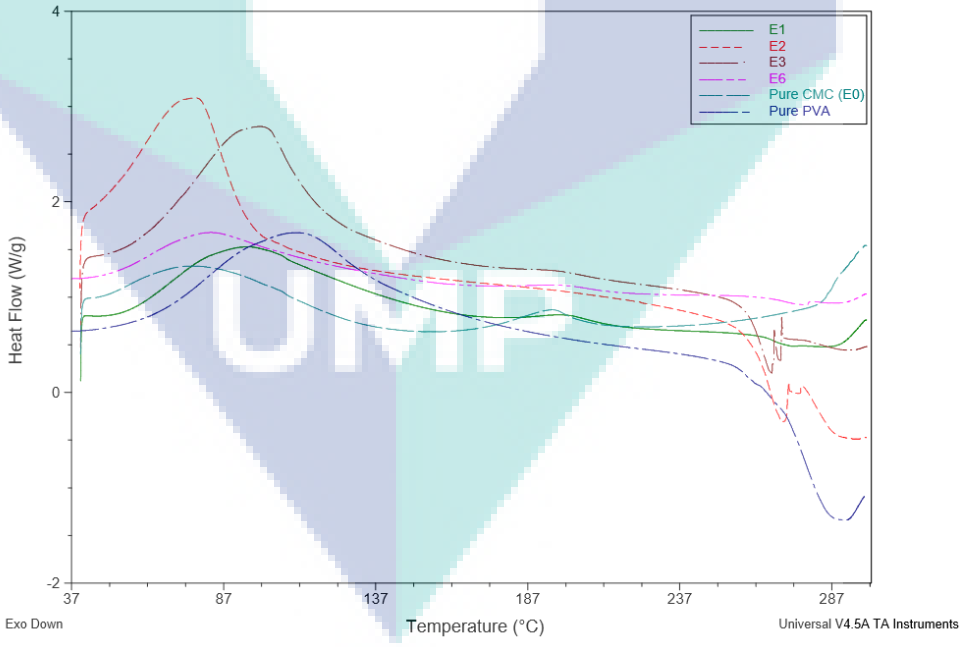

Figure 4 11 DSC thermogram for various composition CMC-PVA BPe system

The information on physical parameters of glass transition temperature (T_g) explain the degree of purity and nature of the substance (Guirguis & Moselhey, 2012). The glass and melting temperature of the BPe system is listed in Table 4.4. Obviously, thermal transition of CMC varied after the incorporation of PVA at different composition. Broad endothermic peaks around 47 to 73 °C and 170 to 184 °C is referring to T_g and T_m of semi-crystalline (El-Sayed et al., 2011) . These observations signify the compatibility between the CMC and PVA which is mainly due to the characteristic of hydroxyl and carboxylate anion group that facilitate the interaction via H-bonding and the result also shows agreement with other report (Abd El- Kader, Shehap, Abo- Ellil, & Mahmoud, 2005; El-Kader, Gaafar, Mahmoud, Bannan, & El-Kader, 2008; El-Sayed et al., 2011). According to (Andreev & Bruce, 2000), T_g is crucial in determining the characteristic of polymer chain in terms of segmental motion that enhance the conductivity.

Table 4 4 Glass and melting phase transition of CMC-PVA BPe system.

Sample	**Glass phase transition**		**Melting phase transition**	
	T_g **(°C)**	ΔH **(J/g)**	T_m **(°C)**	ΔH **(J/g)**
Pure CMC (E0)	55.3	62	173	23.1
Pure PVA	89.7	374	-	-
E1	71.6	236	182	9.12
E2	47.4	174	-	-
E3	73.2	362	181	2.27
E6	60.8	215	184	3.48

The value of T_g decreases to the lowest temperature of 47.4 °C with enthalpy, ΔH of 174 J/g for E2 samples suggesting that the flexibility increases in the CMC/PVA BPe system chain. This suggests the present sample E2 is suitable to act as host polymer in the further expansion of polymer electrolytes system. However, upon the addition of more PVA, the T_g increases as the H-bonding interaction between CMC and PVA become stronger. This result is also in accordance with (Lin, Ito, & Yokoyama, 2017) which states

that H-bonding and T_g is directly related in qualitatively. However, the value of T_g observed for sample E3 and E6 is not quite consistent with the percentage of crystallinity discussed in XRD previously. At higher composition of PVA, optimum number of intermolecular hydrogen bonding leading to more disturbance in the order of PVA molecular chains and creating some free volumes. In 2010, (Napolitano, Pilleri, Rolla, & Wübbenhorst, 2010) pointed to some of the ways in which the presence of free volume could further contribute in the reduction of T_g. This finding corroborates with those of other studies who worked on blending system of polymer which discovered similar inconsistent trend where the discrepancy might be attributed to the interaction between two polymers via inter-molecular H-bonding that could lead to stiffening molecular chain and hence affecting the thermal transition to lower value for sample E6 in comparison to sample (Bao et al., 2018b; Saroj, Krishnamoorthi, & Singh, 2017; S. Wang & Min, 2010).

4.6 Electrical Impedance Spectroscopy (EIS)

4.6.1 Cole-Cole Plot

Figure 4.12 depicts the Cole-Cole plot of CMC-PVA based BPe films at room temperature. The Cole-Cole plot of BPe containing 0, 10, 20, 30 and 40 percent composition of PVA showed by Figure 4.12 (a-e) shows an incomplete semicircle curve. Two regions could be observed as semicircle at high frequency and spike at low frequency. These impedance plots are frequently used to separate the electrical polarization that affects the selected impedance frequency and the impedance of bulk material as reported earlier.

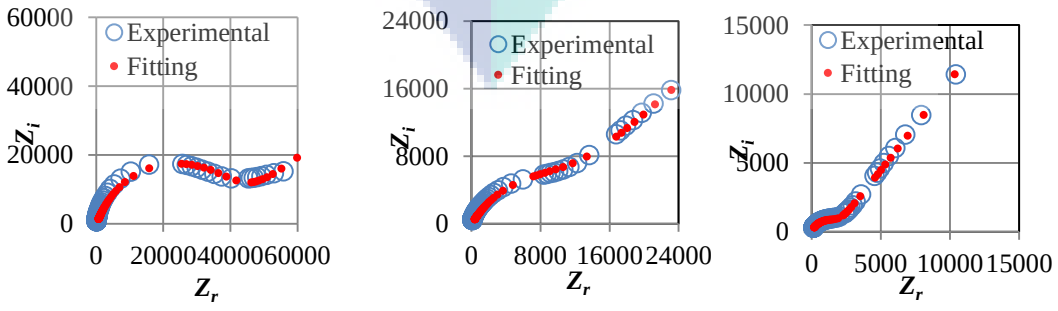

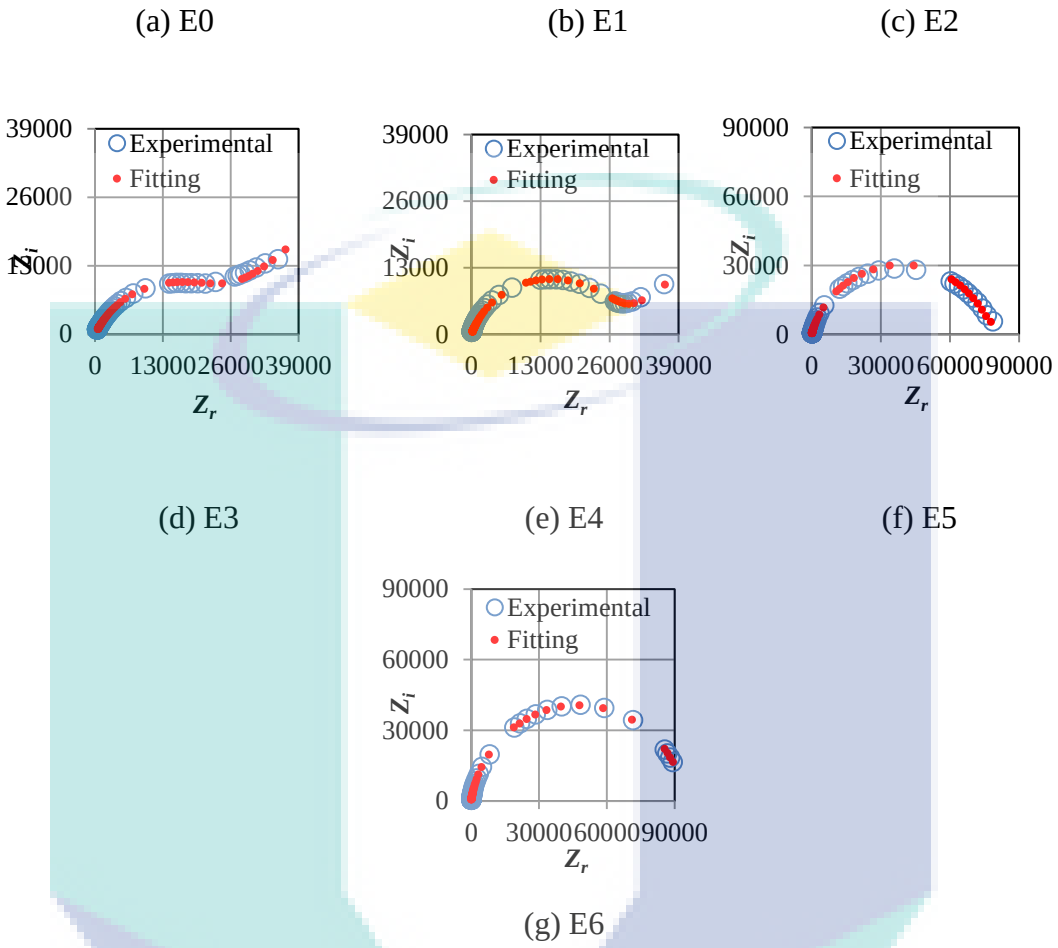

Figure 4 12 Cole-Cole plot of CMC-PVA based bio-polymer blend electrolytes system for composition (a) E0 (b) E1 (c) E2 (d) E3 (e) E4 (f) E5 (g) E6.

In this work, the impedance data for the shows semicircle and spike that can be represented by a parallel combination of bulk resistance (R_b) and constant phase element (CPE). The R_b was determined based on the interception between higher and lower frequency from the Cole-Cole plot of complex impedance [22-23]. CPE was utilized in a model to replace the capacitor to balance the heterogeneity of the BPe system studied in this work. The impedance of CPE (Z_{CPE}) can be represented by the following equation:

$$Z_{CPE} = 1/k(j\omega)^p \text{ where } 0 \leq p \leq 1 \quad (4.1)$$

Or

$$Z_{CPE} = k\,[\cos(p\pi/2) - j\,\sin(p\pi/2)]\,/\omega^{p} \tag{4.2}$$

Variable of k^{-1} corresponds to the capacitance value of the CPE element, ω is the angular frequency where, $\omega = 2\pi f$ (f is frequency), and p is referred to the deviation of the vertical axis in the Z_r versus Z_i plot. The values of Z_r and Z_i associated to the equivalent circuit can be termed as follows:

$$Z_r = \frac{R_b + R_b^2 k_1^{-1} \omega^{P_1} \cos(\frac{\pi p_1}{2})}{1 + 2R_b k_1^{-1} \omega^{p} \cos\left(\frac{\pi p_1}{2}\right) + R_b^2 k_1^{-2} \omega^{2p_1}} + \frac{\cos \pi p_2/2)}{k_2^{-1} \omega p_2} \tag{4.3}$$

$$Z_i = \frac{R_b^2 k_1^{-1} \omega^{P_1} \sin(\frac{\pi p_1}{2})}{1 + 2R_b k_1^{-1} \omega p_1 \cos\left(\frac{\pi p_1}{2}\right) + R_b^2 k_1^{-2} \omega^{2p_1}} + \frac{\sin \pi p_2/2)}{k_2^{-1} \omega p_2} \tag{4.4}$$

Table 4.5 lists the parameter of the circuit elements for all BPe composition studied at room temperature. The formation of semicircle could be explained by the occurrence of a capacitor and a resistor, which is in parallel series. Meanwhile, an inclined spike was due to the effect of electrode polarization, which is the characteristic of ions diffusion process for the bio-polymer blends electrolyte system. This diffusion happens among ions when PVA was incorporated into CMC and causes the insulating properties start to change into semi-conducting material. As shown in Figure 4.12 (c-f), when PVA was incorporated into the CMC the tilted spike has inclined at an angle lesser than 90° along the real axis which might be attributed to heterogeneity between the electrode-biopolymer electrolyte interface and resulting to a decrease in ionic conductivity. These result support previous research conducted by (Samsudin & Isa, 2014), which has explained on the electrical properties of CMC, doped with NH_4Br.

Figure 4.12 (f) and (g) shows the only semicircle curve after the addition of more than 50 percent composition of PVA into the BPe system. This is directly related to the bulk resistance and bulk capacitance of the BPe system. The part of semicircle shown in the Cole-Cole plot can be demonstrated as a parallel resistor attributed to the movable

ions inside the polymer matrix and capacitor due to the motionless polymer chain circuit network. The addition of more PVA in C5 until C7 will destruct the dielectric polarization and lead to greater hindrance to the polymer resulting in an increase in R_b and decreasing the ionic conductivity.

Table 4 5 List of parameters of circuit elements for all BPe system composition at room temperature

Sample	**p_1 (rad)**	**C_1(F)**	**p_2 (rad)**	**C_2 (F)**
E0	0.850	5.5×10^{8}	0.430	5.58×10^{5}
E1	0.775	4.56×10^{8}	0.495	9.90×10^{5}
E2	0.745	5.82×10^{7}	0.585	1.44×10^{6}
E3	0.749	9.60×10^{7}	0.499	8.35×10^{5}
E4	0.810	1.40×10^{8}	0.472	2.05×10^{5}
E5	0.839	2.60×10^{8}	-	-
E6	0.901	8.85×10^{8}	-	-

4.6.2 Conductivity at Room Temperature

Conductivity measurement is conducted in order to reveal the effect of SBE system by addition of PVA into the CMC. Based on the previous analysis, the crystallinity of the BPe system has reduced upon the incorporation of the PVA which was proven by the XRD analysis. In conjunction to these results, the conductivity of the BPe system was further investigated. The conductivity values of BPe system are illustrated in

Figure 4.13 and showed the increasing of conductivity when CMC blended with PVA. The plot shows that sample E2, with composition of 80:20 is the optimum composition for this present work with conductivity ta room temperature is $(9.12 \pm 0.04) \times 10^{-6}$ S/cm. This increment was due to higher amorphous phase and lowest weight loss which was confirmed from XRD and TGA analysis.

PVA is well known with its chain flexibility allowing random intra- and inter-molecular attraction forces between the host polymers which can promote the segmental motion which can increase the chain mobility and hence increasing the conductivity (Prajapati, Roshan, & Gupta, 2010). This is supported by the XRD analysis where crystallinity phase has decreased until sample E2 and hence increasing the conductivity. (Rajeh, Morsi, & Elashmawi, 2019) in his study about the enhancement of spectroscopic and electrical properties of polyethylene oxide/carboxymethyl cellulose blends revealed the increase in amorphous of polymer blend could increase the electrical conductivity. This result also supported by DSC where T_g becomes lower and fasten the chain mobility and hence increasing the conductivity. It can be seen that upon the addition of PVA above 20 % in CMC, the conductivity starts to decrease to a lower value. This can be due to reappearance of crystal peak where huge amount of PVA can trigger the improvement in crystallization of SBE system (Assender & Windle, 1998). Furthermore, excess amount of PVA causes rapid weight loss due to the weak interaction between the CMC and PVA as revealed by FTIR and TGA.

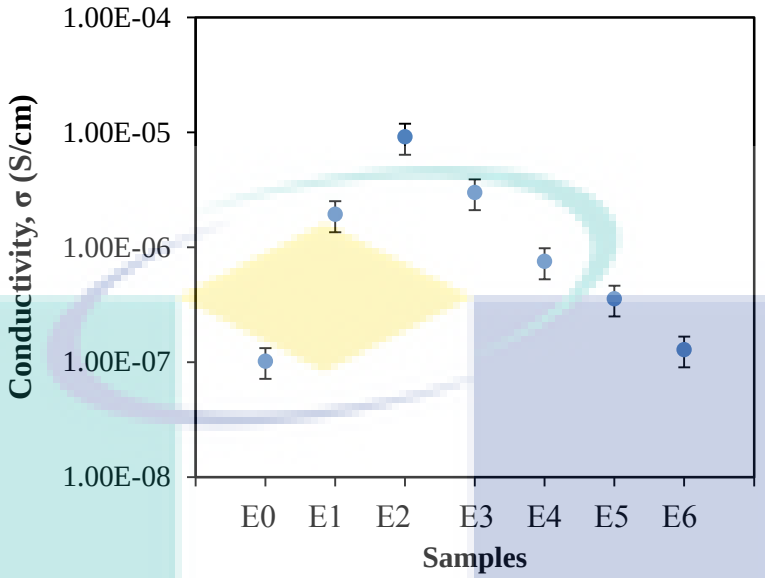

Figure 4 13 Variation plot of conductivity as a function of percentage of PVA incorporate into CMC

The finding reveals that CMC-PVA BPe system possessed relatively higher conductivity as compared to single polymer and also polymer blend as electrolyte systems. Therefore, this present system conveys that the CMC-PVA BPe system is a promising candidate to act as a host for polymer electrolytes system in electrochemical applications. (M. Hafiza & Isa, 2014; Hema, Selvasekerapandian, Sakunthala, Arunkumar, & Nithya, 2008; Isa & Samsudin, 2016; Joge, Kanchan, Sharma, & Gondaliya, 2013; R. Singh et al., 2014)

4.6.3 Electrical Properties Study

The dielectric properties may vary in different types of polymer electrolyte system attributed to several factors including frequency of applied electrical field, temperature, structural characteristics or other external factors. Figure 4.14 (a) and (b) shows the frequency dependence of the real part of the dielectric constant (ε_r) for all composition of CMC-PVA which is also known as stored charge in any material. In the studied range of frequency of 50Hz to 1 MHz, it can be observed ε_r and ε_i increases sharply from low frequency contributed by electrode, molecular and ionic polarization. The dielectric

constant, ε_r was found to increase for the sample E2 which indicated that charge carrier concentration has increased in the space charge accumulation area and later increasing the conductivity (Sudhakar & Selvakumar, 2013). Sample E2 shows the highest value of ε_r may be due to an increase in the heterogeneity in the polymer blend which could increase the free volume. At high frequency, both dielectric properties were showed decreasing trend explained the decreasing rearrangement of dipolar groups and polar segments of the polymer which is no longer capable to react to the applied electric field hence causes electrical relaxation process to happen (Chai & Isa, 2013).

Modulus formalism is important to analyze the ionic conductivity or in further analysis as the loss peak could not be detected in the dielectric loss spectrum. It is a useful application to analyze the electrical response and relaxation of polymer electrolyte system. The real (M_r) and imaginary (M_i) part of complex modulus are derived from their complex permittivity and shown in Figure 4.15. In Figure 4.15 (a), the M_r values were increased proportionally with the increase of frequency. According to (Ramesh & Chai, 2007), the non-zero values of M_r at low frequency suggest that the BPe system was negligible from electrode polarization. Plot of imaginary modulus (M_i) able to evaluate the effect of the smallest capacitance and the largest resistance, hence determine the relaxation process attributed to short or long-range movement of charge carrier. The occurrences of relaxation peaks in the M_i plots in Figure 4.15(b) reveals the characteristic of the SBE system as ionic conductors. The peak position and height of E0 sample at high frequency can be distinguished from other samples in both M_i and M_r spectrum may be due to the bulk effect as CMC is exceptionally stiff which in turn resulting to a decrease in chain mobility. This peaking curve also attributed to the relaxation phenomenon in the polymer electrolyte system.

Compared with CMC, the CMC-PVA based BPe contribute much more to the M_r of the blend, which becomes broadening and lowering down which means that stiffness of CMC has decreased as PVA was added (N. A. Zakaria et al., 2010). At lower frequency, there was a large association between the values of capacitance with electrodes which can be seen by a plateau peak for M_r and this present work result was

in agreement with work done by (Ahmad Salihin Samsudin et al., 2011). Thus, this confirmed that the behaviour of the PBe system work in this study is non-Debye.

Figure 4.16 illustrates the variation of real modulus (M_r) and imaginary modulus (M_i) parts of electrical modulus for the highest conductivity sample containing 80:20 compositions of CMC-PVA (E2). Both figure 4.16 (a) and (b) show long tails at lower frequency indicating that no relaxation peaks at that region. Figure 4.16 (a) shows an increasing trend at higher frequency with no definitive peaks. In addition, the highest peak frequency of the highest conducting BPe sample, E2, presented in Figure 4.16 (b) which was corresponding to the shortest relaxation time (Fadzallah, Noor, Careem, & Arof, 2016). Accordingly, the relaxation time decreases as temperature increases. At higher temperature the ion mobility of the polymer chain has increased and hence increasing the conductivity. This result also supports the work done by (Pradhan, Choudhary, & Samantaray, 2008).

Dielectric loss tangent (tan δ) spectrum of CMC-PVA in Figure 4.17 depicts the dielectric relaxation process which is derived from the ratio $\varepsilon_i/\varepsilon_r$. Sample E0 until E4 exhibits a relaxation peak at high frequency corresponding to the conductivity relaxation process, whereas sample E5 and E6 decreased sharply from lower to higher frequency. The dielectric and conductivity relaxation was evaluated by the reorientation process of dipolar molecules in the polymer which is represented by a peak in the tangent dielectric loss spectrum. The highest conducting sample, E2 exhibits the shortest relaxation time at higher frequency due to the increasing number of segmental motion. Meanwhile slower relaxation process was indicated by higher PVA composition more than 50 percent composition which gives reflection to a lower conductivity. Figure 4.18 presented the plot of tan δ versus log frequency. The trend was clearly observed where tan δ shifts to higher frequency and the height of the peak also increased when temperature increased. Based on the plot of tan δ, the relaxation time, τ can be determined by using the following equation:

$$\tau = 1/\omega_{peak} \qquad (4.5)$$

where ω_{peak} is the angular frequency of the relaxations peak. The temperature dependence of relaxation time for E2 BPe is shown by figure 4.19 with regression value (R^2) of 0.9764. The plot shows good linearity and confirms the conductivity of temperature dependence of the present work BPe system follows the Arrhenius law. The effect of temperature also suggests that there was no phase transition in the BPe containing 80:20 composition of CMC-PVA.

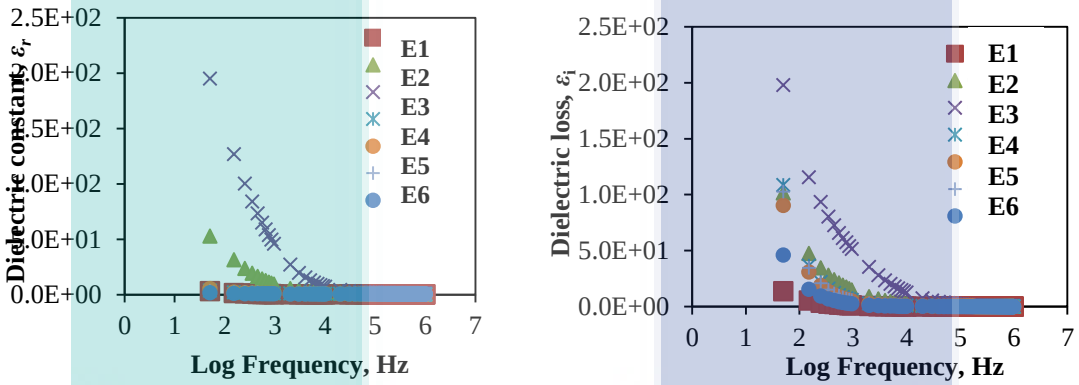

(a) (b)

Figure 4 14 Frequency dependence of (a) dielectric constant (b) dielectric loss for various composition of CMC-PVA at room temperature, 303 K.

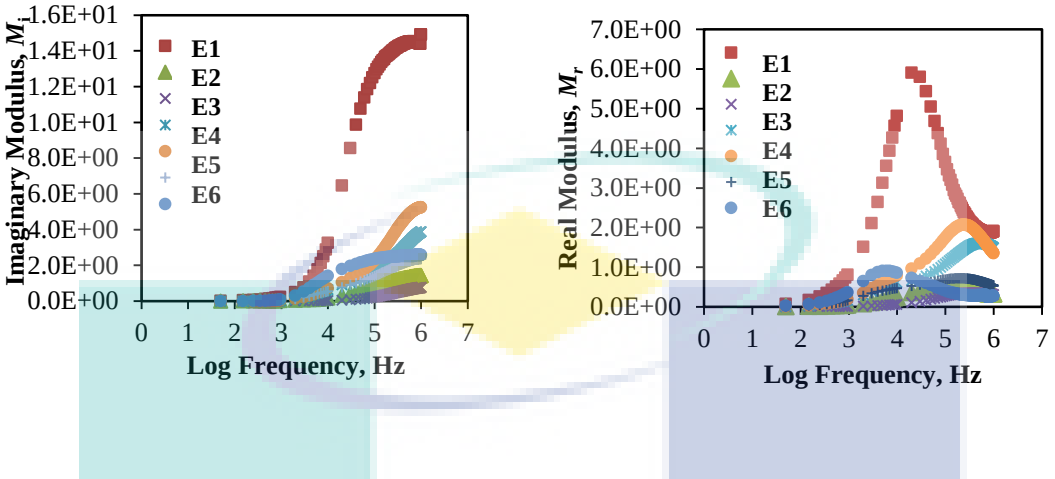

(a) (b)

Figure 4 15 Frequency dependence of (a) real modulus (b) imaginary modulus for various composition of CMC-PVA at room temperature, 303 K.

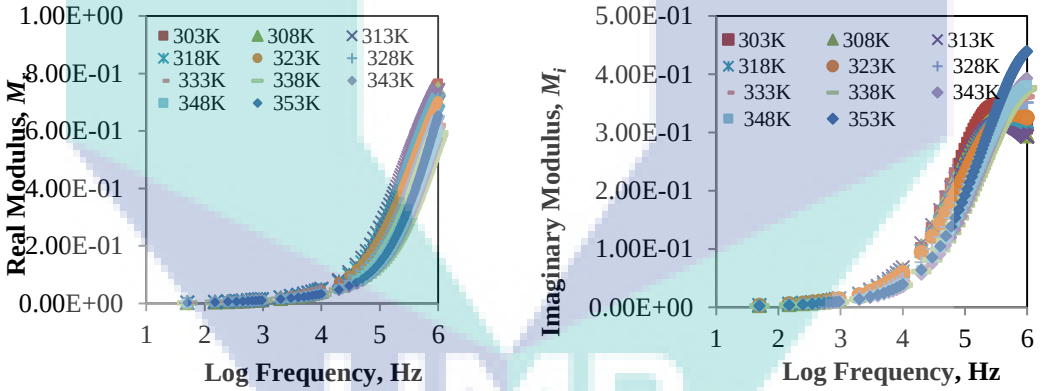

(a) (b)

Figure 4 16 Frequency dependence of (a) real modulus (b) imaginary modulus for the highest conductivity CMC-PVA (E2) at different temperature.

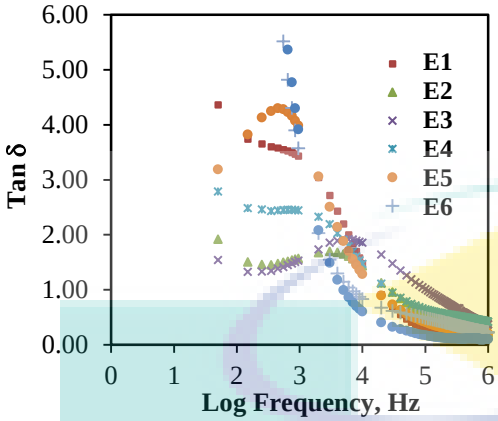

Figure 4 17 The dependence of tan δ on frequency for all compositions of CMC/PVA.

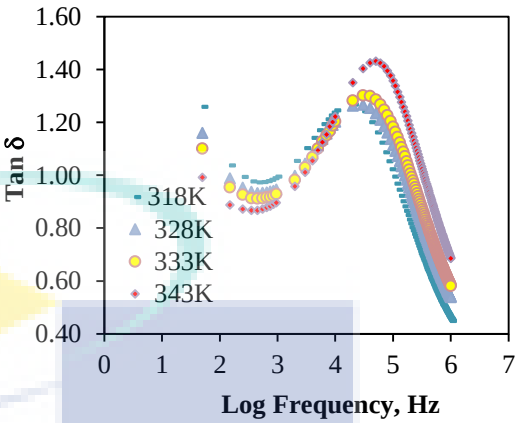

Figure 4 18 The dependence of tan δ on frequency of the highest conductivity CMC/PVA (E2) at different temperature.

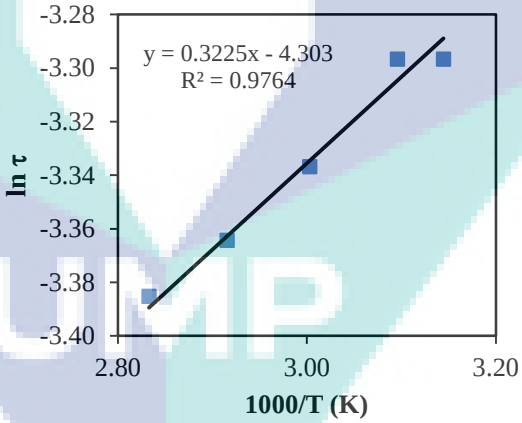

Figure 4 19 The temperature dependence of relaxation time of highest conductivity CMC-PVA (E2).

CHAPTER 5

RESULTS AND DISCUSSION OF POLYMER BLEND-SALT COMPLEX

This chapter discussed results obtained from all the characterization used in this work including the structural and thermal properties of CMC-PVA-NH_4Br biopolymer electrolytes system using Fourier Transform Infrared (FTIR) Spectroscopy, X-ray diffraction (XRD), Differential Scanning Calorimetry (DSC) and Thermo Gravimetric Analysis (TGA). The ionic conduction properties of biopolymer electrolytes system measured via Electrical Impedance Spectroscopy (EIS) and Transference Number Measurement (TNM) and also investigated in this chapter. A further evaluation on performance of solid biopolymer electrolytes system in electrical double layer capacitor (EDLC) via Linear Sweep Voltammetry (LSV), Cyclic Voltammetry (CV) and Galvanostatic Charge-Discharge (GDC) has been explained in this chapter. All the findings in this work is compiled and supported each other following reference from previous work in order to achieve objective 2, 3 and 4.

5.1 Appearance of Blend Polymer Electrolyte

The solid biopolymer electrolytes (SBEs) thin film system based polymer blend CMC-PVA doped with various amount of NH_4Br has been successfully prepared via casting method. The physical appearance of SBEs shows transparent thin film, flexible and free standing as presented in Figure 5.1. These excellent appearance help SBE system properties to show good compatibility with electrodes, ease the

fabrication process, no leakage, low self discharge and elastricity. All the SBE system give the thickness at range of 0.0285 to 0.0696 cm.

Figure 5 1 Solid biopolymer electrolyte thin film.

5.2 Fourier Transform Infrared Spectroscopy Analysis (FTIR)

Infrared radiation is broadly to the part of the electromagnetic spectrum between the visible and microwave regions. Wavenumber region of 4000 to 700 cm^{-1} is believed the great practical use (Ramesh, Leen, Kumutha, & Arof, 2007). FTIR spectroscopy is one of the most important instrument in order to investigate the polymer structure in polymer electryte backbone.

5.2.1 Pure Ammonium Bromide

The FTIR spectra of pure NH_4Br has illustrated in Figure 5.2. A broad intensity band at 3133 cm^{-1} is due to asymmetric stretching vibration of ammonium ion. According to (Ramlli & Isa, 2016) reported that the N-H stretching mode were

detected at ~3176 cm^{-1} and ~3028 cm^{-1}. (Kadir, Aspanut, Majid, & Arof, 2011) also support at that band corresponds to NH_4^+ asymmetric and symmetric vibration mode.

Meanwhile, sharp intense absorption observed at 1402 cm^{-1} were identified as bending mode of N-H. A similar band was also reported by (Samsudin, 2014) and according to (Nik Aziz et al., 2010), NH_4^+ plays important role and influential in functional group to acts as proton donor in present electrolyte. The NH_4^+ ions of NH_4Br are coordinated to the O atom of the ether and to the O-H group in polymer blend CMC-PVA. These interaction will prove that protonation happens and it is visible in the shifting of the funtionl group peaks.

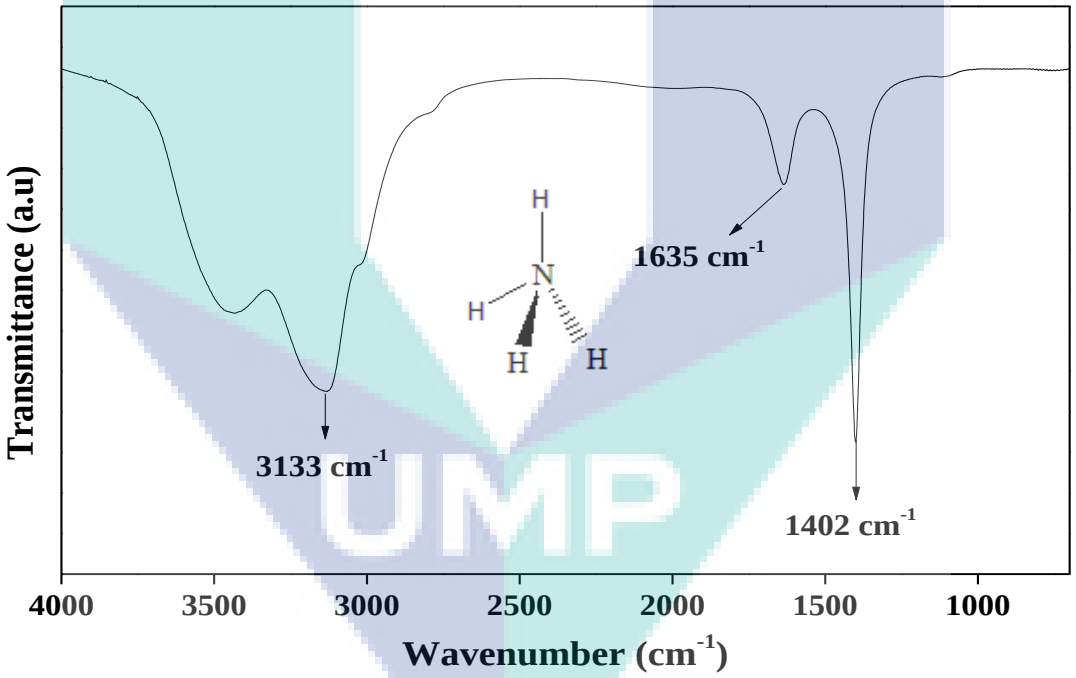

Figure 5 2 FTIR spectra of pure ammonium bromide.

5.2.2 Solid Biopolymer Electrolyte Systems (SBEs)

Infrared spectral analysis also has been used in order to analyse the interactions occurred between atoms and ions in biopolymer electrolytes system. The IR spectra for

polymer blend CMC-PVA doped with various amount of NH_4Br was demonstrated in Figure 5.3. The regions have been divided in 2 regions at 2200 to 900 cm^{-1} and 4000 to 2700 cm^{-1} as plotted in Figure 5.3(a) and 5.3(b), respectively. Based on Figure 5.3(a), the characteristic vibrational band at 1057 cm^{-1} is assigned to ether linkage (C–O–C) stretching vibration of pure CMC (A. Samsudin, H. Lai, & M. Isa, 2014), and slight shift from higher to lower wavenumber was observed from 1057 to 1049 cm^{-1} after the incorporation of NH_4Br. Shift in wavenumber is expected at region 1057 cm^{-1} due to the presence of oxygen which is known as highly electronegative atom from the C-O-C group create an opportunity for the interaction to happen between CMC with added PVA and NH_4Br which may affect the ionic conductivity and crystallinity of present system (N. Rasali & A. Samsudin, 2017). Meanwhile, the functional group of hydroxyl (-OH) with bending vibration was observed at wavenumber of 1323 cm^{-1}. According to (Dai, Huang, & Huang, 2017) and (Dai & Huang, 2017) has reported this band at 1322 cm^{-1} and 1320 cm^{-1}, respectively. Apparently, peak intensity of this group has decreased and shifted to the higher wavenumber at 1325 cm^{-1} upon the addition of NH_4Br. This phenomenon may be explained by the substitution of –OH group with proton (H^+) from NH_4Br to form H-OH in the present system (N. H. Ahmad & M. I. N. Isa, 2016a). Similar behaviour was observed from other research worked by (A. Samsudin et al., 2014) where the shifting in wavenumber occurred when amount of salts increase which could be attributed to the coordination of NH_4^+ ion with polar group present in polymer blend CMC-PVA when NH_4Br was added.

Another obvious complexation can be observed in Figure 5.3(a), the sharp intense absorption at 1590 cm^{-1} corresponds to C=O of COO^- stretching was shifted to the lower wavenumber 1581 cm^{-1} due to the lone pair electron possessed by oxygen will attract NH_4Br molecule to be attached to it and hence induce the protonation process (N. H. Ahmad & M. I. N. Isa, 2015b). In addition, it can be seen that the peaks start to disappear when amount of NH_4Br was added up to AB15 and then slowly shows the appearance of peak at AB25. This phenomenon is believed due to the coordination interaction of COO^- functional group in polymer host and H^+ from NH_4^+ which reflect the protonation between cation and carboxylate group of polymer blend CMC-PVA.

(Mejenom et al., 2018) also support the finding that the peak shifting occurred might be due to the formation of dative bond between H^+ from NH_4Br and nitrogen or oxygen coordinating position in the host polymer blend. It can be noted here that the concentration of H^+ increases with the increasing amount of NH_4Br and thus create more ions to be migrated towards host blend polymer backbone. This migration drives the ions hopping from one site to another site via formation of H-bonding (M. Shukur et al., 2014). The interaction process occurs through structure diffusion (known as Grotthus mechanism) where the ions exchange happens between the complexed sites (Hema et al., 2008). Since this SBE system uses ammonium salt as dopant agent, proton migration (H^+) mechanism is more possible due to the following explanation where two of the four hydrogen atoms of NH_4^+ ions are bound identically, one hydrogen is bound more strictly and the fourth more weakly. The weakly bond H of NH_4^+ can be dissociated more easily and these H^+ can hop from one site to another leaving a vacant site which will be filled by another H^+ ion from a neighbouring site (Du, Bai, Chu, & Qiao, 2010; Kadir et al., 2011). Since this present work used PVA which is partially hydrolysed therefore, there is appearance of new shoulder peak at wavenumber 1712 cm^{-1} belongs to C=O stretching in the acetate group of PVA when AB20 was introduced into the present work (J.-C. Park et al., 2010). However, the peak start to disappear after 25 wt. % of NH_4Br was added in the complexes and appear again at AB35. According to Ramlli et al. (M. Ramlli et al., 2015) & Rajendran et al. (Rajendran et al., 2003), the position and intensity of polar group of polymer is expected to change due to the interaction between the proton (H^+) ion from ammonium salt with the host polymer. This attracts more electrons to CMC-PVA through C=O to form hydrogen.

Based on Figure 5.3(b), there are two peaks observed represented by C-H stretching and O-H stretching. It can be observed the stretching C-H at 2919 cm^{-1} which believed belongs to CMC-PVA has shifted to lower wavenumber and the peak become strong. Later, after the addition of 30 wt. %, the peak become broadened and shift to lower wavenumber. In addition, there is new peak is noticed beyond 30 wt. % NH_4Br in the SBEs system at 3206 cm^{-1} and 3218 cm^{-1} which might be attributed to the presence of asymmetrical N-H stretching from NH_4Br that entrapped in biopolymer

blend thus expected to increase in transport properties. It can be interpreted that ion re-associate and form ion aggregates, resulting the decrement of ionic conductivity in the present system. Similar behaviour has been reported by other similar research work where it is believed the H^+ originate from ammonium salts start to overcrowded when added with vast amount of dopant (N. H. B. Ahmad & M. I. N. B. M. Isa, 2015; Kamarudin & Isa, 2013). The broad band at 3316 cm^{-1} corresponding to O-H stretching is detected in Figure 4.4(b). Upon addition of NH_4Br, the hydroxyl band shifted to higher wavenumber of 3320 cm^{-1} at AB25 which might due the polymer blend of CMC-PVA has interacted with NH_4Br at the O-H band. According to (El-Sawy et al., 2010) and (Krimm, Liang, & Sutherland, 1956), band at 3316 cm^{-1} was correspond to the O-H stretching absorption generated from PVA which has been blended with CMC. When the concentration of 25 wt. % was added into the present system, the wavenumber shifted to higher wavenumber at 3375 cm^{-1}. (M. Shukur et al., 2014) reported that the interaction between starch and chitosan has interacted with NH_4Cl at the O-H group. This phenomenon can be explained in the present work associated with the coordination of NH_4^+ ions with polar groups found in CMC-PVA when NH_4Br is introduced into the system. The shifting in wavenumber for all SBEs system-based CMC-PVA doped with vary amount of NH_4Br at different functional group were summarized in Table 5.1. Based on the elucidation, it is believed that proton H^+ from NH_4^+ have interact with the oxygen from polymer blend CMC-PVA as proposed in Figure 4.5.

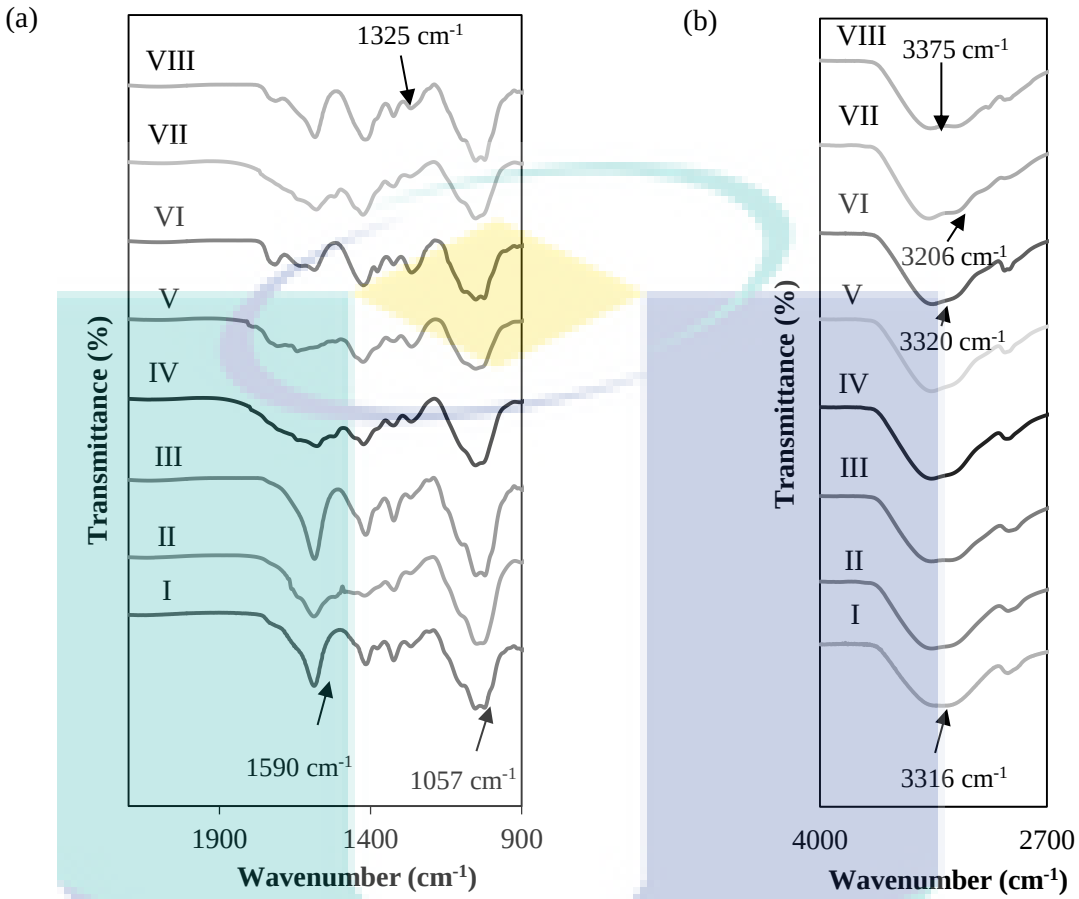

Figure 5 3 (a) and (b) FTIR spectra of (I) AB0, (II) AB5, (III) AB10, (IV) AB15, (V) AB20, (VI) AB25, (VII) AB30 and (VIII) AB35.

Samples	**The functional group (wavenumber, cm^{-1})**						
	C-O stretching	**O-H bending**	**COO^- stretching**	**C=O stretching**	**NH_4^+ stretching**	**C-H stretching**	**O-H stretching**
AB0	1057	1320	1590	-	-	2919	3316
AB5	1048	1328	1588	-	-	2910	3316
AB10	1044	1325	1588	-	-	2900	3317

AB15	1048	1322	-	-	-	2910	3306,3320
AB20	1060	1332	-	1712	-	2918	3320
AB25	1056	1328	1591	1724	-	2919	3320
AB30	1054	1328	1588	-	3206	2910	3374
AB35	1049	1325	1588	1726	3218	2900	3375

Table 5 1 The summary of shifting in wavenumber of the SBEs system.

5.3 X-ray Diffraction Analysis

The structure and crystallization of the polymer matrices can be determined via X-ray diffraction analysis. The X-ray diffractograms of polymer blend CMC-PVA doped with vary amount NH_4Br are depicted in Figure 5.4. It is observed that the peak intensity of polymer blend CMC-PVA decrease from 22º to 20º when NH_4Br was indroduced into the electrolyte system up to AB15. The shifting in peak intensity to the lower 2θ may be attributed to the interaction happen between the host polymer blend and dopant salt, in turn enhance the amorphous phase of SBE systems (Bao et al., 2018a; Moniha, Alagar, Selvasekarapandian, Sundaresan, & Boopathi, 2018; Rajendran et al., 2003). The polymer blend has provided more free volume space and give opportunity for ions to migrate in polymer backbone when an appropriate amount of dopant salt was added. The incorporation of NH_4Br in present work contributes the raising of H^+ protonation which resulting to enhancement in amorphous phase as discussed in FTIR analysis part. In addition, the hump becomes more broaden as increase amaount of NH_4Br and this can be explained due to polymer backbone softened when two polymers were blended together, thus improve its segmental motion. This observation suggests the readily interaction between the ionic dopant and the CMC-PVA, reflecting the amorphous phase (Samsudin et al., 2012). The XRD pattern reveals that most of the peaks belong to pure NH_4Br have disappeared in the blend polymer electrolytes containing 5 to 25 wt. % of NH_4Br and this situation could be possibly due to the complete dissolution of the ammonium salt in the polymer blend matrix. It also can be observed from Figure 5.4, there is appearance of

new peak at AB30 and AB35 which believed belongs to pure NH_4Br. This strongly suggests that at high concentration, the crystallinity of the system increases due to the formation of ion aggregates.

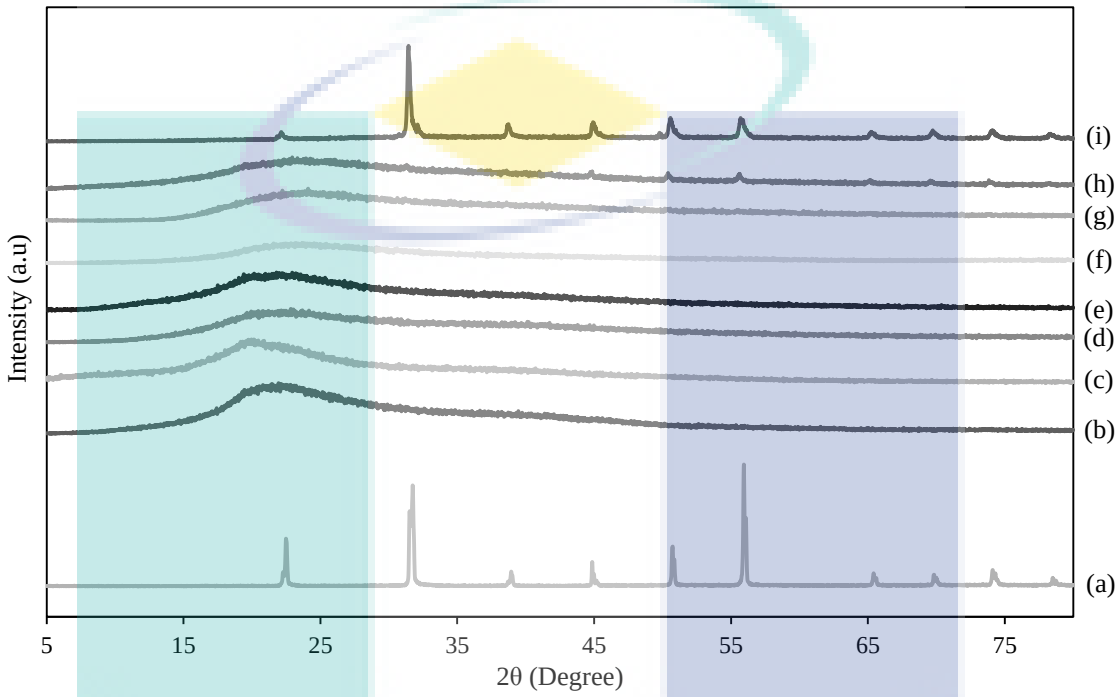

Figure 5 4 XRD patterns of biopolymer electrolytes for (a) pure NH_4Br, (b) AB0, (c) AB5, (d) AB10, (e) AB15, (f) AB20, (g) AB25, (h) AB30 and (i) AB35.

The size of crystallinity has been calculated via full width at half maximum (FHWM) of the peak which retrieved using OriginPro 8.0 sofware. This measurement is needed in order to identify the changes of amorphous phase in present system via Debye-Scherrer approach (Mahakul, Sa, Das, & Mahanandia, 2017; J. Wang et al., 2017).

$$D = \frac{0.94\lambda}{\beta \cos \theta} \tag{5.1}$$

where λ is represent to the wavelength of the X-ray used with value of 1.5406 Å, β is represent to the value FHWM of the peak and θ is represent to the Bragg diffraction angle. The measurement size of crystallinity of XRD patterns for all amount of NH_4Br based biopolymer electrolyte system were tabulated in Table 4.2. As noticed in Table 4.3, the

crystallinity is inversely proportional to the FHWM where the higher value of crystallinity, the lower the value of FHWM (J.-M. Yang & Wang, 2015).

Table 5 2 Crystallite size of all SBEs system.

Sample	2θ(degree)	FHWM (rad)	*D* (Å)
AB0	20.85	0.08	18.29
AB5	21.12	0.12	12.33
AB10	21.7	0.14	10.44
AB15	27.43	0.48	3.11
AB20	23.74	1.26	1.36
AB25	23.99	0.32	4.80
AB30	22.74	0.15	9.75
	47.51	0.73	2.18
	50.42	0.88	1.82
	55.62	0.0051	323.35
	73.93	0.0077	235.92
	79.39	0.13	14.76
AB35	22.15	0.0021	187.81
	31.46	0.0079	191.49
	38.75	0.0056	274.75
	44.97	0.0044	359.06
	50.62	0.0068	235.25
	55.81	0.0077	213.31
	65.3	0.0054	317.77
	69.79	0.0058	306.43
	74.12	0.0059	305.69
	78.34	0.0038	486.29

As reported by Shukur et al. (M. F. Shukur et al., 2014b), the amorphousness of electrolytes can be related with conductivity trend. As increases the amorphous phase, the conductivity also will increase. It can predict from Figure 5.4 that biopolymer electrolyte containing AB20 concentration exhibit the highest conductivity at ambient

temperature since it shows the most amorphousness pattern. Therefore, when above AB20 concentration is added, it shows the decrement of amorphous phase and this might be due to the crystallinity of the polymer electrolytes increased. The presence of new peaks at AB30 and AB35 proved that un-dissociated salt occurred and causes sample to become more crystalline (A. S. Samsudin & M. I. N. Isa, 2012). A substantial portion of the salt is not entrapped in the host polymer and deposited on the surface when film has formed. This situation leads the decrement number of mobile ions in SBEs system thus decrease the ionic conductivity (Liew et al., 2017; Salleh, Aziz, Aspanut, & Kadir, 2016). The amorphous phase contributes towards the protonation of H^+ in host polymer to increase and get agreement with the FTIR observation where H^+ from NH_4Br easily to migrate towards COO^- of CMC-PVA in amorphous state which resulting the increment of conductivity (Buraidah & Arof, 2011a; Rasali, Nagao, & Samsudin, 2018).

5.4 Thermal Stability Studies

The studies of thermal stability of solid biopolymer electrolytes based CM-PVA blend doped with vary amount of NH_4Br has been done via thermogravimetric analysis and differential scanning calorimetry measurement.

5.4.1 Thermogravimetric Analysis (TGA)

Dehydration and decomposition are the main processes associated with the degradation mechanism of polymer electrolytes. Figure 5.5 depicts thermo gravimetric spectra of variuos amount of NH_4Br solid biopolymer electrolytes system. Thermogravimetric analysis (TGA) is a process in which a material is decomposed by heat, which causes bonds within the molecule to be broken. TGA plays an important role in determining thermal stability of the materials. Three distinct decomposition stages have been attained for all the samples in the temperature range of 20–800 °C. From Figure 4.6, it can be observed that the initial weight loss which get from decomposition process were accounted in all the tested samples at the temperature of 100 °C owing to the evaporation of residual solvent and moisture (S. A. Hashmi et al., 1990). The initial weight loss is attributed to the presence of a small amount of moisture influenced from

the uses of distilled water as solvent in SBEs system (Mohamad & Arof, 2007). Further increase in the temperature leads to the de-polymerization of the present biopolymer electrolytes. According to the findings, it can be seen that AB5 undergoes one-step weight loss process with the decomposition temperature of 317 °C.

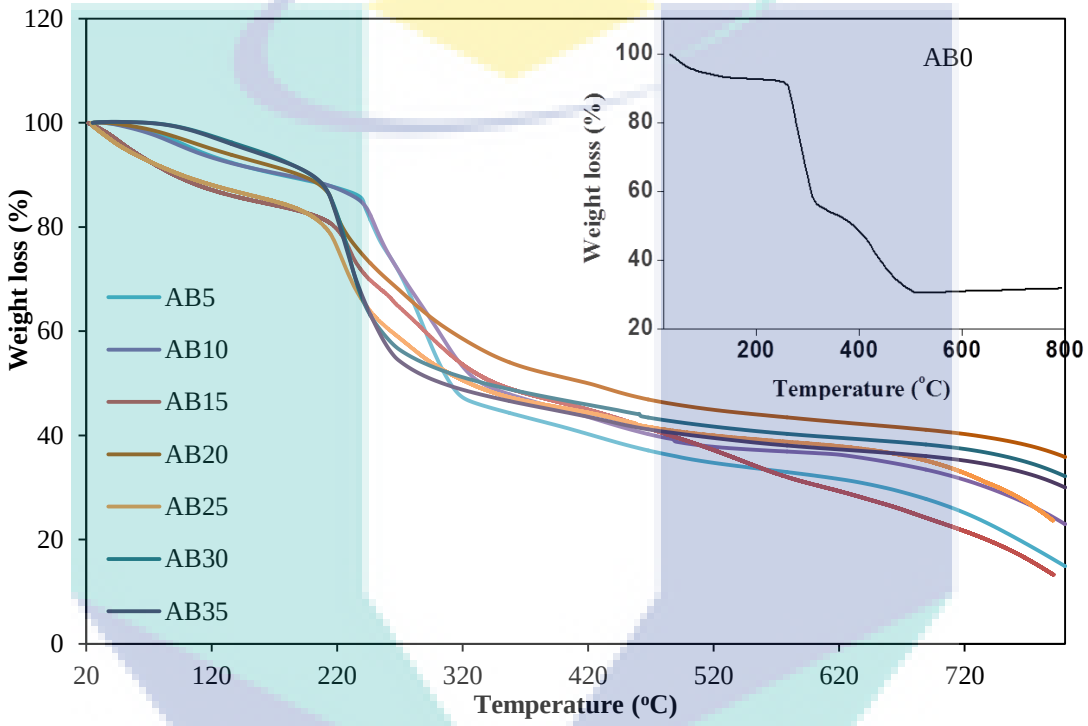

Figure 5 5 TGA curve of biopolymer electrolytes at various amount of NH_4Br.

5.4.2 Differential Scanning Calorimetry Analysis (DSC)

The polymer segmental motions plays an important role in ionic mobility and in conductivity as well (H. Woo, Majid, & Arof, 2013). Heating-cooling-heating (H-C-H) cycle was used in DSC measurements in order to remove any water and moiture of biopolymer electrolyte at first heating cycle (Liew, Ramesh, & Arof, 2015; C.-C. Yang, Lee, & Yang, 2009). Figure 5.6 illustrates DSC thermograms (second heating) of polymer blend CMC-PVA and CMC-PVA with various amount of ammonium salt based biopolymer electrolytes. The glass transition was determined at midpoint of the each transition where the phase transition of polymer is allowed (Hema,

Selvasekerapandian, et al., 2009; Liew, Ramesh, & Arof, 2016b; Sivadevi et al., 2015). The degree of purity and nature of the substance can obtained from the physical parameters of T_g information (Guirguis & Moselhey, 2012). The temperature of glass transition (T_g) for polymer blend CMC-PVA without dopant in present work was detected at 83 ℃. According (M. A. Saadiah & A. S. Samsudin, 2018), the T_g for pure PVA was found to be at 89.7 ℃. The shifting to lower temperature might be due to the interaction between two polymer CMC and PVA via H-bonding and the result get supported with other finding work (Abd El- Kader et al., 2005; El-Kader et al., 2008; El-Sayed et al., 2011; Sudhamani, Prasad, & Sankar, 2003). Moreover, (Iwamoto,

Miya, & Mima, 1979) reported blending PVA into water can reduces the crystallinity of PVA.

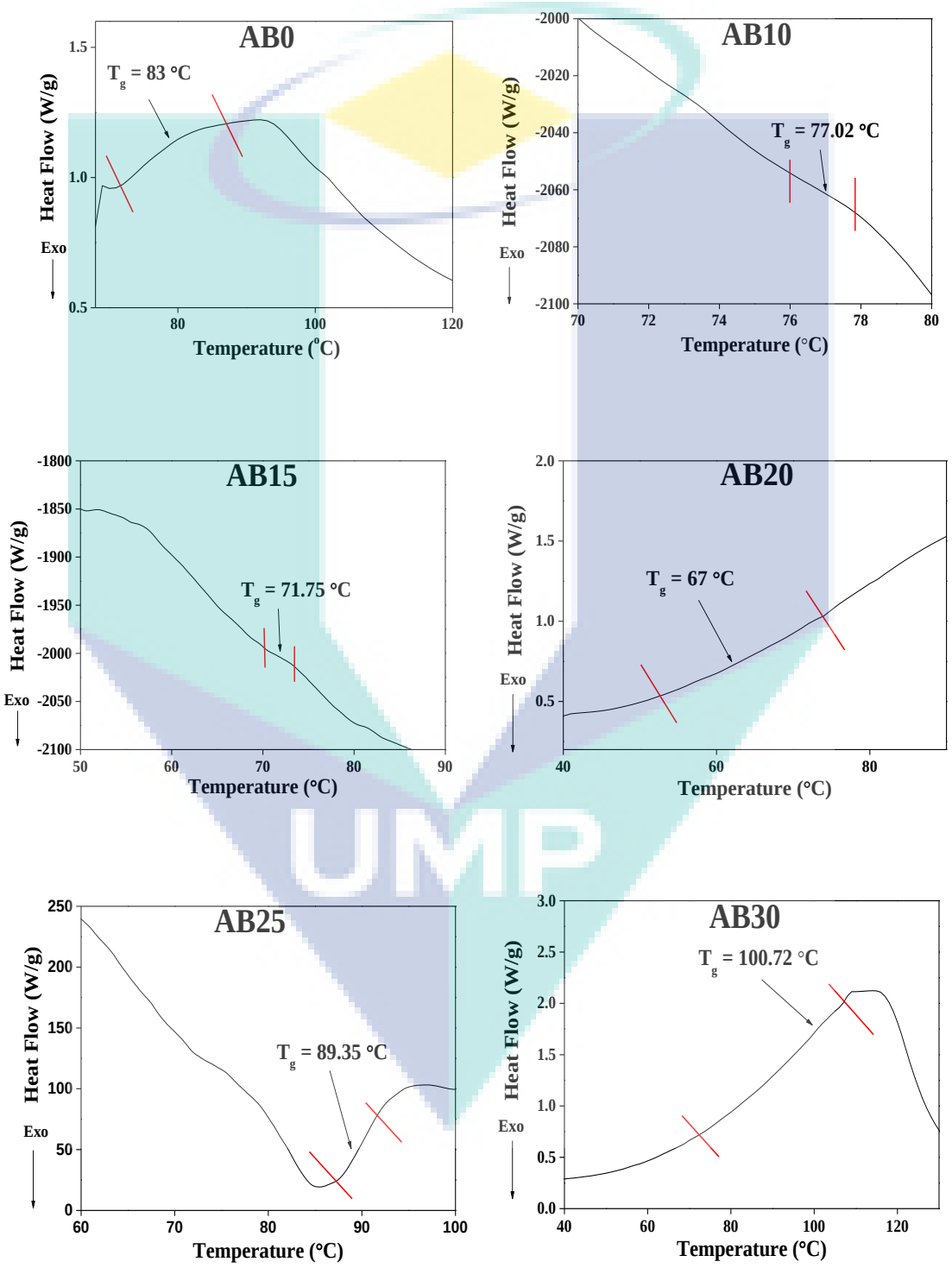

Figure 5 6 DSC Thermograms of polymer blend CMC-PVA (AB0) and selected amount of NH_4Br based biopolymer electrolytes.

Further, addition of dopant salt decrease the T_g of CMC-PVA. Based on Figure 4.7, it is obviouly seen that the thermal transition of polymer blend CMC-PVA varied after different amount of NH_4Br was introduced into the biopolymer electrolyte system. These denotes the plasticization of the salt effect and was noted the T_g decrese drastically up to AB20 (Vijaya et al., 2013). The incorporation of NH_4Br has shifted the glass transition from higher to lower T_g, indicating interaction of the dissociated dopant salt with the polymer blend host, in turn increased the segmental motion and became highly amorphous (Genova et al., 2015; Sudhakar & Selvakumar, 2013). Similar results have been reported by (Sivadevi et al., 2015), for the PVA-PAN blend doped with ammonium thioctanate polymer electrolyte systems. Moreover, the addition of ammonium salt into CMC-PVA matrix results in weakening of the dipole-dipole interaction between the polymer blend host chains, thus make ions to move freely through the network of polymer chain when an electric field is applied (Vijaya et al., 2013). AB20 exhibits the lowest T_g which infers high flexibility of the polymer chain, thus expected the ionic conductivity to improve. Additionally, increasing in T_g increased the crystallinity of the biopolymer electrolytes structure. Apart from that, (Yuhanees, 2017) and (Mizuno, Mitsuiki, & Motoki, 1998) have reported more restriction of segmental motions which may lead the inter and intachain hydrogen bonding to form, thus triggered the crystallinity to increase as T_g increase.

5.5 Electrical Impedance Spectroscopy Studies (EIS)

The data collected from EIS can be used to investigate the impedance spectroscopy, ionic conductivity, temperature dependence, activation energy, dielectric and modulus studies.

5.5.1 Impedance Spectroscopy

Figure 5.7 depicted the complex impedance plot at ambient temperature (303 K)

obtained for CMC-PVA-NH_4Br biopolymer electrolytes system.

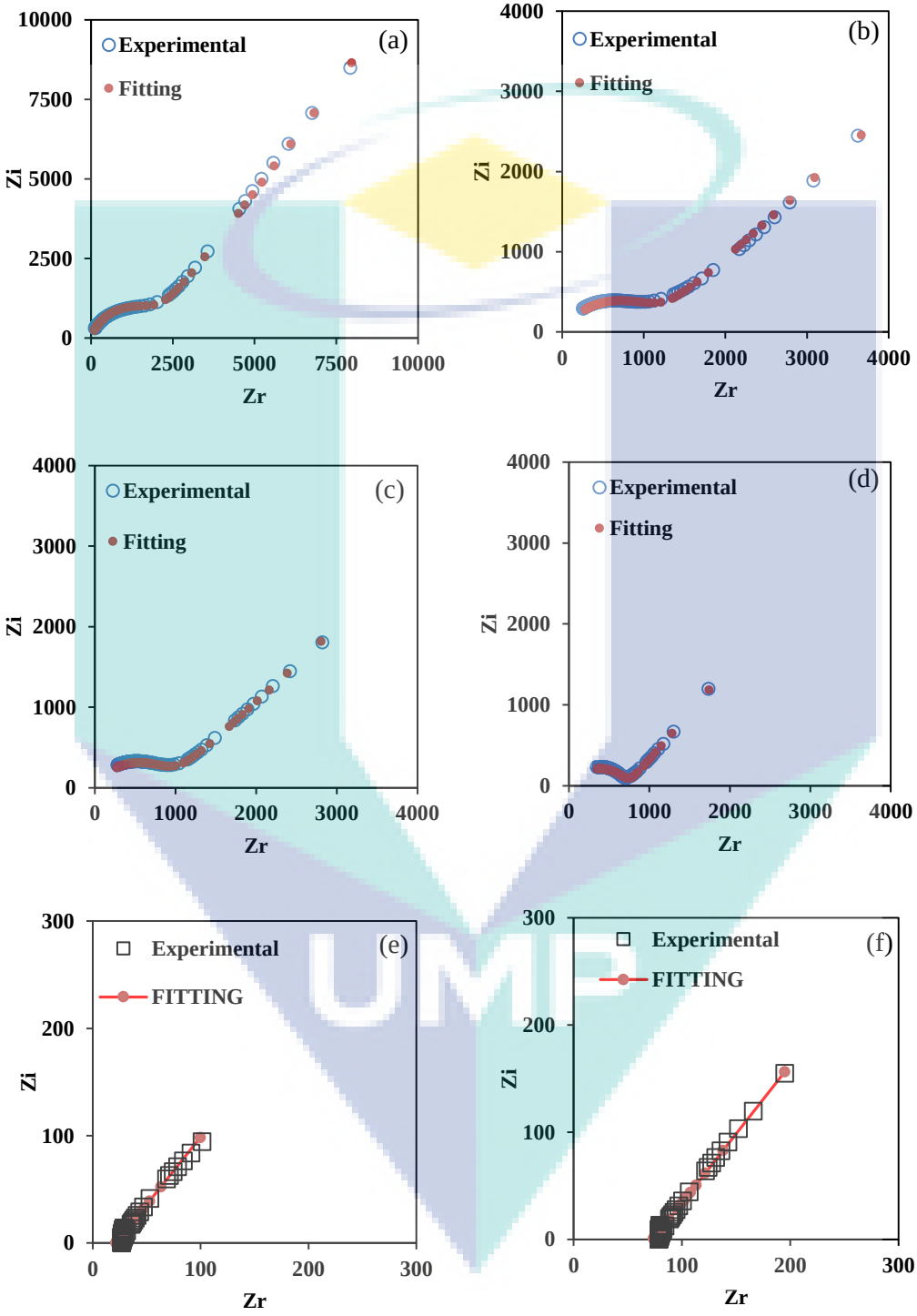

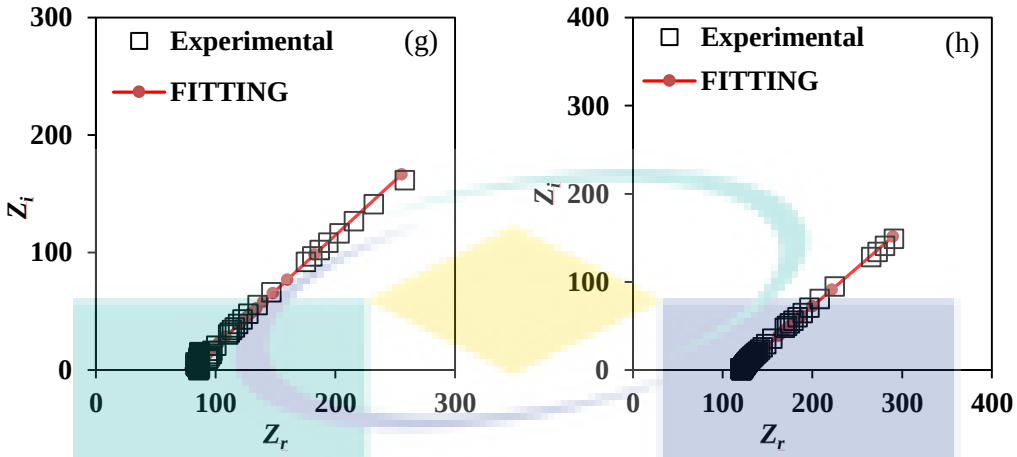

Figure 5 7 (a) AB0, (b) AB5, (c) AB10, (d) AB15, (e) AB20, (f) AB25, (g) AB30 and (h) AB35.

It can be observed from Figure 5.7 that the Cole-Cole plot also known contains of a semicircle at high frequency and spike at low frequency. The semicircle at high frequency is due to the parallel combination of bulk resistance, R_b and bulk capacitance while spike can be fitted with the equivalent circuit consists of R_b and constant phase element (CPE) as presented in Scheme 5.1 (Rudhziah, Ahmad, Ahmad, & Mohamed, 2015; Subramaniyan Selvasekarapandian, Hema, Kawamura, Kamishima, & Baskaran, 2010). The existence of bulk capacitance might be due to the migration of proton in biopolymer electrolytes system while R_b could be due to immobile polymer chains. From Figure 5.7, it can be seen that there is formation of semicircle with a title spike when added AB0 and AB10 into the system. However, beyond AB20, the semicircle disappears in the impedance plot at higher salt concentration and replaced by tilted spike suggesting that only the resistive component of the polymer prevails (Rajeswari, Selvasekarapandian, Sanjeeviraja, Kawamura, & Bahadur, 2014). The value of R_b can be calculated from the intercept of high frequency semicircle or the low frequency spike. The R_b value decrease with the increment of salt concentration where electrolyte containing AB20 has the lowest R_b value at room temperature. The decrement of R_b value as increase the salt content might be due to the mobile charge carrier increase (M. F. Shukur et al., 2014b).

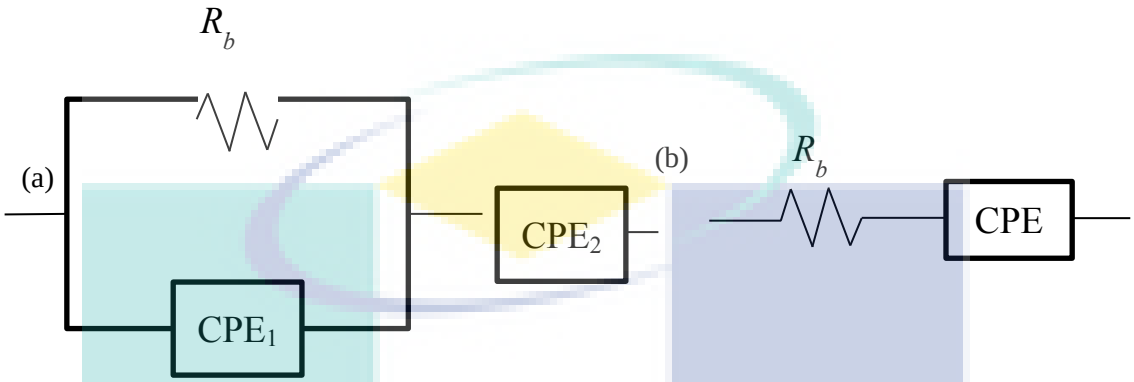

Scheme 5 1 The equivalent circuit of CMC-PVA-NH_4Br biopolymer electrolytes for (a) semicircle with title spike and (b) spike.

The Cole-Cole plot of the electrolyte consists of a semicircle with title spike can be represented by a parallel combination of R_b and CPE that connected in series with another CPE (Teo, Buraidah, Nor, & Majid, 2012). The semicircle ascribes the bulk material while title spike ascribes the electrical double layer. Ionically, a CPE is used in a model instead of a capacitor to compensate for inhomogeneity in the system (Qian et al., 2001). The impedance of CPE (Z_{CPE}) can be represented via equation 4.1 or 4.2 (A. Arof, S. Amirudin, S. Yusof, & I. Noor, 2014; M. Saadiah & A. Samsudin, 2018; N. Shuhaimi, L. Teo, H. Woo, S. Majid, & A. K. Arof, 2012; M. F. Shukur et al., 2014b).

Hence, the real and imaginary parts for Cole-Cole plot containing of a semicircle and title spike can be expressed using equation 4.3 and 4.4 (N. Mazuki, N. Rasali, M. Saadiah, & A. Samsudin, 2018).

The list of parameters for the circuit element of all SBEs system studied at ambient temperature tabulated in Table 5.3. It can be observed that the value of R_b for fitting give almost similar R_b value for experimental.

Table 5 3 The parameter for CMC-PVA-NH_4Br

Sample	R_b *(experimental)* (Ω)	R_b *(theoretical)* (Ω)	p_1 *(rad)*	k_1 *(F)*	p_2 *(rad)*	k_2 *(F)*
AB0	2.44×10^3	1.70×10^3	0.85	8.26×10^{-9}	0.6	1.13×10^{-6}
AB5	1.21×10^3	1.06×10^3	0.68	5.56×10^{-8}	0.48	1.04×10^{-5}
AB10	9.83×10^2	8.83×10^2	0.68	5.56×10^{-8}	0.48	1.41×10^{-5}
AB15	7.32×10^2	7.32×10^2	0.68	5.56×10^{-8}	0.55	2.72×10^{-5}
AB20	2.83×10^1	2.16×10^1	0.579	2.95×10^{-4}	-	-
AB25	7.98×10^1	7.38×10^1	0.578	1.80×10^{-4}	-	-
AB30	8.46×10^1	7.79×10^1	0.48	2.60×10^{-4}	-	-
AB35	1.27×10^2	1.18×10^2	0.46	2.90×10^{-4}	-	-

5.5.2 Ionic Conductivity

The studies of impedance spectroscopy in present work is to investigated the electrical behavior and ionic conductivity of solid biopolymer electrolytes based CMC-PVA-NH_4Br. The electrical studies have been done using electrical impedance spectroscopy (EIS) characterization. Figure 5.8 depicted ionic conductivity of solid biopolymer electrolytes for different NH_4Br concentration at ambient temperature (303K). As plotted in Figure 5.8, it can be seen that the ionic conductivity is increase as amount of NH_4Br increase up to 20 wt. %. These increasing pattern at low concentration could be discussed as ion dissociation thus increase ionic mobility and number of charge carriers (M. A. Ramlli, K. H. Kamarudin, & M. I. N. Isa, 2015; Ramly et al., 2011). From previous work (Ahmad Salihin Samsudin et al., 2011), the optimum ionic conductivity achieved at 1.12×10^{-4} S cm^{-1} for sample containing 25 wt. % NH_4Br. However, in this present work is observed the optimum ionic

conductivity achieved is 3.21 x 10^{-4} S cm^{-1} for sample containing 20 wt. % NH_4Br, suggesting that when CMC was blend with PVA will enhance the ionic conductivity. In addition, at maximum ionic conductivity is suggested that ion hopping mechanism is in stable condition.

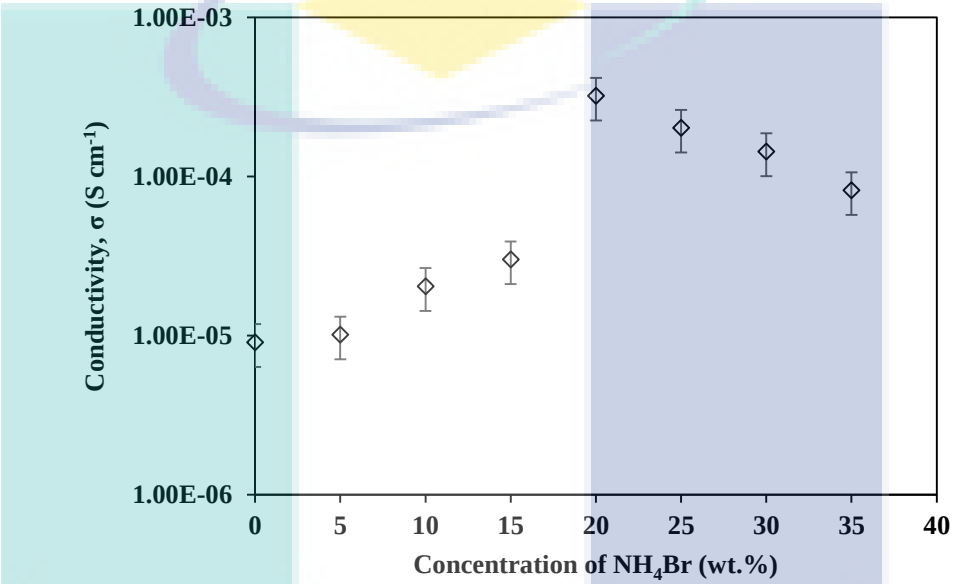

Figure 5 8 Ionic conductivity of solid biopolymer electrolytes system.

However, when beyond 20 wt. % NH_4Br is incorporated in polymer blend CMC-PVA biopolymer electrolyte, the ionic conductivity seem to be decreases. This phenomenon might be due to formation neutral ion pairs in biopolymer electrolytes. In other work, at high salt concentration contribute more free ion which restrict movement of other free ions to move freely from one side to another as number density of mobile ions were decreased, resulting ionic conductivity to be reduce. (Samsudin, Kuan, & Isa, 2011) also supported the present finding were decreasing pattern at higher concentration is attributed to the dipole interaction between free ions and

electrolyte system medium increase thus leads the reduction of mobile ions and ions mobility.

5.5.3 Temperature Dependence

The mechanism of ionic conduction of blend biopolymer electrolytes were analysed via temperature-dependent of ionic conductivity. The temperature dependence of polymer blend CMC-PVA (303K to 353K) and various NH_4Br

concentration (5 to 35 wt. %) at temperature range of 303K to 373K were illustrated in Figure 5.9(a) and 4.11(b), respectively.

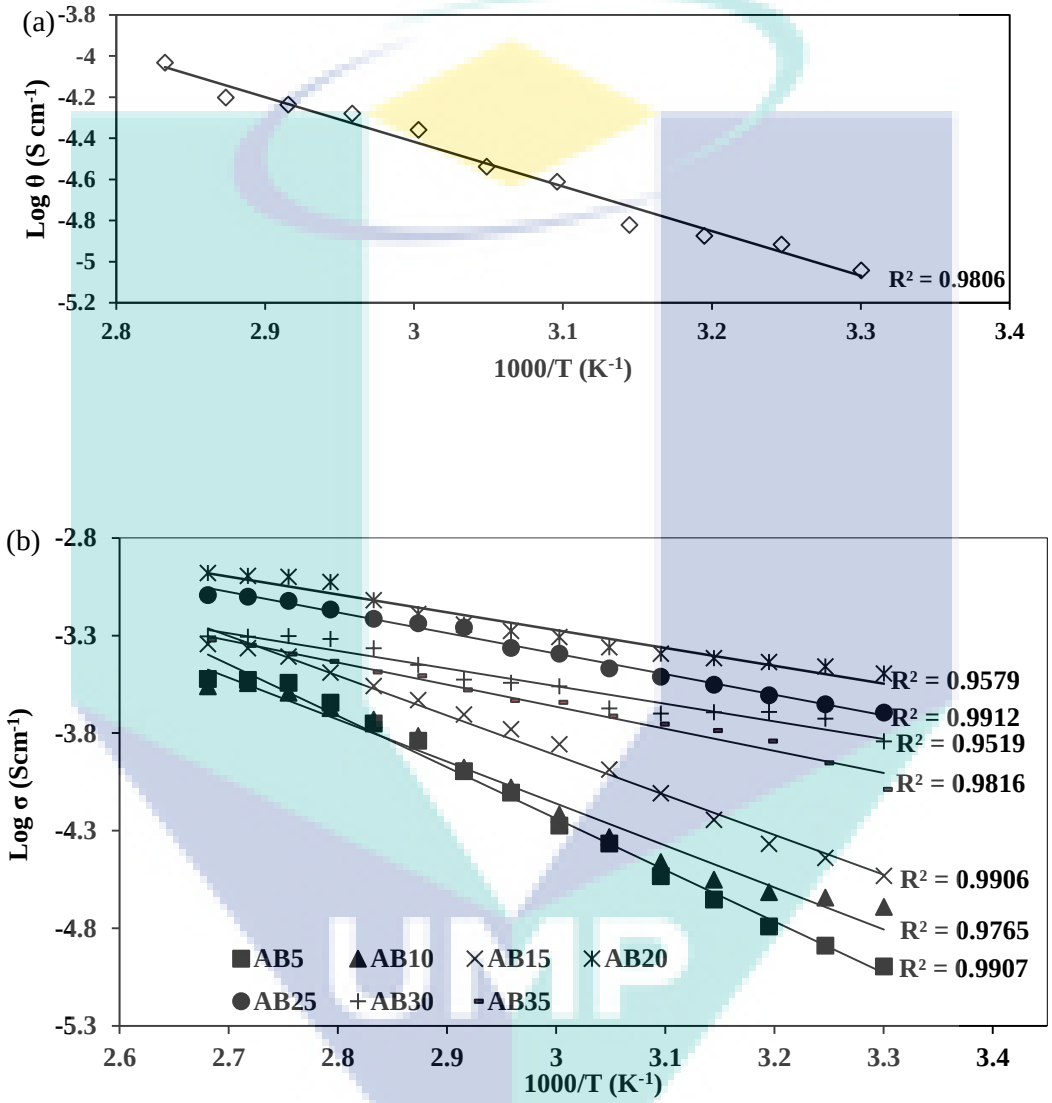

Figure 5 9 (a) Temperature dependence plot of polymer blend CMC-PVA and (b) log conductivity versus 1000/T plot for different NH_4Br concentration

On other hand, it can be observed that the ionic conductivity increase with temperature up to 353K for polymer blend CMC-PVA while at various amount of NH_4Br, the ionic conductivity increase until temperature of 373K. This phenomenon can be inferred as increasing in temperature can improve movement of ion to hop from

one site to another site, resulting enhancement in ionic conductivity. Futhermore, (Deka & Kumar, 2011) has reported that ionic conductivity increase as temperature increase is due to polymer chain flexilibity increase, thus provided more free volume, in turn leads to increment in polymer segmental mobility. The regression values for all sample shows almost close to unity (R^2~1) thus suggesting biopolymer electrolytes based polymer blend CMC-PVA doped with vary amount of NH_4Br obeys Arrhenius behaviour. This indicates that the ionic conductivity mechanism is thermally assisted (Samsudin & Isa, 2014). Arrhenius behaviour can be impressed via relation:

$$\sigma = \sigma_o \, exp^{(\frac{-E_a}{kT})} \tag{5.2}$$

where σ_o represent pre-exponential factor, E_a is activation energy, k is the Boltzmann constant and T is temperature in unit kelvin. There is no abrupt jump with temperature is detected in both figures above, suggesting that there is no phase transition in structure of biopolymer electrolytes within the temperature range investigated (N. F. Mazuki, N. M. J. Rasali, M. A. Saadiah, & A. S. Samsudin, 2018).

5.5.4 Activation Energy

The variation of activation energy at ambient temperature (303K) has been calculated from the log σ versus 1000/T slope and has plotted in Figure 5.10. It is noticable that activation energy is inversely proportional with ionic conductivity trends as value of activation energy decreases when more NH_4Br concentration is added into the biopolymer electrolyte system up to AB20 and back to increase at high concentration. Moreover, sample with highest ionic conductivity possess the lowest activation energy value. This situation can be explains as amount of salt concentration increase can enhanced the ionic conductivity which requires lower energy to ions migrate one site to another in polymer blend matrix. These observation get good aggrement with (Buraidah, Teo, Majid, & Arof, 2009) where they believe the

activation energy is one of the important energy to move ion and thus presupposing that the structure would not change.

Furthermore, the decrement in activation energy as increasing salt concentration also can be related with interaction between polar moleculs in polymer blend and ion of the salt (Baskaran, Selvasekarapandian, Kuwata, Kawamura, & Hattori, 2006). The increment of amorphous nature with increase in salt concentration up to AB20 facilitates the fast of H^+ ion motion in the biopolymer network contribute the decrement of activation energy (Kopitzke, Linkous, Anderson, & Nelson, 2000; Schantz & Torell, 1993; S Selvasekarapandian, Hirankumar, Kawamura, Kuwata, & Hattori, 2005; Srivastava & Chandra, 2000). When beyond AB20, the activation energy start to increase and this might be due to high concentration of ion supply in biopolymer electrolytes difficulities the movement of ions, thus requires more energy to move the ions. The values of E_a for CMC-PVA-NH_4Br studied in this work are in range of 0.25 to 0.12 eV.

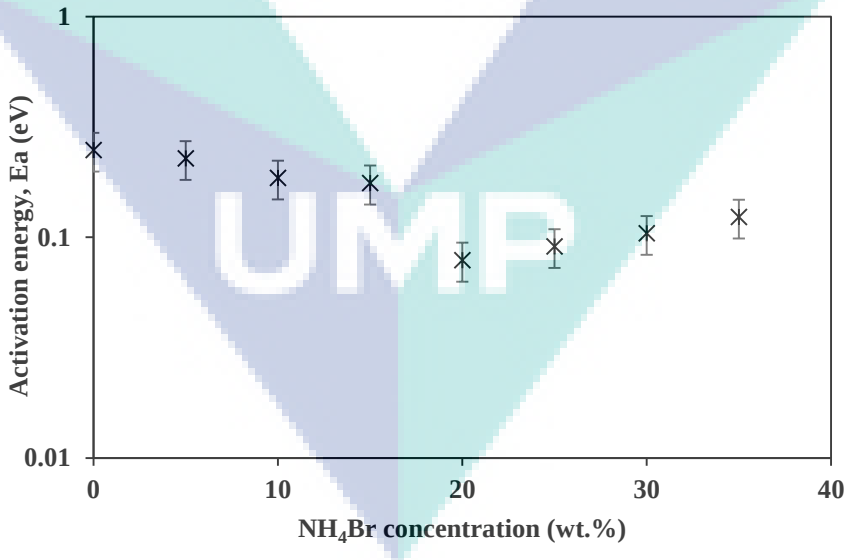

Figure 5 10 The activation energy plot of biopolymer electrolytes system.

5.5.5 Dielectric Studies

Beside to investigate the ionic conductivity behaviour and electrical properties, the data measured via EIS also contains dielectric permittivity and electrical modulus. The studies in dielectric permittivity is to elucidate the dipole relaxation in biopolymer electrolytes. Figure 5.11 depicts the dielectric constant (ε_r) and dielectric loss (ε_i) of various NH_4Br concentration at room temperature (303K). The behaviour of dielectric relaxation provides important insights into ionic transport phenomenon and polarization effect at the electrode/electrolytes interface (Chai & Isa, 2012; M S A Rani, Dzulkurnain, Ahmad, & Mohamed, 2015). The value of both dielectric permitivitty can be derived as follow:

$$z = z_r + z_i \tag{5.3}$$

$$\varepsilon_r = \frac{z_i}{\omega C_o (z_r{}^2 + z_i{}^2)} \tag{5.4}$$

$$\varepsilon_r = \frac{z_r}{\omega C_o (z_r{}^2 + z_i{}^2)} \tag{5.5}$$

where Z_i and Z_r correspond to imaginary part and real part, respectively, of complex permittivity, $\omega = 2\pi f$, f is frequency while $C_o = \varepsilon_o A/t$, ε_o is free space permittivity.

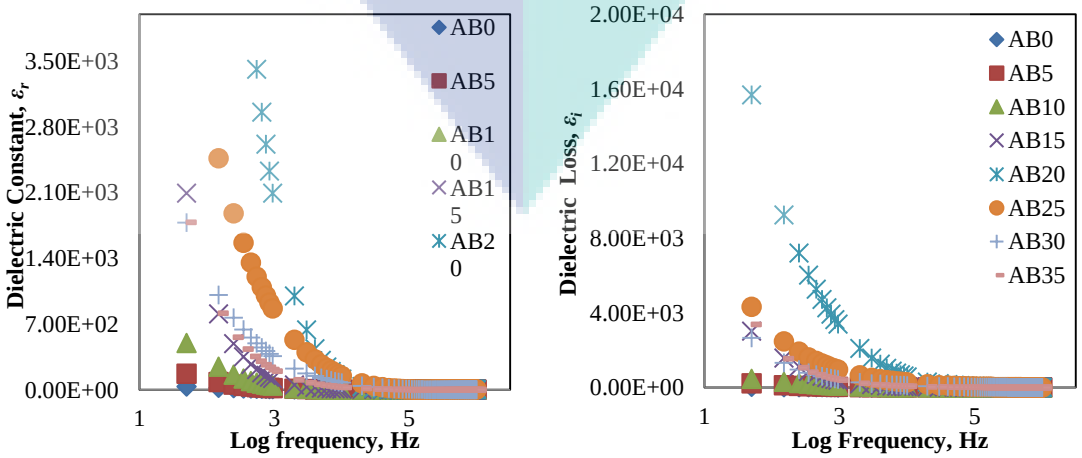

Figure 5 11 Frequency dependence on dielectric constant and dielectric loss for CMC-PVA-NH_4Br systems.

Based on Figure 5.11, the dielectric constant and dielectric loss give almost similar pattern where both is sharply decrease as frequency increase. This phenomenon can be attributed to the effect of electrode polarization which accumulation decrease relate with decreasing both dielectric permittivity. It can be seen that dielectric constant give highest value at low frequency due to the presence of more space charge effect which attributed from charge carriers accumulation near the electrodes (Armstrong, Dickinson, & Willis, 1974; Radha, Selvasekarapandian, Karthikeyan, Hema, & Sanjeeviraja, 2013). The constant value of dielectric constant at high frequency is believe due to periodic reversal of the field occurs so quickly, thus distress the charge carriers to orient themselves in the field direction, in turn leads to decrement in dielectric constant (Hema et al., 2007).

Meanwhile, the very high value of dielectric loss at low frequency also can be explains as free charge carrier motion that builds up within the materials and electrolytes interface (M S A Rani et al., 2015). Moreover, the incorporation of NH_4Br which acts as dopant salt into polymer blend CMC-PVA complexes is expected increase the degree of proton ion (H^+) dissociation and improve the number of free ions. It is also detected in Figure 5.11, both dielectric permittivity shift to high frequency as more amount of NH_4Br concentration is added into biopolymer electrolyte system. These shifting happen is believe due to number density of mobile ions increase which increase the charge storage. According to (A. S. Samsudin & M. I. N. Isa, 2012), the dielectric trends is align with ionic conductivity patterns when NH_4Br was introduced into the electrolyte system. However, above AB20, both dielectric constant and dielectric loss start to decrease and this might be due to ions re-association which leads to density of charge storage to be decrease.

5.5.1 Modulus Studies

A further analysis of electric behavior would be more successfully achieved by dielectric modulus. The real modulus, M_r and imaginary modulus, M_i, can inhibited

the effect of electrode polarization to give a clear indication of electric property of the polymer electrolyte. Figure 5.12 illustrates the frequency dependence on electrical modulus of a real part and imaginary part for biopolymer electrolyes based CMC-PVA doped with vary amount of NH_4Br at ambient temperature.

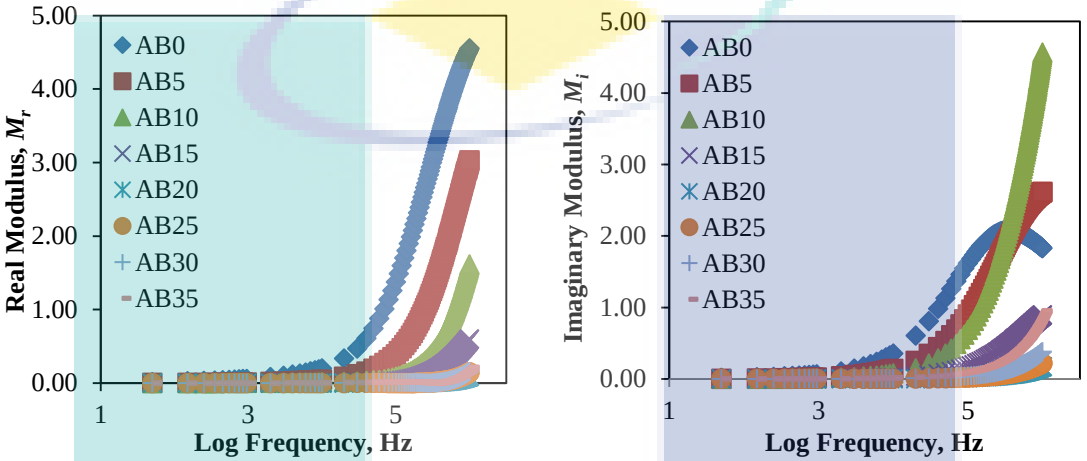

Figure 5 12 Electrical modulus versus frequency for biopolyemer electrolytes containing different NH_4Br concentration.

It is observed from Figure 5.12, both electrical modulus shows increasing patterns with frequency. These increment at high frequency can be explains due to effect of electrode polarization phenomenon. However, in imaginary plot, there is presence of relaxation peak is noticed at high frequency, suggested that the samples is ionic conductor (N. A. M. Noor & M. I. N. Isa, 2015; Ramly et al., 2011). At low frequency, the value of real and imaginary parts are vicinity of zero, indicating that the electrode polarisation contribution is negligible which is the main advantage in modulli studies. The appearance of long tail at low frequency is due to large capacitance associated with the electrodes (Bakar et al., 2015; Nor fatihah Mazuki et al., 2019). It is also noticable in real part plot, the value of real modulus decreasing with incorporation of NH_4Br into the electrolyte system. Sample containing AB20

shows the lowest value compare with others, suggesting the highest ionic conductivity value at room temperature.

5.6 Transport Properties

The FTIR deconvolution method (N. M. J. Rasali & A. S. Samsudin, 2017; N. K. Zainuddin & A. S. Samsudin, 2018) and fitting method (A. K. Arof, S. Amirudin, S. Z. Yusof, & I. M. Noor, 2014) also known as A-N method were used in order to investigate further in transport properties of SBEs system. The comparision between these two method have been made to prove that the result were aligned with each other.

5.6.1 Fourier Transform Infrared Spectroscopy Deconvolution

Fourier transformed infrared spectra of the blended CMC-PVA doped NH_4Br is deconvoluted for primary stretching zone (carbonyl) to isolate and identify the ionic species and polymer segments involved (Yusuf et al., 2016). Figure 5.13 depicts FT-IR deconvolution of SBEs system based blended CMC-PVA doped with various amount of NH_4Br. The region between 1530 and 1670 cm^{-1} is selected where it is believed the most significant complexation has occurred as shown in FTIR analysis section. The region which belongs to COO^- stretching of carboxylate anion of (C=O) is considered where the place that most ion interaction happen when NH_4Br was incorporated into the biopolymer blend systems, resulting peak to shift. These peak assignments are in agreement with findings by (N. Aziz, Majid, & Arof, 2012; Chai & Isa, 2016; N. F. Mazuki, A. F. Fuzlin, et al., 2018; Samsudin et al., 2012) (Ning et al., 2009) (Nik Aziz et al., 2010).

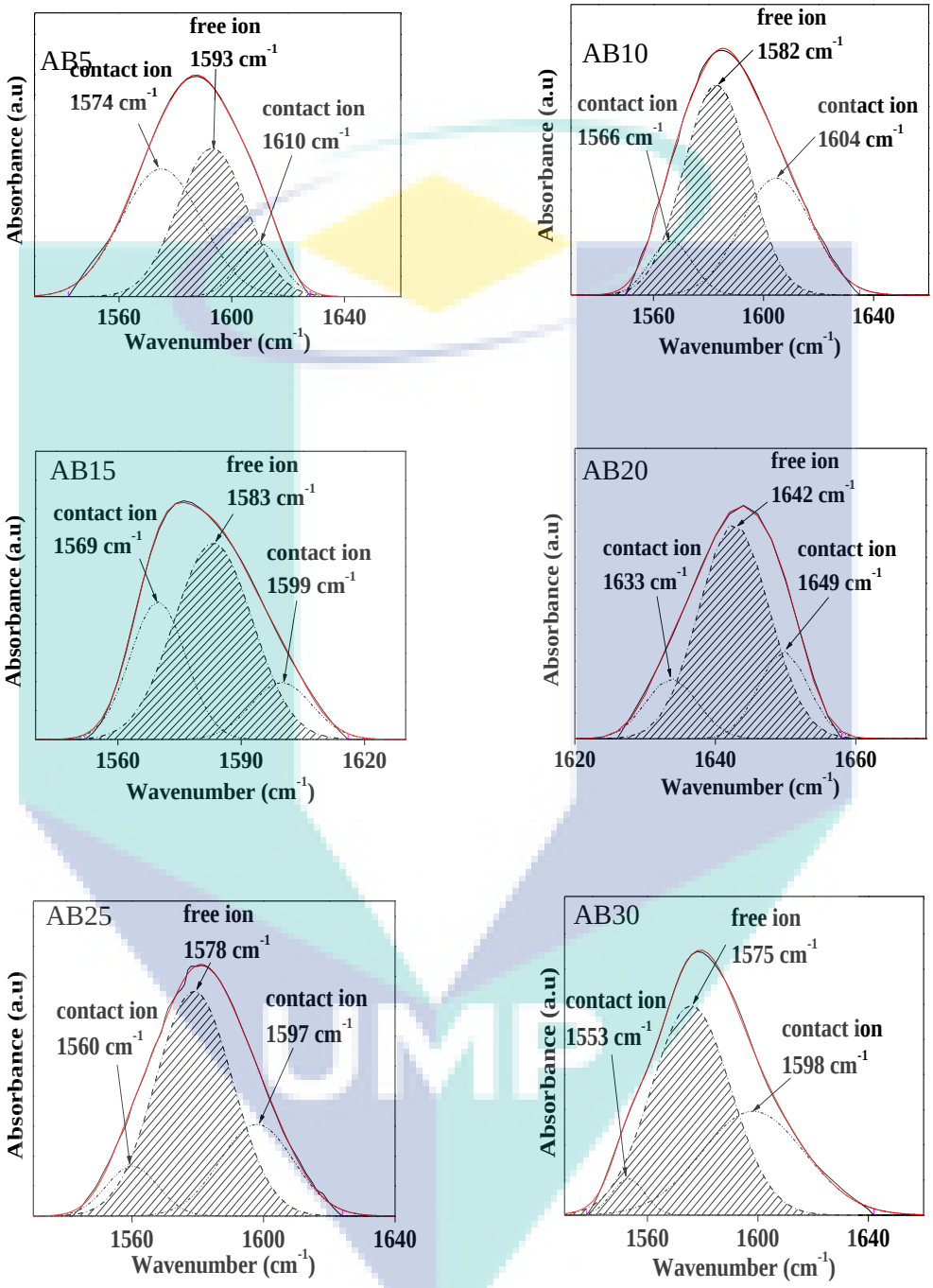
AB5
free ion
1593 cm-1
contact ion
1574 cm-1
contact ion
1610 cm-1
Absorbance (a.u)
1560
1600
1640
Wavenumber (cm-1)
AB10
free ion
1582 cm-1
contact ion
1566 cm-1
contact ion
1604 cm-1
Absorbance (a.u)
1560
1600
1640
Wavenumber (cm-1)
AB15
free ion
1583 cm-1
contact ion
1569 cm-1
contact ion
1599 cm-1
Absorbance (a.u)
1560
1590
1620
Wavenumber (cm-1)
AB20
free ion
1642 cm-1
contact ion
1633 cm-1
contact ion
1649 cm-1
Absorbance (a.u)
1620
1640
1660
Wavenumber (cm-1)
AB25
free ion
1578 cm-1
contact ion
1560 cm-1
contact ion
1597 cm-1
Absorbance (a.u)
1560
1600
1640
Wavenumber (cm-1)
AB30
free ion
1575 cm-1
contact ion
1553 cm-1
contact ion
1598 cm-1
Absorbance (a.u)
1560
1600
1640
Wavenumber (cm-1)

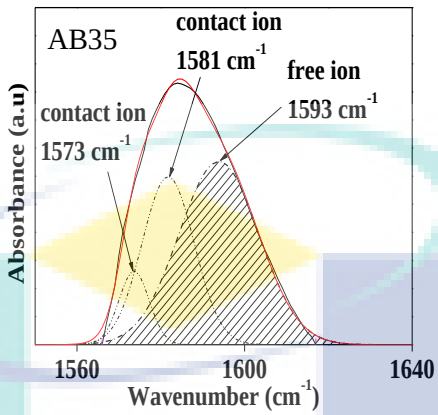

Figure 5 13 FTIR deconvolution spectra of CMC-PVA doped with vary amount of NH_4Br.

The peak at ~1590 cm^{-1} is corresponds to free ion and the peak at ~1575 cm^{-1} and ~1607 cm^{-1} representing contact ions. Free ion also known as ions dissociated from NH_4Br in polymer blend CMC-PVA while contact ion can be assigned as ions aggregate in biopolymer electrolyte system (N. F. Mazuki, A. F. Fuzlin, et al., 2018; Ramlli & Isa, 2016). The area of peaks deconvolution was measured using Gaussian function and the band was fitted via Origin Lab 8.0 software in order to determine the outcome of the carboxylate group in polymer blend CMC-PVA when more NH_4Br concentration was introduced. The free ions and contact ions were determined from the deconvoluted peaks (A. K. Arof et al., 2014; Rodi, Saaid, & Winie, 2017; N. K. Zainuddin & A. S. Samsudin, 2018). The percentage of free ions and V_{Total} are calculated using equation. (5.6) and Eq. (5.7), respectively (Ramlli & Isa, 2016).

$$free\ ions\ (\%) = \frac{A_f}{A_f + A_c} \times 100\% \tag{5.6}$$

$$V_{Total} = \left[\frac{weight}{density}(CMC)\right] + \left[\frac{weight}{density}(PVA)\right] + \left[\frac{weight}{density}(NH_4Cl)\right] \tag{5.7}$$

here A_f represents area under the peak and A_c represents the total area under the peak. The A_f corresponding to free ions and A_c corresponding to contact ions while V_{Total} is the total

volume of SBE system. The number of free mobile ions (η), ionic mobility (μ) and diffusion coefficient (D) can be calculated from FTIR deconvolution via equation (N. F. Mazuki, A. F. Fuzlin, et al., 2018; Rasali et al., 2018):

$$\eta = \frac{M \times N_A}{V_{Total}} \times free\ ions\ (\%) \tag{5.8}$$

$$\mu = \frac{\sigma}{ne} \tag{5.9}$$

$$D = \frac{\mu kT}{e} \tag{5.10}$$

where M is the number of moles of salt concentration, N_A is number of Avogadro constant with value of 6.02 x 10^{23} mol^{-1}, e is electric charge constant with value of 1.602 x 10-19 C, σ is ionic conductivity of SBEs system, k is Boltzmann constant with value of 1.38 x 10-23 J K^{-1} and T is ambient temperature in kelvin (303 K).

Table 5.4 shows free ions, contact ions and total volume for CMC-PVA doped NH_4Br SBEs system. Based on Table 5.4, it could be observed that the free ions increase as increased the NH_4Br concentration and then decreases when beyond AB20 were added into the SBEs system. It is also noticeable that the free ions trend aligned with ionic conductivity pattern while contact ions is inversely proportional to ionic conductivity from previous section. Further, the total volume seems slightly increase as more NH_4Br were incorporated into the present system. These phenomena can be explained as when more ammonium salt was introduced into polymer blend CMC-PVA, it supplies more H^+ ions thus need more space volume. Moreover, dissociation of H^+ from NH_4Br leads free ions percentage increase up to AB20 thus allowing free ions to move freely, resulting the number of charge carrier to increase, in turn improved the ionic conductivity (Sohaimy & Isa, 2015). In other word, the increment of free ions suggests shown more proton (H^+) have been supplied from NH_4Br and thus leads the ionic conductivity to increase. When more concentration above sample AB20 was added into the system, it contributes more H^+ ions thus cause overcrowded ions, resulting ionic conductivity to reduce. The decrement of free ions at higher concentration can be explained as ions association and form ion aggregate which leads the decreasing ionic conductivity of biopolymer

electrolytes (Rajeswari et al., 2014). According (Subramaniyan Selvasekarapandian et al., 2010) and (Chai, Ramlli, & Isa, 2013), the formation of ions aggregates reduced the mobile charge carrier in the electrolytes system.

Table 5 4 Free ions, contact ions and total volume of the CMC-PVA-NH_4Br.

Sample	Free ions (%)	Contact ions (%)	Total volume (cm^{-3})
AB5	44.85	55.15	2.61
AB10	56.41	43.59	2.62
AB15	63.41	36.59	2.63
AB20	66.89	33.11	2.65
AB25	64.89	35.11	2.66
AB30	58.38	41.62	2.68
AB35	57.05	42.95	2.69

5.6.1 Cole-Cole Plot

Further studies on transport properties have been measured via fitting method from Cole-Cole plot. Ionically, this method has been developed by Arof and co-worker in order to calculate the important parameters in transport properties. These method also used data form imedance spectroscopy solely and dependent on electric

double layer (A. K. Arof et al., 2014). Figure 5.14 and 5.15 show the graphs of μ and D and η, respectively for CMC-PVA-NH_4Br based biopolymer electrolyte system.

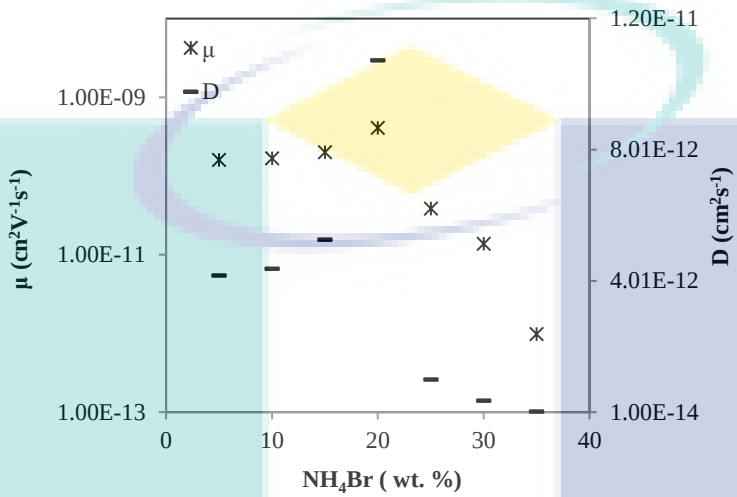

Figure 5 14 Mobility of charge carriers, μ and diffusion coefficient, D versus varied amount of NH_4Br.

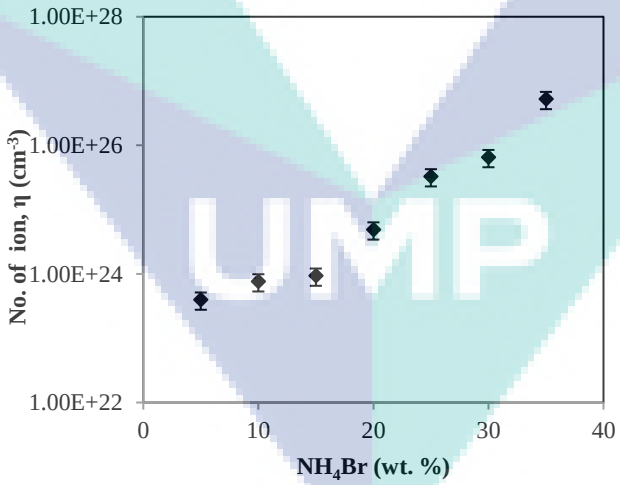

Figure 5 15 Number of ion, η versus varied amount of NH_4Br.

Different with deconvolute FTIR calculation, the parameters of transport properties has been calculated via following equation:

$$D = \frac{(k_2 \varepsilon_r \varepsilon_o A)^2}{\tau_2} \tag{5.11}$$

$$\mu = \frac{eD}{k_b T} \tag{5.12}$$

$$\eta = \frac{\sigma}{e\mu} \tag{5.13}$$

where σ is ionic conductivity, k_b is Boltzmann constant (1.38 x 10^{-23} J K^{-1}) , T is ambient temperature in Kelvin (303 K), $\tau_2 = 1/\omega_2$ also being the minimum imaginary impedance with ω_2 correspond to the angular frequency, e is electric charge constant with a value of 1.602 x 10^{-19} C, k_2 is capacitance k_2^{-1} that obtained from the Cole-Cole plot, ε_o is permittivity constant (8.85 x 10^{-14} F cm^{-1}), A is area of the sample, ε_r is obtained from dielectric constant data from previous section and σ is ionic conductivity of SBEs system. However, equation (5.11) only valid for Cole-Cole consist of semicircle and title spike. The value of D for Cole-Cole plot containing only title spike can be expressed as (I. M. Noor, 2016):

$$D = D_o exp^{[-0.0297\,(ln(D_o))^2 - 1.4348\,(ln(D_o)) - 14.504]} \tag{5.14}$$

where D_o is

$$D_o = \frac{4{k_2}^4 d^2}{R^4 {\omega_2}^3} \tag{5.15}$$

where d is thickness of electrolyte and R is bulk resistance. The value of η, μ and D obtained from fitting method and deconvoluted FTIR were listed in Table 5.5 and 5.6, respectively. As observed in both tables, the values of η, μ and D of the charge carriers

obtained from fitting method follows results obtained from deconvolute FTIR pattern. These methods also get supported with finding by (A. K. Arof et al., 2014; Fadzallah et al., 2016; N. A. M. Noor & Isa, 2019).

Table 5 5 Transport parameter of CMC-PVA-NH_4Br based biopolymer electrolytes obtained from fitting method.

Sample	Mobile ion, η (cm^3)	Ionic mobility, μ ($cm^2V^{-1}s^{-1}$)	Diffusion coefficient, D (cm^2s^{-1})
AB5	1.10×10^{22}	4.25×10^{-9}	1.11×10^{-10}
AB10	2.87×10^{22}	4.44×10^{-9}	1.16×10^{-10}
AB15	4.15×10^{22}	4.52×10^{-9}	1.18×10^{-10}
AB20	7.34×10^{22}	2.72×10^{-8}	7.11×10^{-10}
AB25	9.27×10^{22}	1.36×10^{-8}	3.55×10^{-10}
AB30	1.04×10^{23}	8.59×10^{-9}	2.24×10^{-10}
AB35	1.24×10^{23}	4.10×10^{-9}	1.07×10^{-10}

Table 5 6 Transport parameter of CMC-PVA-NH_4Br based biopolymer electrolytes obtained from FTIR deconvolution method.

Sample	Mobile ion, η (cm^3)	Ionic mobility, μ ($cm^2V^{-1}s^{-1}$)	Diffusion coefficient, D (cm^2s^{-1})
AB5	3.96×10^{23}	1.60×10^{-10}	4.18×10^{-12}
AB10	7.62×10^{23}	1.68×10^{-10}	4.38×10^{-12}
AB15	9.34×10^{23}	2.01×10^{-10}	5.26×10^{-12}
AB20	1.11×10^{24}	1.81×10^{-9}	4.73×10^{-11}
AB25	4.96×10^{25}	2.54×10^{-11}	6.65×10^{-13}
AB30	2.66×10^{27}	3.38×10^{-13}	8.84×10^{-15}
AB35	1.86×10^{31}	2.74×10^{-17}	7.16×10^{-19}

In general, the ionic conductivity totally reflected with the μ equation, however, in the present system it shown value of η shows an increasing pattern as the NH_4Br concentration were increased meanwhile the μ and D are observing to be aligned with the ionic conductivity trend (N. H. B. Ahmad & M. I. N. B. M. Isa, 2015; A. S. Samsudin & M. I. N. Isa, 2012). The number of mobile ions keeps increasing even-thought ionic conductivity decrease for sample above AB20 and this phenomenon might be due to a number of mobile ions had achieved optimum value at highest conductivity sample. In addition, at high NH_4Br concentration will turn the overcrowding H^+ and huge amount of trapped ions need more energy in order to hopping form one site to another, thus, lead to decreasing in ion diffusion and ionic mobility of the present system (Ramlli & Isa, 2016). It also supported by FTIR and XRD analysis at discussed in previous section were H^+ ions from NH_4Br interact towards COO^- of polymer blend CMC-PVA more efficiently as the sample becomes more amorphous which resulting the enhancement of ionic conductivity along with transport properties until reach the optimum value. The drop of μ and D at high concentration can be justified as in the present electrolyte system have been full with overcrowded H^+ ions dissociated from NH_4Br (Ramesh & Ng, 2009; A S Samsudin et al., 2011). The overcrowded ions then cause high crystallinity phase which then create the blocking pathway and make the movement of ions between one site to another in host polymer difficult. In turn, high energy value is needed for ion to migrate from one site to another site.

5.7 Transference Number Measurement Analysis (TNM)

Electronic and ionic transference number measurement is conducted in order to determine the mechanism of conducting species of the SBEs systems, indicating the ionic conductivity of the sample either being more cationic than anionic or otherwise (Azlan & Isa, 2011). Normalized polarization current, I versus time, t for all SBEs system is plotted in Figure 5.16. It can be observed from Figure 5.16 that the decrement initial total current, I_i correspond to the increased of time until become saturated and constant in the fully depleted situation. At the steady state, electrons migrate across the electrolyte and interfaces and triggered cell to polarize and current to flows. This is might be occurred due to ionic currents passing through an ion-blocking electrode fall drastically with time

if the electrolyte is primary ionic (Koksbang & Skou, 1995; Sundaramahalingam, Nallamuthu, Manikandan, Vanitha, & Muthuvinayagam, 2018). Since ionic can be attributed to cation and anion, the possible ionic mobility in biopolymer electrolyte systems might due to H^+ or NH_3^+ or NH_4^+ or Br^- which believed from NH_4Br (M. N. Hafiza, Muhamaruesa, & Isa, 2017).

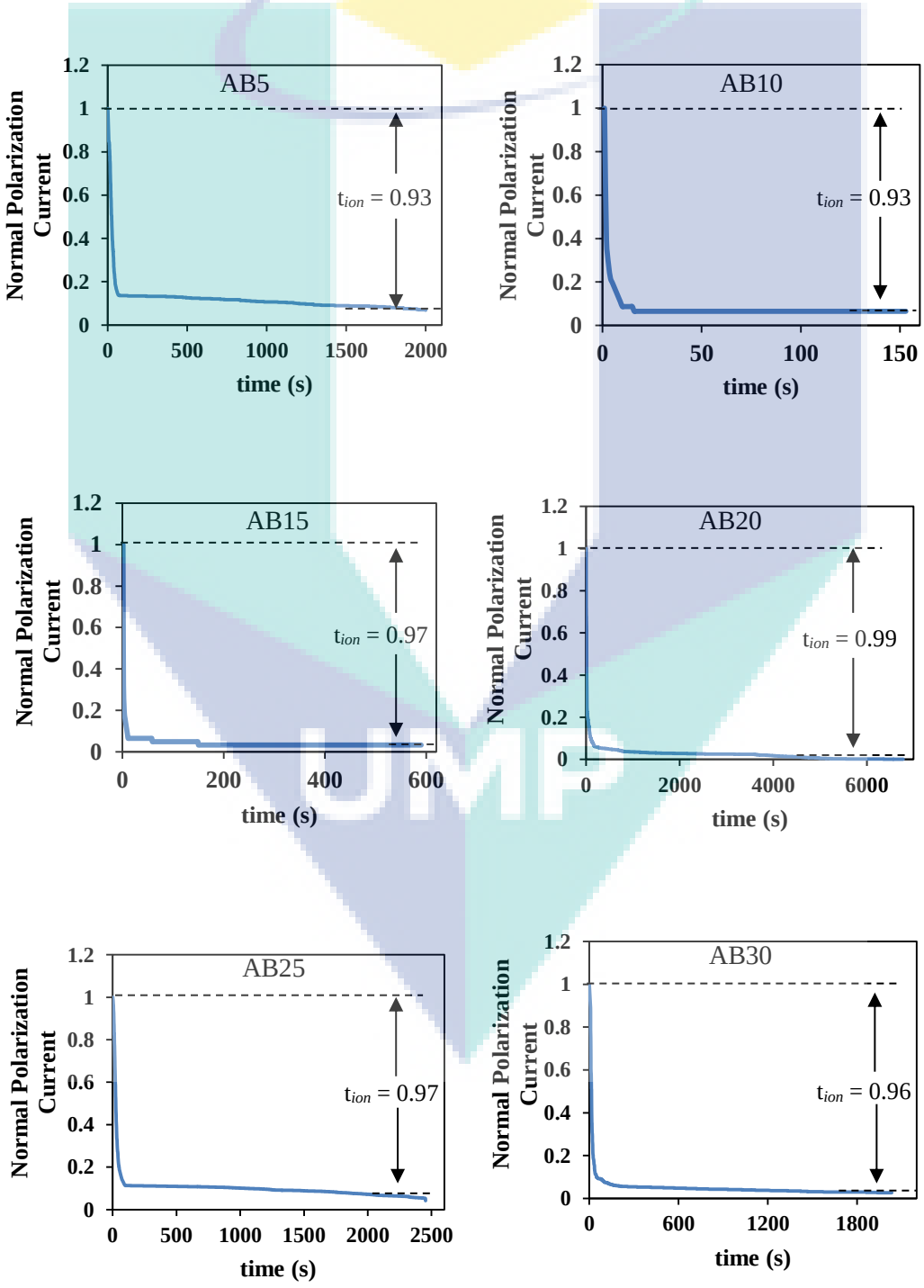

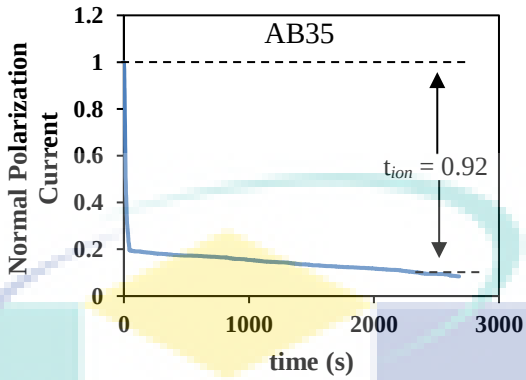

Figure 5 16 Polarization current as a function of time for all SBEs system at varied amount of NH_4Br.

From the graph of normal polarization current versus time, the transference numbers can be calculated using the equations of

$$t_{ion} = \frac{I_i - I_f}{I_i} \tag{5.16}$$

$$t_{ion} = \frac{I_f}{I_i} \tag{5.17}$$

where I_i is the initial current and I_f is the final current (Hema et al., 2007; Muthuvinayagam & Gopinathan, 2015; Selvalakshmi, Vijaya, Selvasekarapandian, & Premalatha, 2017). The incorporation of NH_4Br into the polymer blends CMC-PVA biopolymer electrolyte systems led to an increase in ionic transference number (t_{ion}) which due to cation from NH_4Br increases as increase the concentration (Cheng, Zhu, Huang, Lu, & Yang, 2007). The present systems has comparative study with previous work reported by Samsudin et al. (A S Samsudin et al., 2011) where the biopolymer electrolyte systems based CMC-NH_4Br is more cationic than anionic conductor.

From Figure 5.16 reveals t_{ion} obtained for all samples (AB5 to AB35) is at range of 0.92 to 0.99 thus shows almost absolute ionic conductor. The finding result is in line with earlier literature (M. F. Shukur & M. F. Z. Kadir, 2015; Vijaya et al., 2013) that found the values of t_{ion} in the range of 0.91 to 0.98. Moreover, it is detected sample with highest ionic conductivity value (AB20) possess the highest value of t_{ion} with 0.99 which is follows ionic conductivity trend. This can be considering that the charge transport in the present systems is predominantly ions (Achari, Reddy, Sharma, & Rao, 2007; Dhatarwal et al., 2018).

5.7.1 Cation Studies

Further studies on cationic transference number (t_{H^+}) was carried out in order to confirm the t_{H^+} ion conduction in polymer blend CMC-PVA doped with 20 wt. % biopolymer electrolyte system. It is also an important study to investigate the performance of the SPE film from its application point of view (Manjuladevi et al., 2017). H^+ transport number was identify via combination of complex impedance and transference number measurement. The current relation curve during dc polarization

and complex impedance after polarization for SBE containing AB20 using reversible electrodes were potrys in Figure 5. 17and 5.18, respectively.

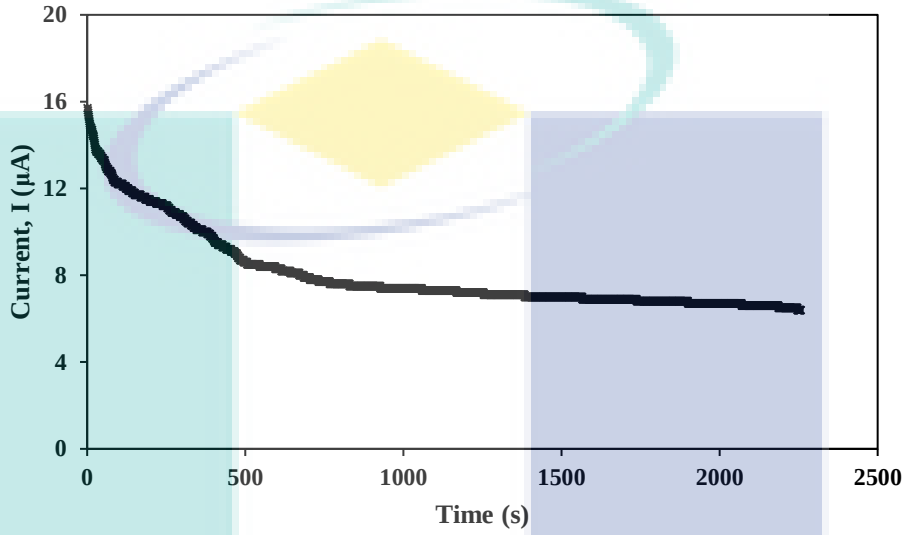

Figure 5 17 Current relaxation curve during dc polarization

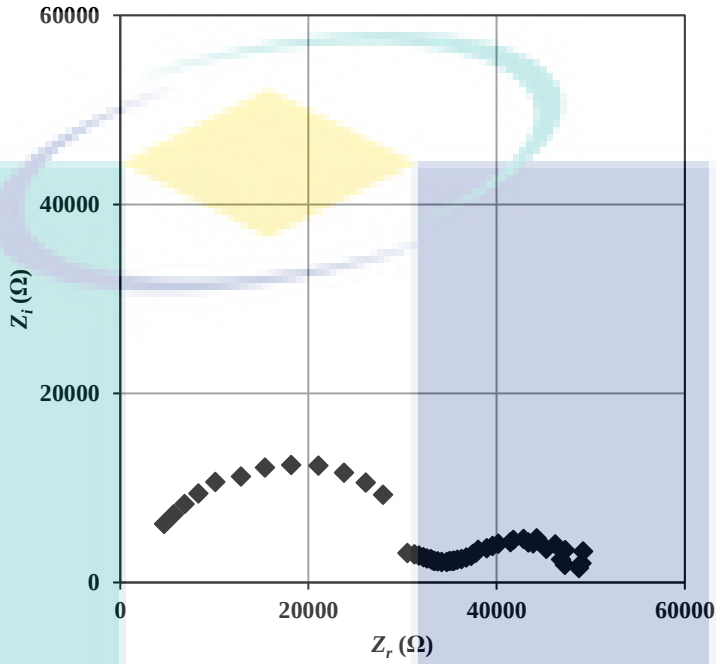

Figure 5 18 Complex impedance diagram for CMC-PVA+20 wt. % NH_4Br biopolymer electrode using non-blocking maganese electrode.

From the curves, the cationic transference number was calculated via the following equation (Bhargav et al., 2009; Manjuladevi et al., 2017):

$$t_{H^+} = \frac{R_b}{\left(\frac{\Delta V}{I_{ss}}\right) - R_c} \tag{5.18}$$

where R_b is bulk resistance (3.41 x 10^4 Ω), R_c is the resistance of electrode/electrolyte interface (1.46 x 10^4 Ω), ΔV is the potential voltage applied in DC and I_{ss} is current at steady state. (Watanabe & Nishimoto, 1995) have pointed out that this method will not give the exact value of cation transport number in a condition where ionic association occurred in the polymeric network as it is likely to happen in such a relatively low polarity media.

The CMC-PVA+20 wt. % NH_4Br biopolymer electrolyte was sandwiched between two manganese electrodes. In present work, manganese was chosen as reversible electrode since proton is expected to be a mobile species in the polymer blend complex. In addition, manganese is widely used as electrode for intercalation of proton in proton batteries (M. F. Z. Kadir et al., 2010; Ng & Mohamad, 2006; A. S. Samsudin et al., 2014; Shukur et al., 2013). The semicircle curve as shown in Figure 5.18 is attributed to the reversible nature of the manganese electrodes and hence has confirms the H^+ ion conduction in the biopolymer electrolyte (Kumar, Hashmi, & Pandey, 2011). The value of cation transference number is calculated to be 0.31, suggesting that total ionic conduction is predominantly anionic conduction. Based on finding work reported by (Geiculescu et al., 2006), the transference number for cation never reached unity value indicates that even for very large and multiply charged anions, there is still contribution of an anionic to the overall ionic conductivity. (H. J. Woo et al., 2011) reported poly(ϵ-caprolactone) incorporated with NH_4SCN possess $t_H{}^+$ value of 0.21 while (Bhargav et al., 2009) reported polyvinyl alcohol shows $t_H{}^+$ value of 0.27.

5.8 Performance of Electrical Double Layer Capacitor (EDLC)

5.8.1 Linear Sweep Voltammetry Analysis (LSV)

LSV measurement was carried out in present work in order to investigate tha stability of electrochemical operating window of the highset conducting CMC-PVA-NH_4Br SBE for device application (Shukur et al., 2013; M. F. Shukur, R. Ithnin, & M. F. Z. Kadir, 2014a). The electrochemical stability which also known as working cell potential range of SBE is one of the important parameter insight to be applied for its application in electrochemical devices such as any storage energy and proton

battery (N. A. M. Noor & Isa, 2019; A. S. Samsudin et al., 2014). Figure 5.19 plotted the potential window for sample containing AB20.

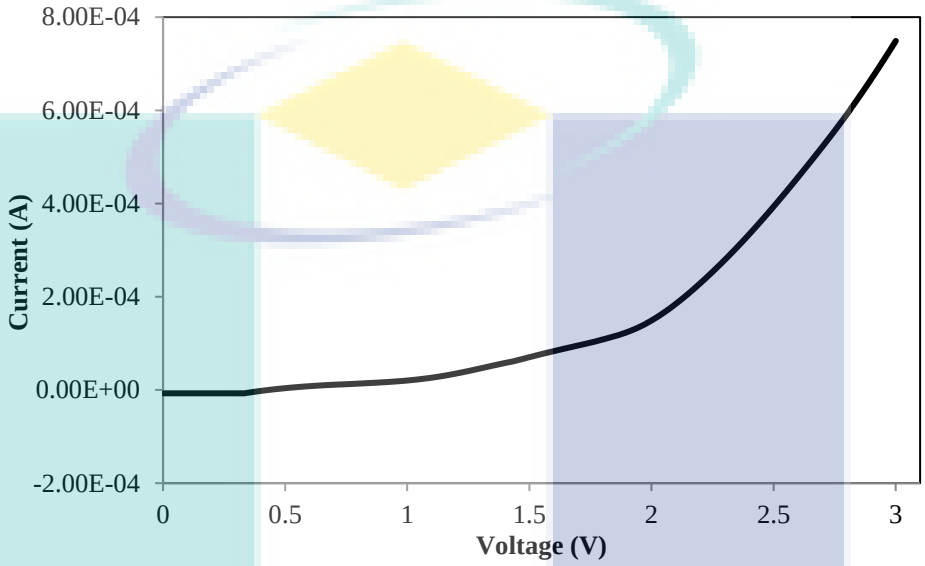

Figure 5 19 LSV response of SBE system of highest ionic conductivity.

It can be seen from Figure 5.19, there is no obvious current is detected through the electrode potential from open circuit potential to 1.55 V. The electrochemical stability of polymer blend CMC-PVA doped with AB20 biopolymer electrolyte was found to be stable up to 1.55 V on the stainless-steel electrodes. In addition, the current onset was observed at 1.55 V which indicating at that point the breakdown voltage of biopolymer electrolyte have occurred (Kadir & Arof, 2011). The present finding is in good agreement with previously reported by (Y. M. Yusof et al., 2014) where polymer blend PVA-chitosan doped with NH_4Br possess the breakdown voltage to be at 1.57 V. Further, (Kadir & Arof, 2011) also reported their work on PVA-chitosan blend polymer electrolyte membrane containing NH_4NO_3 exhibited the breakdown voltage of ~1.70 V at ambient temperature. The operating window voltage for SBE containing AB20 revealed the significant value which suitable to be applied as devices such as energy storage and protonic batteries since the minimum requirement electrochemical window for device is ~1 (Ng & Mohamad, 2008; Pratap, Singh, & Chandra, 2006; Rauh, 1999).

5.8.2 Cyclic Voltammetry Analysis (CV)

The performance of the most conducting biopolymer electrolyte based polymer blend CMC-PVA doped NH_4Br system as application in energy storage was investigate via cyclic voltammetry (CV). Figure 5.20 potrays the CV curve for SBE system at different scan rate from 2 to 50 mV s^{-1}.

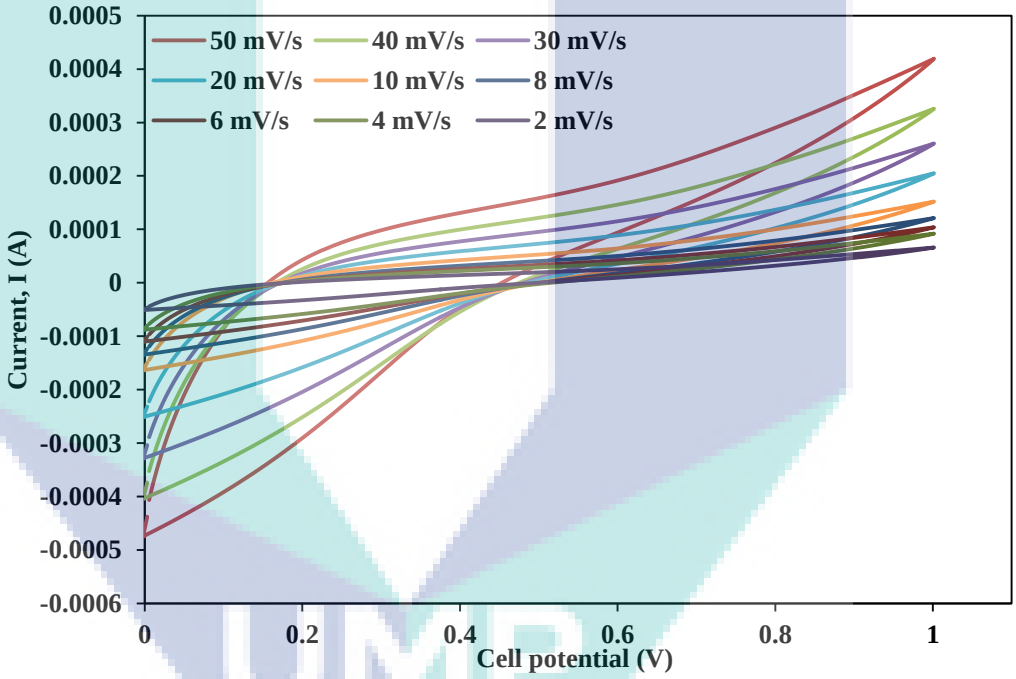

Figure 5 20 Cyclic Voltammetry of the highest conducting SBE at vary scan rate.

It can be observed from Figure 5.20 that the CV curve become thinner when low current density was applied, indicating the stored charge on the electrode surface decrease, in turn enhance the energy loss (M. F. Shukur & M. F. Z. Kadir, 2015). Moreover, there is no catiodic and anionic peaks were detected in all CV curve and this situation is suggested might be due to materials type used in present work. From CV curve, the specific capacitance, C_{sp} can be determined and the values were tabulated in Table 4.8. The C_{sp} were calculated using follows relation (W. Chen,

Beidaghi, et al., 2010; W. Chen, Fan, Gu, Bao, & Wang, 2010; M. H. Hamsan, M. F. Shukur, & M. F. Z. Kadir, 2017; M. F. Shukur et al., 2014a; M. F. Shukur & M. F. Z. Kadir, 2015):

$$C_{sp} = \int_{V_1}^{V_2} \frac{I(V)dV}{2(V_2 - V_1)mv} \tag{5.19}$$

where I (V) is the area under the graph which measured in OriginPro 8 sofware, (V_2 – V_1) is the potential window, m is the mass of activated carbon electrode in gram and v is the potential scan rate (Vs^{-1}). It is noticeable in Table 5.7, the C_{sp} value decrease as scan rate increase and these phenomenon can be explained as the inaccessible portion for ion to diffuse at the electrode/electrolyte interface (Nadiah et al., 2017). The C_{sp} of lowest scan rate possess higher value with 7.82 F g^{-1}.

Table 5 7 List of specific capacitances obtained from CV curve.

Scan rate (mV s^{-1})	**C_{sp} (F g^{-1})**
2	7.82
4	5.37
6	4.21
8	3.84
10	3.07
20	2.71
30	2.32
40	2.16
50	2.07

In addition, the results were found that the ionic conductivity can influence the C_{sp} value since the most conducting sample can promote more mobile charge carrier with

high mobility transported in the high conductive polymer matrix. Thus, it can enhance the formation of double layer and improve the energy storage capability in energy storage application. (Liew et al., 2016b) also support the present finding where the most conducting biopolymer electrolyte infers high ionic transportation within the polymer matrix. Furthermore, large amounts of free ions would be transported in the biopolymer electrolytes and then absorbed onto the carbon pore forming charge accumulation at the electrode/electrolyte region. This situation thus leads to formation of electrical double layer (Francis et al., 2016).

5.8.3 Galvanostatic Charge-Discharge Analysis (GCD)

Further study on charge discharge performance of highest conducting electrolytes based polymer blend CMC-PVA doped NH_4Br was carried out. Figure 5.21 demonstrate the GCD curve of SBE system at different current density and selected specific capacitance and ESR value versus current density. It can be seen clearly from Figure 5.21(a) that at discharge curve, the abrupt jump in voltage increase when high current density were applied in present work. The abrupt jump at discharge curve known as internal resistance (IR). In order to investigate the performance of charge discharge, the equivalent series resistance (ESR) have been calculated and plotted in Figure 5.21(b). It can be noticeable that the ESR value is in inversely proportional to specific capacitance where current density with 0.1 mA g^{-1} exhibits the lowest ESR value and highest in specific capacitance. It can be explained that at high current density, the heat dissipated may cause a significant temperature rise, affect the operation of the circuit and degrade the capacitor, resulting ESR to increase. Further, a significant amount of voltage drop occurs across the resistance have reduce the portion of the useful energy in the application. In addition, a high ESR value

degrades the performance might be attributed to the I^2R losses, noise and higher voltage drop.

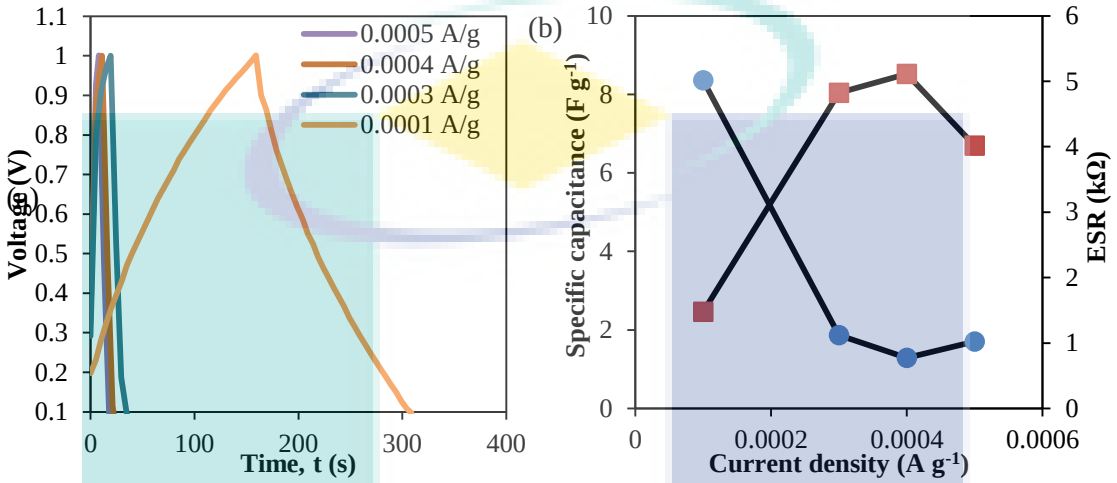

Figure 5 21 (a) GCD plot for varied current density and (b) specific capacitance and ESR versus current density of highest conducting sample.

Figure 5.22 illustrates a typical galvanostatic charge-discharge curve of EDLC comprising of the most conducting biopolymer electrolyte at selected cycles with current density of 0.1 mA g^{-1}. It can be observed that the cell potential limits were set to be between 0 to 1 V. However, the cell potential was started at 0.18 V in this study, indicating that the internal resistance of the cell which increase from the interface of electrode/electrolyte and polymer electrolyte (Arof et al., 2012; Mitra, Shukla, & Sampath, 2001). Similar cases in sudden drop of voltage at discharge curve due to existance of these resistance during the process. On other hand, the internal resistance or commanly called as ohmic loss also triggered due to active materials and inter fluid between the current collector in SBEs system (M. Shukur & M. Kadir, 2015). Further, the increment of internal resistance contribute the amount of mobile charge carrier to increase which in turn depletion of polymer electrolyte. According to (Arof et al.,

2012), they have reported that the internal resistance can be reduced by increasing the percentage efficiency of EDLC more than 90%.

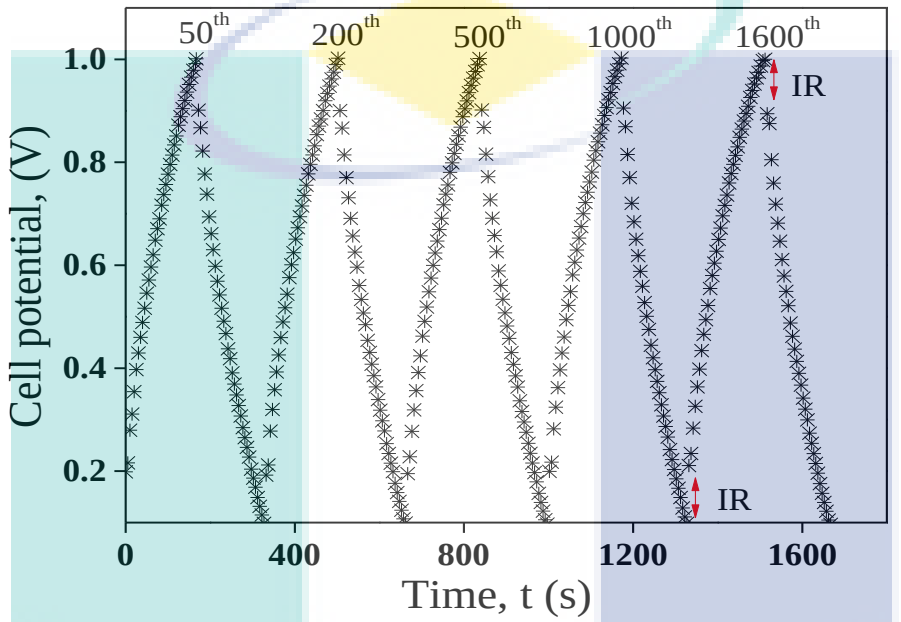

Figure 5 22 Charge-discharge performances of EDLCs at selected cycles.

The specific capacitance and ESR of EDLC for current density of 0.1 mA g^{-1} was plotted in Figure 5.23. It is noticeable the long term cycling performance of EDLC cell containing SBE system with 20 wt.% NH_4Br up to 1600 cycles and the specific capacitance shows almost constant value, which confirms the fabricated EDLC capacitive behavior (S. Hashmi, Kumar, & Tripathi, 2007; M. Shukur & M. Kadir, 2015). The finding has found the specific capacitance in this work to be at ~8.35 F g^{-1} and have potential to be applied in energy storage application using present work material (Arof et al., 2012). (Yusof, Majid, Kasmani, Illias, & Kadir, 2014) have reported the specific capacitance for EDLC cell with starch-chitosan-NH_4I-glycerol polymer electrolyte is 1.82 F g^{-1}, which is lower than in this work. In other hand,

(Sudhakar & Selvakumar, 2012) have studied that few ions still remain in the polymer matrix during charging time, subsequently effects the charge-discharged process.

Furthermore, there have been several studies in the literature reporting that the value of specific capacitance relies on conductivity (Liew, Ramesh, & Arof, 2014a; Lim, Teoh, Liew, & Ramesh, 2014; Pandey, Kumar, & Hashmi, 2010). The relationship between C_{sp} and conductivity is suggested due to ionic mobility plays important parameter in transport properties, thus can influence the performance of EDLC (Yu, Chabot, & Zhang, 2013). From impedance study earlier, the ionic conductivity was recorded to be at 3.21 x 10^{-4} S cm^{-1} for sample containing 20 wt. % of NH_4Br at room temperature. The result is in the lines of earlier literature (M. F. Shukur, R. Ithnin, & M. F. Z. Kadir, 2014c) that found the C_{sp} value for polymer electrolyte based starch-chitosan-NH_4Br as application in EDLC device is 1.17 F g^{-1} possess highest ionic conductivity of 9.72 x 10^{-5} S cm^{-1}. The finding further get agreement with result reported by (S. R. Majid, 2007) where chitosan-H_3PO_4 doped

NH_4NO_3 based polymer electrolyte revealed the ionic conductivity of 10^{-4} S cm^{-1} shows the C_{sp} to be at 0.216 to 0.220 F g^{-1}.

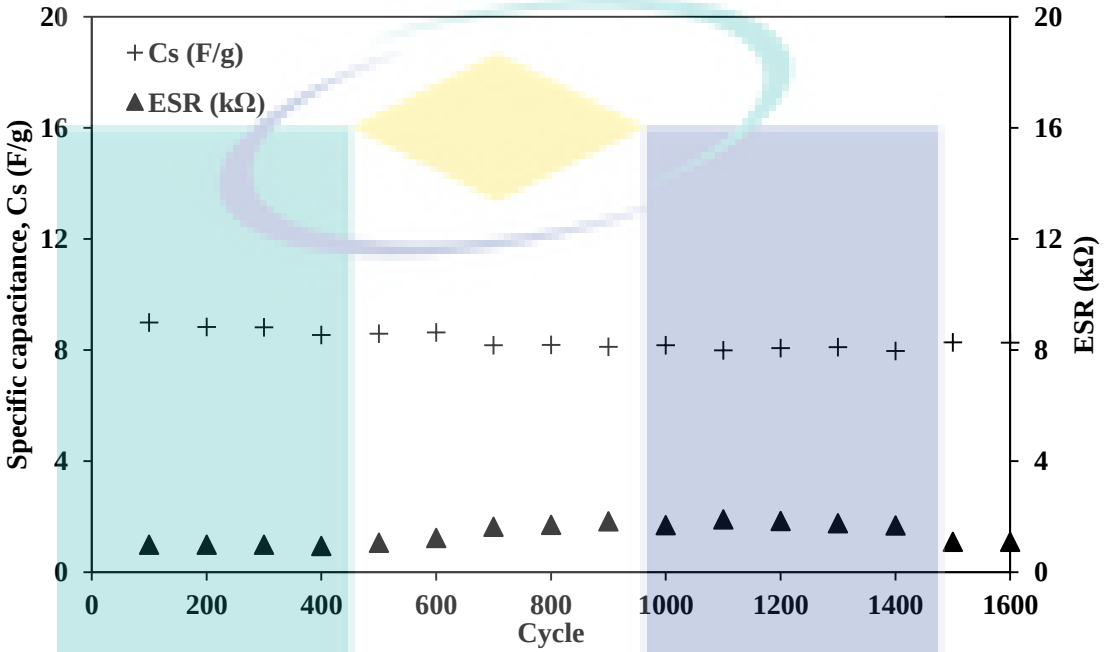

Figure 5 23 Specific capacitance and ESR performance for 20 wt. % NH_4Br electrolytes at 0.1 mA g^{-1}.

Moreover, ESR also have correlation with conductivty where lowest ESR gives higher in conductivity (Lim et al., 2014). This situation can be expalined as concentaration of ions from electrolytes and electrical conductivity from the electrode. The ESR is calculated from voltage drop and has found the to be at ~1.48 kΩ in present work. From the ESR value plotted in Figure 5.23, it is observed these value to be almost consistent, suggesting that the nature of cations in the biopolymer electrolyte containing varied salts does not significantly affects the internal resistance of the EDLC (S. Hashmi et al., 2007). Figure 5.24 demonstrate the power density and energy density versus number of cycles using current density of 0.1 mA g^{-1}. The values of power density and energy density has been evaluated and were observed to be at ~1.94 kW kg^{-1} and ~3.05 Wh kg^{-1}, respectively. The comparative study of energy density and power density between proton battery and supercapacitor with previous research (Ambika et al., 2018;

M. H. Hamsan et al., 2017; Johari, Kudin, Ali, Winie, & Yahya, 2009; Liew et al., 2014a; Samsudin & Isa, 2015; N. E. A. Shuhaimi, L. P. Teo, H. J. Woo, S. R. Majid, & A. K. Arof, 2012) which using H^+ ions as carrier was carried out and plotted in Figure 5.25. It could say that the present work was comparable with other previous works and have potential to be use in energy storage application since it gives higher value in energy density and power density.

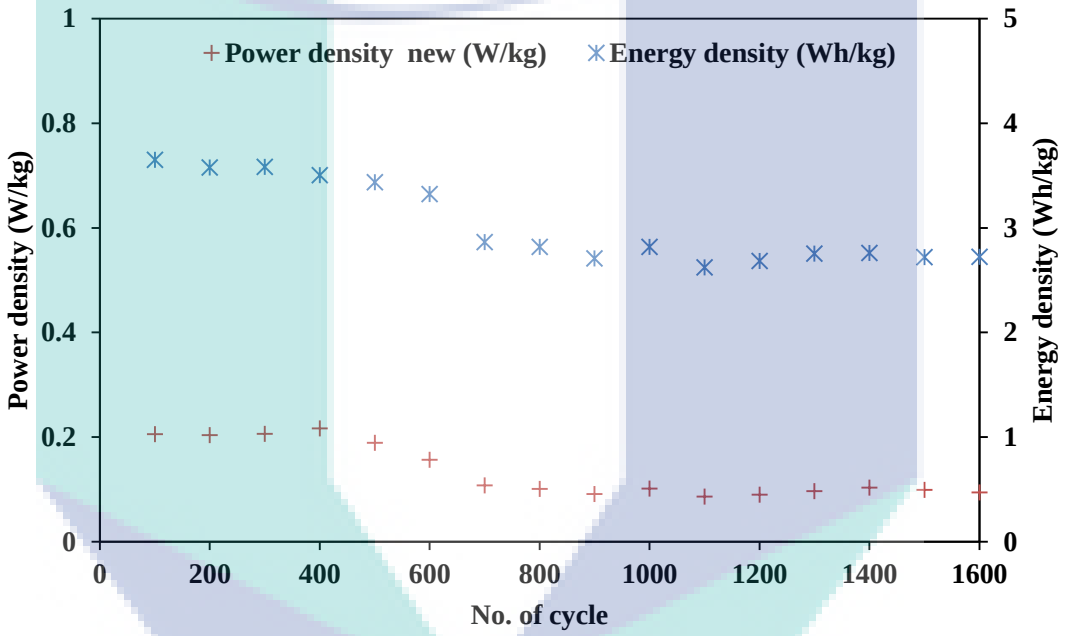

Figure 5 24 Power density and energy density versus number of cycles of cell EDLC.

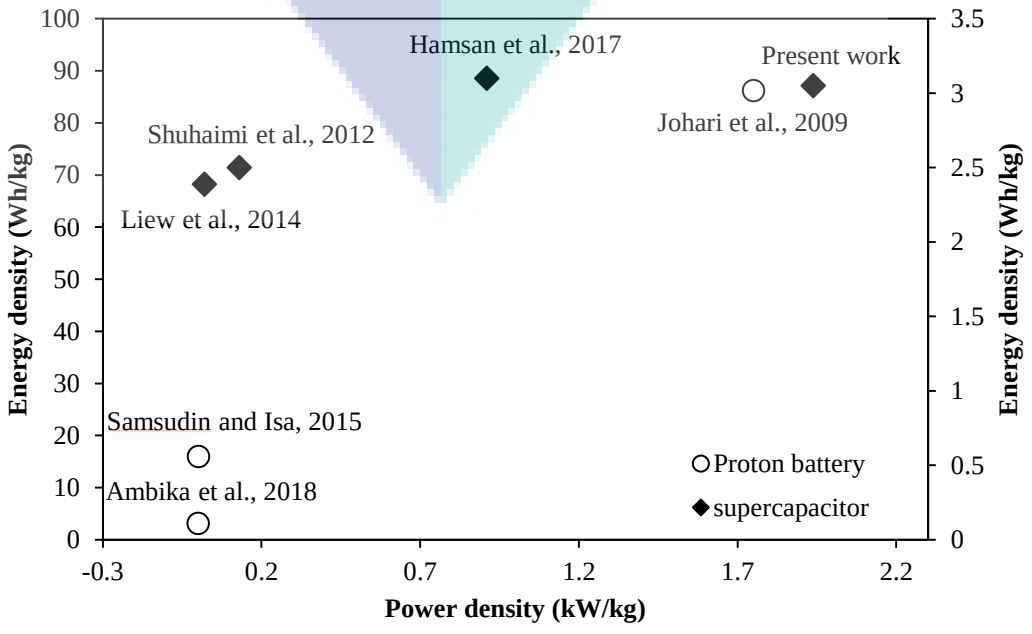

Figure 5 25 Comparable studies of energy density and power density from previous research

CHAPTER 6

CONCLUSION AND RECOMMEDATIONS

6.1 Conclusion

The present study was designed to determine the performance of materials used as biopolymer electrolytes (SBEs) to be applied in energy storage application and has confirms its capability in EDLC. The present work has been characterized to study the electrical and structural properties of solid biopolymer electrolytes.

As a conclusion, a new system have been discovered and successfully prepared by solution casting technique containing CMC-PVA doped with various amount of NH_4Br based biopolymer electrolytes. The SBEs film prepared shows transparent and clear without phase seperation. The amorphous nature and interaction between polymer blend CMC-PVA with NH_4Br were investigated via FTIR spectroscopy analysis and XRD analysis to correlate the ionic conductivity of SBEs. FTIR analysis reveals the complexation happen when NH_4Br was incorporated in polymer blend CMC-PVA by protonation (H^+) which suggesting has take place at carboxylate anion (COO-) group of pure CMC. The interaction between polymer blend host and dopant

salt was suggested as shown in Scheme 6.1. Further, FTIR analysis also has proven these interaction occurred via Grotthus mechanism.

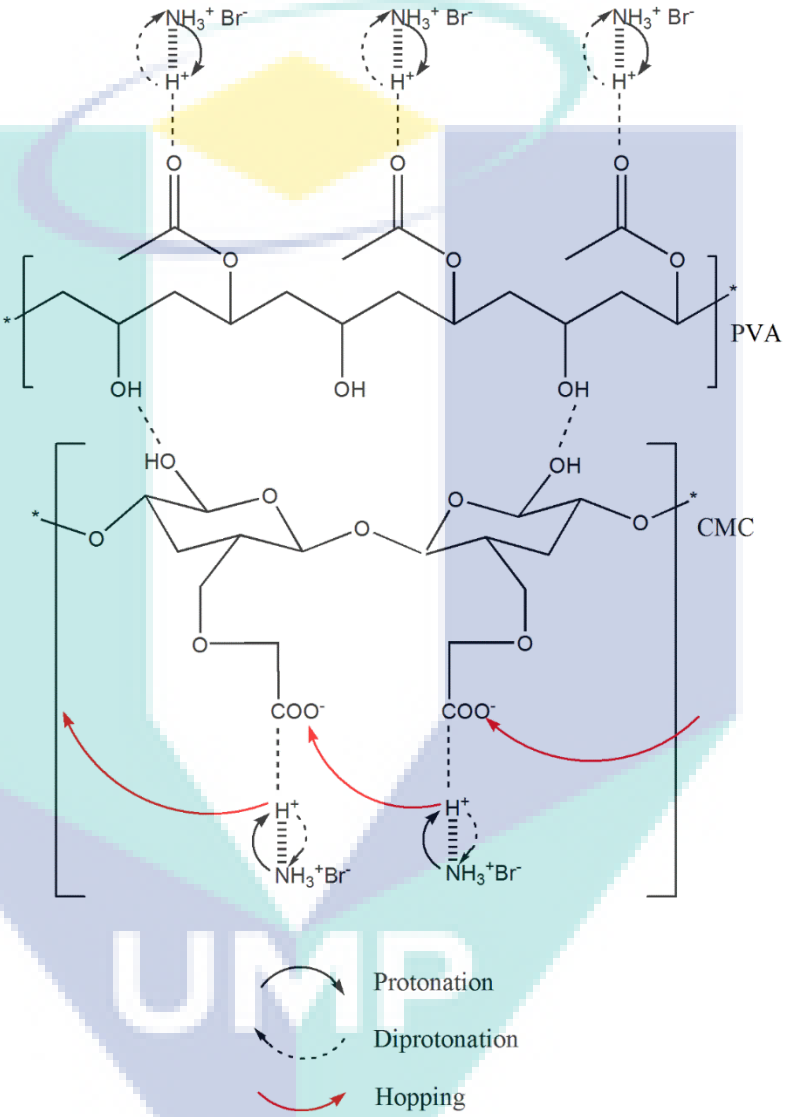

Scheme 6 1 Schematic diagram of interaction between CMC-PVA and NH_4Br.

The XRD peak intensity shows a gradully decrease upon addition of 5 wt. % NH_4Br due to an improvement in the amorphous nature of the SBE, thus discovered the intermolecular H-bonding leads the degree of crystallinity to reduced. The crystallite size of all SBEs have been calculated and has confirms sample with AB20 shows the amorphous phase. TGA results exhibits the thermal stability of polymer

blend CMC-PVA has been increased by the introduction of NH_4Br. The thermogravimetric analysis has proved that the effect of NH_4Br in polymer blend host has increase the decomposition temperature, T_d and decrease the total weight loss, resulting in the enhancement of thermal stability in SBEs. The lowest glass transition temperature, T_g value given by AB20 is another proof that AB20 is highly amorphous compared to other amount of NH_4Br.

The incorporation of different amount NH_4BR which acts as dopant salt in polymer blend CMC-PVA improved the ionic conductivity in biopolymer electrolytes. Present work has revealed the highest ionic conductivity is 3.21×10^{-4} S cm^{-1} for sample containing 20 wt. % of NH_4Br at room temperature. The ionic conductivity increase at low amount of dopant salt can be attributed to the charge carrier increase. While decline in ionic conductivity at high amount of NH_4Br is suggested due to formation ion pairs that form neutral species, in turn deductes number of free ions, consequently reduces the ionic conductivity. The temperature dependence of all SBE systems follows Arrhenius behaviour and thermally activated. The most conducting electrolytes indicates the lowest activation energy of 0.08 eV, suggesting ions to move freely and does needs more energy for ions to hop from one site to another site in polymer backbone. The frequency dependence of both dielectric modulus were found to be non-Debye type.

Further studies on transport properties was carried out via deconvoluted FTIR method and fitting method from cole-cole plot. Both method reveals the number of ions mobility and diffusion coefficient can influence ionic conductivity behavior. In addition, TNM results has obtained the maximum total t_{ion} was 0.99, while t_{H^+} was 0.31 for the most conducting electrolyte. The stability of electrochemical windows has been investigated via LSV and has observed the voltage breakdown at 1.55 V. The EDLC cell containing CMC-PVA doped 20 wt. % NH4Br exhibits the specific capacitance value of 7.82 F g^{-1} which obtained from CV analysis for scan rate 2 mV s^{-1}. The charge discharged performance of EDLC further was characterized via GCD analysis and has found to be stable up to 1600 cycles. The specific capacitance

obtanined from GCD curve was ~8.35 F g^{-1}. The higher in ionic conductivity is believed can influence the increment of specific capacitance value in present work. The abrupt jump in voltage at discharge process elucidated as due to ohmic loss. The power density and energy density has been calculated and recorded to be ~1.94 kW kg^{-1} and ~3.05 Wh kg^{-1}, respectively. The present finding provides evidence that SBE based polymer blend CMC-PVA doped NH_4Br is a potential candidate that can be utilized for fabrication on application of EDLC.

6.2 Recommendations

For future work, a few significant steps must be improved in order to enhanced electrolyte in term of electrical, mechanical, thermal strength and physical of CMC-PVA-NH_4Br biopolymer electrolytes. Herewith some suggestions and opinions based on research finding that can be emphasized for better system in future:

- In order to enhanced the efficiency of solubility of PVA, it is recommended to use other solvent instead distilled water such as Dimethylformamide (DMF) (Sivadevi et al., 2015) and Dimethyl sulfoxide (DMSO) (Rajeswari et al., 2011).

- Enhanced the ionic conductivity via adding plasticizers. Plastiziers can be works as function of dissociate the dopant salt, thus helps increase the ability of polymer electrolytes (Osman, Ibrahim, & Arof, 2001).

- Further study can be evaluated via Field Emission Scanning Electron Microscopy (FESEM) and Density Functional Theory (DFT) characterization in order to studies in detailed the surface structure of SBEs to confirms the

homogeneity of the system. The DFT analysis can provides information of molecule structure of the polymer which can be correlated with FTIR analysis.

REFERENCES

Abbas, Q., Mirzaeian, M., Ogwu, A. A., Mazur, M., & Gibson, D. (2018). Effect of physical activation/surface functional groups on wettability and electrochemical performance of carbon/activated carbon aerogels based electrode materials for electrochemical capacitors. International Journal of Hydrogen Energy.

Abd El- Kader, F., Shehap, A., Abo- Ellil, M., & Mahmoud, K. (2005). Relaxation phenomenon of poly (vinyl alcohol)/sodium carboxy methyl cellulose blend by thermally stimulated depolarization currents and thermal sample technique. Journal of Applied Polymer Science, 95(6), 1342-1353.

Abdelgawad, A. M., Hudson, S. M., & Rojas, O. J. (2014). Antimicrobial wound dressing nanofiber mats from multicomponent (chitosan/silver-NPs/polyvinyl alcohol) systems. Carbohydrate Polymers, 100, 166-178.

Achari, V. B., Reddy, T., Sharma, A., & Rao, V. N. (2007). Electrical, optical, and structural characterization of polymer blend (PVC/PMMA) electrolyte films. Ionics, 13(5), 349-354.

Ahmad, N., & Isa, M. (2016). Characterization of un-plasticized and propylene carbonate plasticized carboxymethyl cellulose doped ammonium chloride solid biopolymer electrolytes. Carbohydrate Polymers, 137, 426-432.

Ahmad, N. H., & Isa, M. I. N. (2015a). Conduction mechanism of solid biopolymer electrolytes system based on carboxymethyl cellulose--ammonium chloride. American-Eurasian Journal of Sustainable Agriculture, 9, 1-7.

Ahmad, N. H., & Isa, M. I. N. (2015b). Structural and Ionic Conductivity Studies of CMC Based Polymerelectrolyte Doped with NH_4Cl. Paper presented at the Advanced Materials Research.

Ahmad, N. H., & Isa, M. I. N. (2016a). Characterization of un-plasticized and propylene carbonate plasticized carboxymethyl cellulose doped ammonium chloride solid biopolymer electrolytes. Carbohydrate Polymers, 137, 426-432.

Ahmad, N. H., & Isa, M. I. N. (2016b). Ionic conductivity and electrical properties of carboxymethyl cellulose-NH_4Cl solid polymer electrolytes. Journal of Engineering Science and Technology, 839-847.

Ahmad, N. H., & Isa, M. I. N. M. (2015). Conduction mechanism of solid biopolymer electrolytes system based on carboxymethyl cellulose--ammonium chloride. American-Eurasian Journal of Sustainable Agriculture, 1-8.

Ahmad, N. H. B., & Isa, M. I. N. B. M. (2015). Proton conducting solid polymer electrolytes based carboxymethyl cellulose doped ammonium chloride: ionic conductivity and transport studies. International Journal of Plastics Technology, 19(1), 47-55.

Ahmad, Z., & Isa, M. I. N. (2012). Ionics conduction via correlated barrier hoping mechanism in CMC-SA solid biopolymer electrolytes. International Journal of Latest Research in Science and Technology, 1, 2278-5299.

Aishova, A., Mentbayeva, A., Isakhov, B., Batyrbekuly, D., Zhang, Y., & Bakenov, Z. (2018). Gel polymer electrolytes for lithium-sulfur batteries. Materials Today: Proceedings, 5(11), 22882-22888.

Alakanandana, A., Subrahmanyam, A. R., & Siva Kumar, J. (2016). Structural and Electrical Conductivity studies of pure PVA and PVA doped with Succinic acid polymer electrolyte system. Materials Today: Proceedings, 3(10, Part B), 3680-3688.

Albdiry, M., & Yousif, B. (2013). Morphological structures and tribological performance of unsaturated polyester based untreated/silane-treated halloysite nanotubes. Materials & Design.

Ambika, C., Karuppasamy, K., Vikraman, D., Lee, J. Y., Regu, T., Raj, T. A. B., . . . Kim, H.-S. (2018). Effect of dimethyl carbonate (DMC) on the electrochemical and cycling properties of solid polymer electrolytes (PVP-MSA) and its application for proton batteries. Solid State Ionics, 321, 106-114.

Andersson, M. P., & Uvdal, P. (2005). New scale factors for harmonic vibrational frequencies using the B3LYP density functional method with the triple-ζ basis set 6-311+ G (d, p). The Journal of Physical Chemistry A, 109(12), 2937-2941.

Andreev, Y. G., & Bruce, P. G. (2000). Polymer electrolyte structure and its implications. Electrochimica Acta, 45(8-9), 1417-1423.

Appetecchi, G., Croce, F., Gerace, F., Panero, S., Passerini, S., Spila, E., & Scrosati, B. (1994). New concepts in primary and rechargeable solid state lithium polymer batteries. MRS Online Proceedings Library Archive, 369.

Armand, M., Endres, F., MacFarlane, D. R., Ohno, H., & Scrosati, B. (2011). Ionic-liquid materials for the electrochemical challenges of the future. In Materials For Sustainable Energy: A Collection of Peer-Reviewed Research and Review Articles from Nature Publishing Group (pp. 129-137): World Scientific.

Armstrong, R. D., Dickinson, T., & Willis, P. M. (1974). The AC impedance of powdered and sintered solid ionic conductors. Journal of electroanalytical Chemistry and interfacial electrochemistry, 53(3), 389-405.

Arof, A., Amirudin, S., Yusof, S., & Noor, I. (2014). A method based on impedance spectroscopy to determine transport properties of polymer electrolytes. Physical Chemistry Chemical Physics, 16(5), 1856-1867.

Arof, A. K., Amirudin, S., Yusof, S. Z., & Noor, I. M. (2014). A method based on impedance spectroscopy to determine transport properties of polymer electrolytes. Physical Chemistry Chemical Physics, 16(5), 1856-1867.

Arof, A. K., Kufian, M. Z., Syukur, M. F., Aziz, M. F., Abdelrahman, A. E., & Majid, S. R. (2012). Electrical double layer capacitor using poly (methyl methacrylate)–C_4BO_8Li gel polymer electrolyte and carbonaceous material from shells of mata kucing (Dimocarpus longan) fruit. Electrochimica Acta, 74, 39-45.

Assender, H. E., & Windle, A. H. (1998). Crystallinity in poly (vinyl alcohol). 1. An X-ray diffraction study of atactic PVOH. Polymer, 39(18), 4295-4302.

Awada, H., & Daneault, C. (2015). Chemical Modification of Poly(Vinyl Alcohol) in Water (Vol. 5).

Aziz, N., Majid, S., & Arof, A. K. (2012). Synthesis and characterizations of phthaloyl chitosan-based polymer electrolytes. Journal of Non-Crystalline Solids, 358(12-13), 1581-1590.

Aziz, N. N., Idris, N., & Isa, M. (2010). Proton conducting polymer electrolytes of methylcellulose doped ammonium fluoride: Conductivity and ionic transport studies. International Journal of Physical Sciences, 5(6), 748-752.

Azlan, A. L., & Isa, M. I. N. (2011). Proton conducting biopolymer electrolytes based on tapioca starch-NH_4NO_3. Solid State Science and Technology Letters, 18(1), 124-129.

Bakar, N. Y. A., Muhamaruesa, N. H. M., Aniskari, N. A. B., & Isa, M. I. N. (2015). Electrical studies of carboxy methycellulose-chitosan blend biopolymer doped

dodecyltrimethyl ammonium bromide solid electrolytes. American Journal of Applied Sciences, 12(1), 40.

Bao, J., Qu, X., Qi, G., Huang, Q., Wu, S., Tao, C., Chen, C. (2018a). Solid electrolyte based on waterborne polyurethane and poly (ethylene oxide) blend polymer for all-solid-state lithium ion batteries. Solid State Ionics, 320, 55-63.

Bao, J., Qu, X., Qi, G., Huang, Q., Wu, S., Tao, C., Chen, C. (2018b). Solid electrolyte based on waterborne polyurethane and poly(ethylene oxide) blend polymer for all-solid-state lithium ion batteries. Solid State Ionics, 320, 55-63.

Baskaran, R., Selvasekarapandian, S., Kuwata, N., Kawamura, J., & Hattori, T. (2006). Conductivity and thermal studies of blend polymer electrolytes based on PVAc–PMMA. Solid State Ionics, 177(26-32), 2679-2682.

Becke, A. D. (1993). Density- functional thermochemistry. III. The role of exact exchange. The Journal of chemical physics, 98(7), 5648-5652.

Bertuzzi, M. A., Vidaurre, E. C., Armada, M., & Gottifredi, J. (2007). Water vapor permeability of edible starch based films. Journal of Food Engineering, 80(3), 972-978.

Bhargav, P. B., Mohan, V. M., Sharma, A. K., & Rao, V. V. R. N. (2009). Investigations on electrical properties of (PVA: NaF) polymer electrolytes for electrochemical cell applications. Current Applied Physics, 9(1), 165-171.

Böckenfeld, N., Jeong, S., Winter, M., Passerini, S., & Balducci, A. (2013). Natural, cheap and environmentally friendly binder for supercapacitors. Journal of Power Sources, 221, 14-20.

Bose, P., Deb, D., & Bhattacharya, S. (2019). Lithium-polymer battery with ionic liquid tethered nanoparticles incorporated P (VDF-HFP) nanocomposite gel polymer electrolyte. Electrochimica Acta.

Brandt, A., & Balducci, A. (2014). Theoretical and practical energy limitations of organic and ionic liquid-based electrolytes for high voltage electrochemical double layer capacitors. Journal of Power Sources, 250, 343-351.

Buraidah, M., & Arof, A. (2011a). Characterization of chitosan/PVA blended electrolyte doped with NH4I. Journal of Non-Crystalline Solids, 357(16-17), 3261-3266.

Buraidah, M., & Arof, A. (2011b). Characterization of chitosan/PVA blended electrolyte doped with NH 4 I. Journal of Non-Crystalline Solids, 357(16), 3261-3266.

Buraidah, M., Teo, L., Majid, S., & Arof, A. (2009). Ionic conductivity by correlated barrier hopping in NH4I doped chitosan solid electrolyte. Physica B: Condensed Matter, 404(8-11), 1373-1379.

Burke, A. (2000). Ultracapacitors: why, how, and where is the technology. Journal of Power Sources, 91(1), 37-50.

Chai, M. N., & Isa, M. I. N. (2011). Carboxyl methylcellulose solid polymer electrolytes: Ionic conductivity and dielectric study. J. Curr. Eng. Res, 1(2), 23-27.

Chai, M. N., & Isa, M. I. N. (2012). Investigation on the conduction mechanism of carboxyl methylcellulose-oleic acid natural solid polymer electrolyte. International Journal of Advanced Technology & Engineering Research, 2(6), 36-39.

Chai, M. N., & Isa, M. I. N. (2013). Electrical characterization and ionic transport properties of carboxyl methylcellulose-oleic acid solid polymer electrolytes. International Journal of Polymer Analysis and Characterization, 18(4), 280-286.

Chai, M. N., & Isa, M. I. N. (2016). Novel proton conducting solid bio-polymer electrolytes based on carboxymethyl cellulose doped with oleic acid and plasticized with glycerol. Scientific reports, 6, 27328.

Chai, M. N., Ramlli, M. A., & Isa, M. I. N. (2013). Proton conductor of propylene carbonate–plasticized carboxyl methylcellulose–based solid polymer electrolyte. International Journal of Polymer Analysis and Characterization, 18(4), 297-302.

Chen, J., Asano, M., Maekawa, Y., & Yoshida, M. (2008). Fuel cell performance of polyetheretherketone-based polymer electrolyte membranes prepared by a two-step grafting method. Journal of Membrane Science, 319(1-2), 1-4.

Chen, W., Beidaghi, M., Penmatsa, V., Bechtold, K., Kumari, L., Li, W., & Wang, C. (2010). Integration of carbon nanotubes to C-MEMS for on-chip supercapacitors. IEEE Transactions on Nanotechnology, 9(6), 734-740.

Chen, W., Fan, Z., Gu, L., Bao, X., & Wang, C. (2010). Enhanced capacitance of manganese oxide via confinement inside carbon nanotubes. Chemical Communications, 46(22), 3905-3907.

Cheng, H., Zhu, C., Huang, B., Lu, M., & Yang, Y. (2007). Synthesis and electrochemical characterization of PEO-based polymer electrolytes with room temperature ionic liquids. Electrochimica Acta, 52(19), 5789-5794.

Chew, K., Ng, T., & How, Z. (2013). Conductivity and microstructure study of PLA-based polymer electrolyte salted with lithium perchloride, LiClO4. Int J Electrochem Sci, 8(5).

Choudhary, S., & Sengwa, R. (2013). Effects of preparation methods on structure, ionic conductivity and dielectric relaxation of solid polymeric electrolytes. Materials Chemistry and Physics, 142(1), 172-181.

Coleman, M. M., & Painter, P. C. (1995). Hydrogen bonded polymer blends. Progress in Polymer Science, 20(1), 1-59.

Coleman, M. M., Skrovanek, D. J., Hu, J., & Painter, P. C. (1988). Hydrogen bonding in polymer blends. 1. FTIR studies of urethane-ether blends. Macromolecules, 21(1), 59-65. doi:10.1021/ma00179a014

Cuevas, J. C., Heurich, J., Pauly, F., Wenzel, W., & Schön, G. (2003). Theoretical description of the electrical conduction in atomic and molecular junctions. Nanotechnology, 14(8), R29.

Dai, H., & Huang, H. (2017). Enhanced swelling and responsive properties of pineapple peel carboxymethyl cellulose-g-poly (acrylic acid-co-acrylamide) superabsorbent hydrogel by the introduction of carclazyte. Journal of Agricultural and Food Chemistry, 65(3), 565-574.

Dai, H., Huang, Y., & Huang, H. (2017). Eco-friendly polyvinyl alcohol/carboxymethyl cellulose hydrogels reinforced with graphene oxide and bentonite for enhanced adsorption of methylene blue. Carbohydrate Polymers, 185, 1-11.

Daniliuc, L., & David, C. (1996). Intermolecular interactions in blends of poly (vinyl alcohol) with poly (acrylic acid): 2. Correlation between the states of sorbed water and the interactions in homopolymers and their blends. Polymer, 37(23), 5219-5227.

Debeaufort, F., Voilley, A., & Meares, P. (1994). Water vapor permeability and diffusivity through methylcellulose edible films. Journal of Membrane Science, 91(1-2), 125-133.

Deka, M., & Kumar, A. (2011). Electrical and electrochemical studies of poly (vinylidene fluoride)–clay nanocomposite gel polymer electrolytes for Li-ion batteries. Journal of Power Sources, 196(3), 1358-1364.

DeMerlis, C., & Schoneker, D. (2003). Review of the oral toxicity of polyvinyl alcohol (PVA). Food and Chemical Toxicology, 41(3), 319-326.

Dhatarwal, P., Choudhary, S., & Sengwa, R. J. (2018). Electrochemical performance of Li+-ion conducting solid polymer electrolytes based on PEO–PMMA blend matrix incorporated with various inorganic nanoparticles for the lithium ion batteries. Composites Communications, 10, 11-17.

Du, J., Bai, Y., Chu, W., & Qiao, L. (2010). Synthesis and performance of proton conducting chitosan/NH4Cl electrolyte. Journal of Polymer Science Part B: Polymer Physics, 48(3), 260-266.

Durán-Guerrero, J. G., Martínez-Rodríguez, M. A., Garza-Navarro, M. A., González-González, V. A., Torres-Castro, A., & De La Rosa, J. R. (2018). Magnetic nanofibrous materials based on CMC/PVA polymeric blends. Carbohydrate Polymers, 200, 289-296.

El-Gamal, S., El Sayed, A. M., & Abdel-Hady, E. (2017). Effect of Cobalt Oxide Nanoparticles on the Nano-scale Free Volume and Optical Properties of Biodegradable CMC/PVA Films. Journal of Polymers and the Environment, 1-10.

El-Kader, F. A., Gaafar, S., Mahmoud, K., Bannan, S., & El-Kader, M. A. (2008). Effects of the Composition Ratio, Eosin Addition, and c Irradiation on the Dielectric Properties of Poly (vinyl Alcohol)/Glycogen Blends. Journal of Applied Polymer Science, 110, 1281-1288.

El-Sawy, N., El-Arnaouty, M., & Ghaffar, A. A. (2010). γ-Irradiation effect on the non-cross-linked and cross-linked polyvinyl alcohol films. Polymer-Plastics Technology and Engineering, 49(2), 169-177.

El-Sayed, S., Mahmoud, K., Fatah, A., & Hassen, A. (2011). DSC, TGA and dielectric properties of carboxymethyl cellulose/polyvinyl alcohol blends. Physica B: Condensed Matter, 406(21), 4068-4076.

El Sayed, A., & El-Gamal, S. (2015). Synthesis and investigation of the electrical and dielectric properties of Co 3 O 4/(CMC+ PVA) nanocomposite films. Journal of Polymer Research, 22(5), 97.

Fadzallah, I., Noor, I., Careem, M., & Arof, A. (2016). Investigation of transport properties of chitosan-based electrolytes utilizing impedance spectroscopy. Ionics, 22(9), 1635-1645.

Faraji, M., & Abedini, A. (2019). Fabrication of electrochemically interconnected MoO3/GO/MWCNTs/graphite sheets for high performance all-solid-state symmetric supercapacitor. International Journal of Hydrogen Energy, 44(5), 2741-2751.

Fenton, D. (1973). Complexes of alkali metal ions with poly (ethylene oxide). Polymer, 14, 589.

Feuillade, G., & Perche, P. (1975). Ion-conductive macromolecular gels and membranes for solid lithium cells. Journal of Applied Electrochemistry, 5(1), 63-69.

Francis, K., Liew, C.-W., Ramesh, S., & Ramesh, K. (2016). Ionic liquid enhanced magnesium-based polymer electrolytes for electrical double-layer capacitors. Ionics, 22(6), 919-925.

Fuzlin, A. F., Rasali, N. M. J., & Samsudin, A. S. (2018). Effect on Ammonium Bromide in dielectric behavior based Alginate Solid Biopolymer electrolytes. Paper presented at the IOP Conference Series: Materials Science and Engineering.

Gaaz, T., Sulong, A., Akhtar, M., Kadhum, A., Mohamad, A., & Al-Amiery, A. (2015). Properties and applications of polyvinyl alcohol, halloysite nanotubes and their nanocomposites. Molecules, 20(12), 22833-22847.

Gale, E., Wirawan, R. H., Silveira, R. L., Pereira, C. S., Johns, M. A., Skaf, M. S., & Scott, J. L. (2016). Directed discovery of greener cosolvents: New cosolvents for use in ionic liquid based organic electrolyte solutions for cellulose dissolution. ACS Sustainable Chemistry & Engineering, 4(11), 6200-6207.

Geiculescu, O. E., Rajagopal, R., Creager, S. E., DesMarteau, D. D., Zhang, X., & Fedkiw, P. (2006). Transport properties of solid polymer electrolytes prepared from oligomeric fluorosulfonimide lithium salts dissolved in high molecular weight poly (ethylene oxide). The Journal of Physical Chemistry B, 110(46), 23130-23135.

Genova, F. K. M., Selvasekarapandian, S., Karthikeyan, S., Vijaya, N., Pradeepa, R., & Sivadevi, S. (2015). Study on blend polymer (PVA-PAN) doped with lithium bromide. Polymer Science Series A, 57(6), 851-862.

Guirguis, O. W., & Moselhey, M. T. (2012). Thermal and structural studies of poly (vinyl alcohol) and hydroxypropyl cellulose blends. Natural Science, 4(1), 57.

Guo, L., Sato, H., Hashimoto, T., & Ozaki, Y. (2010). FTIR study on hydrogen-bonding interactions in biodegradable polymer blends of poly (3-hydroxybutyrate) and poly (4-vinylphenol). Macromolecules, 43(8), 3897-3902.

Hafiza, M., & Isa, M. (2014). Ionic conductivity and conduction mechanism studies of CMC/chitosan biopolymer blend electrolytes. Research Journal of Recent Sciences, 2277, 2502.

Hafiza, M. N., Bashirah, A. N. A., Bakar, N. Y., & Isa, M. I. N. (2014). Electrical properties of carboxyl methylcellulose/chitosan dual-blend green polymer doped with ammonium bromide. International Journal of Polymer Analysis and Characterization, 19(2), 151-158.

Hafiza, M. N., Muhamaruesa, M. R., & Isa, M. I. N. (2017). Transport studies of carboxymethyl cellulose/chitosan-ammonium bromide biopolymer blend electrolytes as an ionic conductor. Journal of Sustainability Science and Management Special Issue Number 2: Fundamental Interdisciplinary Pathways To Future Sustainability, 2, 58-64.

Hamsan, M., Shukur, M., & Kadir, M. (2017). The effect of NH 4 NO 3 towards the conductivity enhancement and electrical behavior in methyl cellulose-starch blend based ionic conductors. Ionics, 23(5), 1137-1154.

Hamsan, M. H., Shukur, M. F., & Kadir, M. F. Z. (2017). NH_4NO_3 as charge carrier contributor in glycerolized potato starch-methyl cellulose blend-based polymer electrolyte and the application in electrochemical double-layer capacitor. Ionics, 23(12), 3429-3453.

Hashmi, S., Kumar, A., & Tripathi, S. (2007). Experimental studies on poly methyl methacrylate based gel polymer electrolytes for application in electrical double layer capacitors. Journal of Physics D: Applied Physics, 40(21), 6527.

Hashmi, S. A., Kumar, A., Maurya, K. K., & Chandra, S. (1990). Proton-conducting polymer electrolyte. I. The polyethylene oxide+ NH_4ClO_4 system. Journal of Physics D: Applied Physics, 23(10), 1307.

Hashmi, S. A., Latham, R. J., Linford, R. G., & Schlindwein, W. S. (1997). Studies on all solid state electric double layer capacitors using proton and lithium ion

conducting polymer electrolytes. Journal of the Chemical Society, Faraday Transactions, 93(23), 4177-4182.

Hatta, F., Kudin, T., Subban, R., Ali, A., Harun, M., & Yahya, M. (2009). Plasticized PVA/PVP–KOH alkaline solid polymer blend electrolyte for electrochemical cells. Functional Materials Letters, 2(03), 121-125.

Hayes, R., Warr, G. G., & Atkin, R. (2015). Structure and nanostructure in ionic liquids. Chemical Reviews, 115(13), 6357-6426.

Hema, M., Selvasekarapandian, S., Arunkumar, D., Sakunthala, A., & Nithya, H. F. T. I. R. (2009). FTIR, XRD and ac impedance spectroscopic study on PVA based polymer electrolyte doped with NH_4X (X= Cl, Br, I). Journal of Non-Crystalline Solids, 355(2), 84-90.

Hema, M., Selvasekarapandian, S., Nithya, H., Sakunthala, A., & Arunkumar, D. (2009). Structural and ionic conductivity studies on proton conducting polymer electrolyte based on polyvinyl alcohol. Ionics, 15(4), 487-491.

Hema, M., Selvasekerapandian, S., & Hirankumar, G. (2007). Vibrational and impedance spectroscopic analysis of poly (vinyl alcohol)-based solid polymer electrolytes. Ionics, 13(6), 483-487.

Hema, M., Selvasekerapandian, S., Hirankumar, G., Sakunthala, A., Arunkumar, D., & Nithya, H. (2009). Structural and thermal studies of PVA: NH4I. Journal of Physics and Chemistry of Solids, 70(7), 1098-1103.

Hema, M., Selvasekerapandian, S., Sakunthala, A., Arunkumar, D., & Nithya, H. (2008). Structural, vibrational and electrical characterization of PVA–NH_4Br polymer electrolyte system. Physica B: Condensed Matter, 403(17), 2740-2747.

Hohenberg, P., & Kohn, W. (1964). Inhomogeneous electron gas. Physical review, 136(3B), B864.

Huang, Y., Huang, Y., Liu, B., Cao, H., Zhao, L., Song, A., . . . Zhang, Z. (2018). Gel polymer electrolyte based on p (acrylonitrile-maleic anhydride) for lithium ion battery. Electrochimica Acta, 286, 242-251.

Ibrahim, A. A., Adel, A. M., El–Wahab, Z. H. A., & Al–Shemy, M. T. (2011). Utilization of carboxymethyl cellulose based on bean hulls as chelating agent. Synthesis, characterization and biological activity. Carbohydrate Polymers, 83(1), 94-115.

Isa, M., & Samsudin, A. (2016). Potential study of biopolymer-based carboxymethylcellulose electrolytes system for solid-state battery application. International Journal of Polymeric Materials and Polymeric Biomaterials, 65(11), 561-567.

Iwamoto, R., Miya, M., & Mima, S. (1979). Determination of crystallinity of swollen poly (vinyl alcohol) by laser Raman spectroscopy. Journal of Polymer Science: Polymer Physics Edition, 17(9), 1507-1515.

Jenkins, R., & Snyder, R. L. (2012). Diffraction theory: Wiley Online Library.

Jiang, Y., Yan, X., Ma, Z., Mei, P., Xiao, W., You, Q., & Zhang, Y. (2018). Development of the peo based solid polymer electrolytes for all-solid state lithium ion batteries. Polymers, 10(11), 1237.

Joge, P., Kanchan, D. K., Sharma, P., & Gondaliya, N. (2013). Effect of nano-filler on electrical properties of PVA-PEO blend polymer electrolyte.

Johari, N. A., Kudin, T. I. T., Ali, A. M. M., Winie, T., & Yahya, M. Z. A. (2009). Studies on cellulose acetate-based gel polymer electrolytes for proton batteries. Materials Research Innovations, 13(3), 232-234.

Kadir, M., Majid, S., & Arof, A. (2010). Plasticized chitosan–PVA blend polymer electrolyte based proton battery. Electrochimica Acta, 55(4), 1475-1482.

Kadir, M. F. Z., & Arof, A. K. (2011). Application of PVA–chitosan blend polymer electrolyte membrane in electrical double layer capacitor. Materials Research Innovations, 15(sup2), s217-s220.

Kadir, M. F. Z., Aspanut, Z., Majid, S. R., & Arof, A. K. (2011). FTIR studies of plasticized poly (vinyl alcohol)–chitosan blend doped with NH_4NO_3 polymer electrolyte membrane. Spectrochimica Acta Part A: Molecular and Biomolecular Spectroscopy, 78(3), 1068-1074.

Kadir, M. F. Z., Majid, S. R., & Arof, A. K. (2010). Plasticized chitosan–PVA blend polymer electrolyte based proton battery. Electrochimica Acta, 55(4), 1475-1482.

Kadir, M. F. Z., Salleh, N. S., Hamsan, M. H., Aspanut, Z., Majid, N. A., & Shukur, M. F. (2018). Biopolymeric electrolyte based on glycerolized methyl cellulose with NH_4Br as proton source and potential application in EDLC. Ionics, 24(6), 1651-1662.

Kalaiselvimary, J., Pradeepa, P., Sowmya, G., Edwinraj, S., & Prabhu, M. R. (2016). Electrical characterization of proton conducting polymer electrolyte based on bio polymer with acid dopant. Paper presented at the AIP Conference Proceedings.

Kamarudin, K. H., & Isa, M. I. N. (2013). Structural and DC Ionic conductivity studies of carboxy methylcellulose doped with ammonium nitrate as solid polymer electrolytes. International Journal of Physical Sciences, 8(31), 1581-1587.

Khiar, A. S. A., & Arof, A. K. (2011). Electrical properties of starch/chitosan-NH_4NO_3 polymer electrolyte. WASET, 59, 23-27.

Kibi, Y., Saito, T., Kurata, M., Tabuchi, J., & Ochi, A. (1996). Fabrication of high-power electric double-layer capacitors. Journal of Power Sources, 60(2), 219-224.

Kim, H.-S., Kum, K.-S., Cho, W.-I., Cho, B.-W., & Rhee, H.-W. (2003). Electrochemical and physical properties of composite polymer electrolyte of poly (methyl methacrylate) and poly (ethylene glycol diacrylate). Journal of Power Sources, 124(1), 221-224.

Kim, J.-K., Cheruvally, G., Li, X., Ahn, J.-H., Kim, K.-W., & Ahn, H.-J. (2008). Preparation and electrochemical characterization of electrospun, microporous membrane-based composite polymer electrolytes for lithium batteries. Journal of Power Sources, 178(2), 815-820.

Klug, H. P., & Alexander, L. E. (1974). X-ray diffraction procedures: for polycrystalline and amorphous materials. X-Ray Diffraction Procedures: For Polycrystalline and Amorphous Materials, 2nd Edition, by Harold P. Klug, Leroy E. Alexander, pp. 992. ISBN 0-471-49369-4. Wiley-VCH, May 1974., 992.

Koduru, H., Marinov, Y., Hadjichristov, G., & Scaramuzza, N. (2019). Characterization of polymer/liquid crystal composite based electrolyte membranes for sodium ion battery applications. Solid State Ionics, 335, 86-96.

Koh, M. H. (2013). Preparation and characterization of carboxymethyl cellulose from sugarcane bagasse. UTAR,

Koksbang, R., & Skou, E. (1995). Transference number measurements on a hybrid polymer electrolyte. Electrochimica Acta, 40(11), 1701-1706.

Kokubo, H., Sano, R., Murai, K., Ishii, S., & Watanabe, M. (2018). Ionic polymer actuators using poly (ionic liquid) electrolytes. European Polymer Journal, 106, 266-272.

Kopitzke, R. W., Linkous, C. A., Anderson, H. R., & Nelson, G. L. (2000). Conductivity and water uptake of aromatic- based proton exchange membrane electrolytes. Journal of the Electrochemical Society, 147(5), 1677-1681.

Krimm, S., Liang, C., & Sutherland, G. (1956). Infrared spectra of high polymers. V. Polyvinyl alcohol. Journal of Polymer Science Part A: Polymer Chemistry, 22(101), 227-247.

Krumova, M., Lopez, D., Benavente, R., Mijangos, C., & Perena, J. (2000). Effect of crosslinking on the mechanical and thermal properties of poly (vinyl alcohol). Polymer, 41(26), 9265-9272.

Kubo, S., & Kadla, J. F. (2003). The formation of strong intermolecular interactions in immiscible blends of poly (vinyl alcohol)(PVA) and lignin. Biomacromolecules, 4(3), 561-567.

Kumar, Y., Hashmi, S., & Pandey, G. (2011). Ionic liquid mediated magnesium ion conduction in poly (ethylene oxide) based polymer electrolyte. Electrochimica Acta, 56(11), 3864-3873.

Kuutti, L., Haavisto, S., Hyvarinen, S., Mikkonen, H., Koski, R., Peltonen, S., . . . Kyllönen, H. (2011). Properties and flocculation efficiency of cationized biopolymers and their applicability in papermaking and in conditioning of pulp and paper sludge. BioResources, 6(3), 2836-2850.

Lee, C., Yang, W., & Parr, R. G. (1988). Development of the Colle-Salvetti correlation-energy formula into a functional of the electron density. Physical review B, 37(2), 785.

Liew, C.-W., Arifin, K., Kawamura, J., Iwai, Y., Ramesh, S., & Arof, A. (2017). Effect of halide anions in ionic liquid added poly (vinyl alcohol)-based ion conductors for electrical double layer capacitors. Journal of Non-crystalline solids, 458, 97-106.

Liew, C.-W., Ramesh, S., & Arof, A. (2014a). Good prospect of ionic liquid based-poly (vinyl alcohol) polymer electrolytes for supercapacitors with excellent electrical, electrochemical and thermal properties. International Journal of Hydrogen Energy, 39(6), 2953-2963.

Liew, C.-W., Ramesh, S., & Arof, A. (2014b). Investigation of ionic liquid-based poly (vinyl alcohol) proton conductor for electrochemical double-layer capacitor. High Performance Polymers, 26(6), 632-636.

Liew, C.-W., Ramesh, S., & Arof, A. (2015). Characterization of ionic liquid added poly (vinyl alcohol)-based proton conducting polymer electrolytes and electrochemical studies on the supercapacitors. International Journal of Hydrogen Energy, 40(1), 852-862.

Liew, C.-W., Ramesh, S., & Arof, A. K. (2016a). Enhanced capacitance of EDLCs (electrical double layer capacitors) based on ionic liquid-added polymer electrolytes. Energy, 109, 546-556.

Liew, C.-W., Ramesh, S., & Arof, A. K. (2016b). Investigation of ionic liquid-doped ion conducting polymer electrolytes for carbon-based electric double layer capacitors (EDLCs). Materials & Design, 92, 829-835.

Lim, C.-S., Teoh, K., Liew, C.-W., & Ramesh, S. (2014). Electric double layer capacitor based on activated carbon electrode and biodegradable composite polymer electrolyte. Ionics, 20(2), 251-258.

Lin, Y.-C., Ito, K., & Yokoyama, H. (2017). Solid polymer electrolyte based on crosslinked polyrotaxane. Polymer.

Liu, S., Tao, D., Bai, H., & Liu, X. (2012). Cellulose- nanowhisker- templated synthesis of titanium dioxide/cellulose nanomaterials with promising photocatalytic abilities. Journal of Applied Polymer Science, 126(S1), E282-E290.

Lu, Q., Fu, J., Chen, L., Shang, D., Li, M., Xu, Y., . . . Shi, L. (2019). Polymeric polyhedral oligomeric silsesquioxane ionic liquids based solid polymer electrolytes for lithium ion batteries. Journal of Power Sources, 414, 31-40.

Mahakul, P. C., Sa, K., Das, B., & Mahanandia, P. (2017). Structural investigation of the enhanced electrical, optical and electrochemical properties of MWCNT incorporated Poly [3-hexylthiophene-2, 5-diyl] composites. Materials Chemistry and Physics, 199, 477-484.

Mahdavinia, G. R., Massoudi, A., Baghban, A., & Shokri, E. (2014). Study of adsorption of cationic dye on magnetic kappa-carrageenan/PVA nanocomposite hydrogels. Journal of Environmental Chemical Engineering, 2(3), 1578-1587.

Majid, S., & Arof, A. K. (2005). Proton-conducting polymer electrolyte films based on chitosan acetate complexed with NH4NO3 salt. Physica B: Condensed Matter, 355(1-4), 78-82.

Majid, S. R. (2007). High Molecular Weight Chitosan as Polymer Electrolyte for Electrochemical Devices. Jabatan Fizik, Fakulti Sains, Universiti Malaya,

Manjuladevi, R., Thamilselvan, M., Selvasekarapandian, S., Mangalam, R., Premalatha, M., & Monisha, S. (2017). Mg-ion conducting blend polymer electrolyte based on poly (vinyl alcohol)-poly (acrylonitrile) with magnesium perchlorate. Solid State Ionics, 308, 90-100.

Mazuki, N., Rasali, N., Saadiah, M., & Samsudin, A. (2018). Irregularities trend in electrical conductivity of CMC/PVA-NH4Cl based solid biopolymer electrolytes. Paper presented at the AIP Conference Proceedings.

Mazuki, N. F., Fuzlin, A. F., Saadiah, M. A., & Samsudin, A. S. (2018). An investigation on the abnormal trend of the conductivity properties of CMC/PVA-doped NH_4Cl-based solid biopolymer electrolyte system. Ionics, 1-11.

Mazuki, N. f., Nagao, Y., & Samsudin, A. S. (2019). Immittance Response on Carboxymethyl Cellulose Blend with Polyvinyl Alcohol-Doped Ammonium Bromide-Based Biopolymer Electrolyte. Makara Journal Of Technology, 22(3), 167-170.

Mazuki, N. F., Rasali, N. M. J., Saadiah, M. A., & Samsudin, A. S. (2018). Irregularities trend in electrical conductivity of CMC/PVA-NH_4Cl based solid biopolymer electrolytes. Paper presented at the AIP Conference Proceedings.

Meena, K., Muthu, K., Meenatchi, V., Rajasekar, M., Bhagavannarayana, G., & Meenakshisundaram, S. (2014). Spectrochimica acta part A: molecular and biomolecular spectroscopy. Spectrochimica Acta Part A: Molecular and Biomolecular Spectroscopy, 124, 663-669.

Mejenom, A. A., Hafiza, M. N., & Mohamad Isa, M. I. N. (2018). X-Ray diffraction and infrared spectroscopic analysis of solid biopolymer electrolytes based on dual blend carboxymethyl cellulose-chitosan doped with ammonium bromide. ASM Sci. J. Special Issue, 11, 37-46.

Mindemark, J., Lacey, M. J., Bowden, T., & Brandell, D. (2018). Beyond PEO—alternative host materials for Li+-conducting solid polymer electrolytes. Progress in Polymer Science, 81, 114-143.

Mitra, S., Shukla, A., & Sampath, S. (2001). Electrochemical capacitors with plasticized gel-polymer electrolytes. Journal of Power Sources, 101(2), 213-218.

Mizuno, A., Mitsuiki, M., & Motoki, M. (1998). Effect of crystallinity on the glass transition temperature of starch. Journal of Agricultural and Food Chemistry, 46(1), 98-103.

Mohamad, A., Mohamed, N., Yahya, M., Othman, R., Ramesh, S., Alias, Y., & Arof, A. (2003). Ionic conductivity studies of poly (vinyl alcohol) alkaline solid polymer electrolyte and its use in nickel–zinc cells. Solid State Ionics, 156(1-2), 171-177.

Mohamad, A. A., & Arof, A. K. (2007). Plasticized alkaline solid polymer electrolyte system. Materials Letters, 61(14-15), 3096-3099.

Mohamad, A. A., Mohamed, N. S., Yahya, M. Z. A., Othman, R., Ramesh, S., Alias, Y., & Arof, A. K. (2003). Ionic conductivity studies of poly (vinyl alcohol) alkaline solid polymer electrolyte and its use in nickel–zinc cells. Solid State Ionics, 156(1-2), 171-177.

Mokhtar, M., Herianto, E., Talib, M. Z. M., Ahmad, A., Tasirin, S. M., & Daud, W. (2016). A short review on alkaline solid polymer electrolyte based on polyvinyl alcohol (PVA) as polymer electrolyte for electrochemical devices applications. International Journal of Applied Engineering Research, 11(19), 10009-10015.

Moniha, V., Alagar, M., Selvasekarapandian, S., Sundaresan, B., & Boopathi, G. (2018). Conductive bio-polymer electrolyte iota-carrageenan with ammonium nitrate for application in electrochemical devices. Journal of Non-Crystalline Solids, 481, 424-434.

Moon, R. J., Martini, A., Nairn, J., Simonsen, J., & Youngblood, J. (2011). Cellulose nanomaterials review: structure, properties and nanocomposites. Chemical Society Reviews, 40(7), 3941-3994.

Muthuvinayagam, M., & Gopinathan, C. (2015). Characterization of proton conducting polymer blend electrolytes based on PVdF-PVA. Polymer, 68, 122-130.

Nadiah, N., Omar, F. S., Numan, A., Mahipal, Y., Ramesh, S., & Ramesh, K. (2017). Influence of acrylic acid on ethylene carbonate/dimethyl carbonate based liquid

electrolyte and its supercapacitor application. International Journal of Hydrogen Energy, 42(52), 30683-30690.

Napolitano, S., Pilleri, A., Rolla, P., & Wübbenhorst, M. (2010). Unusual Deviations from Bulk Behavior in Ultrathin Films of Poly(tert-butylstyrene): Can Dead Layers Induce a Reduction of Tg? ACS Nano, 4(2), 841-848. doi:10.1021/nn9014517

Nawaz, H., Casarano, R., & El Seoud, O. A. (2012). First report on the kinetics of the uncatalyzed esterification of cellulose under homogeneous reaction conditions: a rationale for the effect of carboxylic acid anhydride chain-length on the degree of biopolymer substitution. Cellulose, 19(1), 199-207.

Ng, L., & Mohamad, A. (2006). Protonic battery based on a plasticized chitosan-NH4NO3 solid polymer electrolyte. Journal of Power Sources, 163(1), 382-385.

Ng, L., & Mohamad, A. (2008). Effect of temperature on the performance of proton batteries based on chitosan–NH4NO3–EC membrane. Journal of Membrane Science, 325(2), 653-657.

Nik Aziz, N. A., Idris, N. K., & Isa, M. I. N. (2010). Solid polymer electrolytes based on methylcellulose: FT-IR and ionic conductivity studies. International Journal of Polymer Analysis and Characterization, 15(5), 319-327.

Ning, W., Xingxiang, Z., Haihui, L., & Benqiao, H. (2009). 1-Allyl-3-methylimidazolium chloride plasticized-corn starch as solid biopolymer electrolytes. Carbohydrate Polymers, 76(3), 482-484.

Noor, I. M. (2016). Characterization and transport properties of pva–libob based polymer electrolytes with application in dye sensitized solar cells. University of Malaya,

Noor, N. A. M., & Isa, M. (2015). Ionic Conductivity and Dielectric Properties of CMC Doped NH4SCN Solid Biopolymer Electrolytes. Advanced Materials Research, 1107, 230.

Noor, N. A. M., & Isa, M. I. N. (2015). Ionic conductivity and dielectric properties of CMC doped NH_4SCN solid biopolymer electrolytes. Advanced Materials Research, 1107, 230.

Noor, N. A. M., & Isa, M. I. N. (2019). Investigation on transport and thermal studies of solid polymer electrolyte based on carboxymethyl cellulose doped ammonium

thiocyanate for potential application in electrochemical devices. International Journal of Hydrogen Energy, 44, 8298-8306.

Numan, A., Duraisamy, N., Omar, F. S., Mahipal, Y., Ramesh, K., & Ramesh, S. (2016). Enhanced electrochemical performance of cobalt oxide nanocube intercalated reduced graphene oxide for supercapacitor application. RSC Advances, 6(41), 34894-34902.

Omar, F. S., Numan, A., Duraisamy, N., Bashir, S., Ramesh, K., & Ramesh, S. (2016). Ultrahigh capacitance of amorphous nickel phosphate for asymmetric supercapacitor applications. RSC Advances, 6(80), 76298-76306.

Orio, M., Pantazis, D. A., & Neese, F. (2009). Density functional theory. Photosynthesis research, 102(2-3), 443-453.

Osman, Z., Ibrahim, Z. A., & Arof, A. K. (2001). Conductivity enhancement due to ion dissociation in plasticized chitosan based polymer electrolytes. Carbohydrate Polymers, 44(2), 167-173.

Pandey, G., Kumar, Y., & Hashmi, S. (2010). Ionic liquid incorporated polymer electrolytes for supercapacitor application.

Park, C.-H., Park, M., Yoo, S.-I., & Joo, S.-K. (2006). A spin-coated solid polymer electrolyte for all-solid-state rechargeable thin-film lithium polymer batteries. Journal of Power Sources, 158(2), 1442-1446.

Park, J.-C., Ito, T., Kim, K.-O., Kim, K.-W., Kim, B.-S., Khil, M.-S., . . . Kim, I.-S. (2010). Electrospun poly (vinyl alcohol) nanofibers: effects of degree of hydrolysis and enhanced water stability. Polymer Journal, 42(3), 273.

Polu, A. R., & Rhee, H.-W. (2017). Ionic liquid doped PEO-based solid polymer electrolytes for lithium-ion polymer batteries. International Journal of Hydrogen Energy, 42(10), 7212-7219.

Pradhan, D. K., Choudhary, R., & Samantaray, B. (2008). Studies of structural, thermal and electrical behavior of polymer nanocomposite electrolytes. Express Polymer Letters, 2(9), 630-638.

Prajapati, G., Roshan, R., & Gupta, P. (2010). Effect of plasticizer on ionic transport and dielectric properties of PVA–H3PO4 proton conducting polymeric electrolytes. Journal of Physics and Chemistry of Solids, 71(12), 1717-1723.

Pratap, R., Singh, B., & Chandra, S. (2006). Polymeric rechargeable solid-state proton battery. Journal of Power Sources, 161(1), 702-706.

Qian, X., Gu, N., Cheng, Z., Yang, X., Wang, E., & Dong, S. (2001). Impedance study of (PEO) 10LiClO4–Al2O3 composite polymer electrolyte with blocking electrodes. Electrochimica acta, 46(12), 1829-1836.

Quartarone, E., & Mustarelli, P. (2011). Electrolytes for solid-state lithium rechargeable batteries: recent advances and perspectives. Chemical Society Reviews, 40(5), 2525-2540.

Radha, K. P., Selvasekarapandian, S., Karthikeyan, S., Hema, M., & Sanjeeviraja, C. (2013). Synthesis and impedance analysis of proton-conducting polymer electrolyte PVA: NH_4F. Ionics, 19(10), 1437-1447.

Rajantharan, S. (2011). Investigation on the effect of ionic liquid and ionic mixture in biodegradable polymer electrolytesunder. UTAR,

Rajeh, A., Morsi, M. A., & Elashmawi, I. S. (2019). Enhancement of spectroscopic, thermal, electrical and morphological properties of polyethylene oxide/carboxymethyl cellulose blends: Combined FT-IR/DFT. Vacuum, 159, 430-440.

Rajendran, S., Sivakumar, M., & Subadevi, R. (2003). Effect of salt concentration in poly (vinyl alcohol)-based solid polymer electrolytes. Journal of Power Sources, 124(1), 225-230.

Rajendran, S., Sivakumar, M., & Subadevi, R. (2004). Investigations on the effect of various plasticizers in PVA–PMMA solid polymer blend electrolytes. Materials Letters, 58(5), 641-649.

Rajeswari, N., Selvasekarapandian, S., Karthikeyan, S., Prabu, M., Hirankumar, G., Nithya, H., & Sanjeeviraja, C. (2011). Conductivity and dielectric properties of polyvinyl alcohol–polyvinylpyrrolidone poly blend film using non-aqueous medium. Journal of Non-Crystalline Solids, 357(22-23), 3751-3756.

Rajeswari, N., Selvasekarapandian, S., Sanjeeviraja, C., Kawamura, J., & Bahadur, S. A. (2014). A study on polymer blend electrolyte based on PVA/PVP with proton salt. Polymer bulletin, 71(5), 1061-1080.

Ramesh, S., & Chai, M. F. (2007). Conductivity, dielectric behavior and FTIR studies of high molecular weight poly (vinylchloride)–lithium triflate polymer electrolytes. Materials Science and Engineering: B, 139(2-3), 240-245.

Ramesh, S., Leen, K. H., Kumutha, K., & Arof, A. (2007). FTIR studies of PVC/PMMA blend based polymer electrolytes. Spectrochimica Acta Part A: Molecular and Biomolecular Spectroscopy, 66(4-5), 1237-1242.

Ramesh, S., Liew, C.-W., & Ramesh, K. (2011). Evaluation and investigation on the effect of ionic liquid onto PMMA-PVC gel polymer blend electrolytes. Journal of Non-Crystalline Solids, 357(10), 2132-2138.

Ramesh, S., & Lu, S. (2012). Enhancement of ionic conductivity and structural properties by BMIMTf ionic liquid in P (VdF-HFP)-based polymer electrolytes. Journal of Applied Polymer Science, 126, 484-492.

Ramesh, S., & Ng, K. Y. (2009). Characterization of polymer electrolytes based on high molecular weight PVC and Li_2SO_4. Current Applied Physics, 9(2), 329-332.

Ramesh, S., & Wen, L. C. (2010). Investigation on the effects of addition of SiO 2 nanoparticles on ionic conductivity, FTIR, and thermal properties of nanocomposite PMMA–LiCF 3 SO 3–SiO 2. Ionics, 16(3), 255-262.

Ramlli, M., & Isa, M. (2015). Conductivity study of carboxyl methyl cellulose solid biopolymer electrolytes (SBE) doped with ammonium fluoride. Research Journal of Recent Sciences, 2277, 2502.

Ramlli, M., Kamarudin, K., & Isa, M. (2015). Ionic conductivity and structural analysis of carboxymethyl cellulose doped with ammonium fluoride as solid biopolymer electrolytes. American-Eurasian Journal of Sustainable Agriculture, 46-52.

Ramlli, M. A., & Isa, M. I. N. (2015). Solid Biopolymer Electrolytes Based Carboxymethyl Cellulose Doped With Ammonium Fluoride: Ionic Transport and Conduction Mechanism. Polymers from Renewable Resources, 6(2), 55.

Ramlli, M. A., & Isa, M. I. N. (2016). Structural and ionic transport properties of protonic conducting solid biopolymer electrolytes based on Carboxymethyl cellulose doped with ammonium fluoride. The Journal of Physical Chemistry B, 120(44), 11567-11573.

Ramlli, M. A., Kamarudin, K. H., & Isa, M. I. N. (2015). Ionic conductivity and structural analysis of carboxymethyl cellulose doped with ammonium fluoride as solid

biopolymer electrolytes. American-Eurasian Journal of Sustainable Agriculture, 46-52.

Ramly, K., Isa, M. I. N., & Khiar, A. S. A. (2011). Conductivity and dielectric behaviour studies of starch/PEO+ x wt-% NH_4NO_3 polymer electrolyte. Materials Research Innovations, 15(sup2), 82-85.

Ramya, C., Selvasekarapandian, S., Hirankumar, G., Savitha, T., & Angelo, P. (2008). Investigation on dielectric relaxations of PVP–NH4SCN polymer electrolyte. Journal of Non-Crystalline Solids, 354(14), 1494-1502.

Ramya, C. S., Selvasekarapandian, S., Hirankumar, G., Savitha, T., & Angelo, P. C. (2008). Investigation on dielectric relaxations of PVP–NH_4SCN polymer electrolyte. Journal of Non-Crystalline Solids, 354(14), 1494-1502.

Rani, M. S. A., Dzulkurnain, N. A., Ahmad, A., & Mohamed, N. S. (2015). Conductivity and dielectric behavior studies of carboxymethyl cellulose from kenaf bast fiber incorporated with ammonium acetate-BMATFSI biopolymer electrolytes. International Journal of Polymer Analysis and Characterization, 20(3), 250-260.

Rani, M. S. A., Rudhziah, S., Ahmad, A., & Mohamed, N. S. (2014). Biopolymer electrolyte based on derivatives of cellulose from kenaf bast fiber. Polymers, 6(9), 2371-2385.

Rasali, N., Nagao, Y., & Samsudin, A. (2018). Enhancement on amorphous phase in solid biopolymer electrolyte based alginate doped NH 4 NO 3. Ionics.

Rasali, N., & Samsudin, A. (2017). Ionic transport properties of protonic conducting solid biopolymer electrolytes based on enhanced carboxymethyl cellulose-NH 4 Br with glycerol. Ionics, 1-12.

Rasali, N. M. J., & Samsudin, A. S. (2017). Ionic transport properties of protonic conducting solid biopolymer electrolytes based on enhanced carboxymethyl cellulose-NH_4Br with glycerol. Ionics, 24, 1639-1650.

Rauh, R. D. (1999). Electrochromic windows: an overview. Electrochimica Acta, 44(18), 3165-3176.

Razzak, M. T., & Darwis, D. (2001). Irradiation of polyvinyl alcohol and polyvinyl pyrrolidone blended hydrogel for wound dressing. Radiation Physics and Chemistry, 62(1), 107-113.

Riaz, U., & Ashraf, S. M. (2014). Characterization of polymer blends with FTIR spectroscopy. Characterization of Polymer Blends: Miscibility, Morphology and Interfaces, 625-678.

Rodi, I., Saaid, F., & Winie, T. (2017). PEMA-LiCF3SO3 polymer electrolytes: Assessment of conductivity and transport properties. Paper presented at the AIP Conference Proceedings.

Rozali, M., & ISA, M. I. N. M. (2014). Electrical behaviour of carboxy methyl cellulose doped adipic acid solid biopolymer electrolyte. International Journal of Material Science.

Rudhziah, S., Ahmad, A., Ahmad, I., & Mohamed, N. (2015). Biopolymer electrolytes based on blend of kappa-carrageenan and cellulose derivatives for potential application in dye sensitized solar cell. Electrochimica acta, 175, 162-168.

Saadiah, M., & Samsudin, A. (2018). Electrical study on Carboxymethyl Cellulose-Polyvinyl alcohol based bio-polymer blend electrolytes. Paper presented at the IOP Conference Series: Materials Science and Engineering.

Saadiah, M. A., & Samsudin, A. S. (2018). Electrical study on Carboxymethyl Cellulose-Polyvinyl alcohol based bio-polymer blend electrolytes. Paper presented at the IOP Conference Series: Materials Science and Engineering.

Saadiah, M. A., Zhang, D., Nagao, Y., Muzakir, S. K., & Samsudin, A. S. (2019). Reducing crystallinity on thin film based CMC/PVA hybrid polymer for application as a host in polymer electrolytes. Journal of Non-Crystalline Solids, 511, 201-211.

Salleh, N. S., Aziz, S. B., Aspanut, Z., & Kadir, M. F. Z. (2016). Electrical impedance and conduction mechanism analysis of biopolymer electrolytes based on methyl cellulose doped with ammonium iodide. Ionics, 22(11), 2157-2167.

Samad, Y. A., Asghar, A., & Hashaikeh, R. (2013). Electrospun cellulose/PEO fiber mats as a solid polymer electrolytes for Li ion batteries. Renewable Energy, 56, 90-95.

Samir, M. A., Chazeau, L., Alloin, F., Cavaillé, J.-Y., Dufresne, A., & Sanchez, J.-Y. (2005). POE-based nanocomposite polymer electrolytes reinforced with cellulose whiskers. Electrochimica Acta, 50(19), 3897-3903.

Samsudin, A., & Isa, M. (2012a). Characterization of carboxy methylcellulose doped with DTAB as new types of biopolymer electrolytes. Bulletin of Materials Science, 35(7), 1123-1131.

Samsudin, A., & Isa, M. (2012b). Structural and ionic transport study on CMC doped NH4Br: A new types of biopolymer electrolytes. J. Appl. Sci, 12(2), 174-179.

Samsudin, A., Lai, H., & Isa, M. (2014). Biopolymer materials based carboxymethyl cellulose as a proton conducting biopolymer electrolyte for application in rechargeable proton battery. Electrochimica Acta, 129, 1-13.

Samsudin, A. S. (2014). Development of carboxymethyl cellulose based proton conducting biopolymer electrolytes and its application in solid-state proton battery. Terengganu: Universiti Malaysia Terengganu,

Samsudin, A. S., & Isa, M. I. N. (2012). Structural and ionic transport study on CMC doped NH_4Br: A new types of biopolymer electrolytes. J. Appl. Sci, 12(2), 174-179.

Samsudin, A. S., & Isa, M. I. N. (2014). Conductivity and transport properties study of plasticized carboxymethyl cellulose (CMC) based solid biopolymer electrolytes (SBE). Paper presented at the Advanced Materials Research.

Samsudin, A. S., & Isa, M. I. N. (2015). CONDUCTIVITY STUDY ON PLASTICIZED SOLID BIO-ELECTROLYTES CMC-NH_4BR AND APPLICATION IN SOLID-STATE PROTON BATTERIES. Jurnal Teknologi, 78(6-5).

Samsudin, A. S., Isa, M. I. N., & Mohamad, N. (2011). New types of biopolymer electrolytes: Ionic conductivity study on CMC doped with NH_4Br. Journal of current engineering research, 1(1), 7-11.

Samsudin, A. S., Khairul, W. M., & Isa, M. I. N. (2012). Characterization on the potential of carboxy methylcellulose for application as proton conducting biopolymer electrolytes. Journal of Non-Crystalline Solids, 358(8), 1104-1112.

Samsudin, A. S., Kuan, E. C. H., & Isa, M. I. N. (2011). Investigation of the potential of proton-conducting biopolymer electrolytes based methyl cellulose-glycolic acid. International Journal of Polymer Analysis and Characterization, 16(7), 477-485.

Samsudin, A. S., Lai, H. M., & Isa, M. I. N. (2014). Biopolymer materials based carboxymethyl cellulose as a proton conducting biopolymer electrolyte for application in rechargeable proton battery. Electrochimica Acta, 129, 1-13.

Saroj, A., Krishnamoorthi, S., & Singh, R. (2017). Structural, thermal and electrical transport behaviour of polymer electrolytes based on PVA and imidazolium based ionic liquid. Journal of Non-Crystalline Solids, 473, 87-95.

Schantz, S., & Torell, L. (1993). Evidence of dissolved ions and ion pairs in dilute poly (propylene oxide)-salt solutions. Solid State Ionics, 60(1-3), 47-53.

Scott, A. P., & Radom, L. (1996). Harmonic vibrational frequencies: an evaluation of Hartree− Fock, Møller− Plesset, quadratic configuration interaction, density functional theory, and semiempirical scale factors. The Journal of Physical Chemistry, 100(41), 16502-16513.

Seddon, K., & Holbrey, J. (1999). Ionic liquids. Clean Products and Processes, 1, 223-236.

Selvalakshmi, S., Vijaya, N., Selvasekarapandian, S., & Premalatha, M. (2017). Biopolymer agar- agar doped with NH_4SCN as solid polymer electrolyte for electrochemical cell application. Journal of Applied Polymer Science, 134(15), 44702.

Selvasekarapandian, S., Hema, M., Kawamura, J., Kamishima, O., & Baskaran, R. (2010). Characterization of PVA–NH_4NO_3 polymer electrolyte and its application in rechargeable proton battery. Journal of the Physical Society of Japan, 79(Suppl. A), 163-168.

Selvasekarapandian, S., Hirankumar, G., Kawamura, J., Kuwata, N., & Hattori, T. (2005). 1H solid state NMR studies on the proton conducting polymer electrolytes. Materials Letters, 59(22), 2741-2745.

Shuhaimi, N., Teo, L., Woo, H., Majid, S., & Arof, A. K. (2012). Electrical double-layer capacitors with plasticized polymer electrolyte based on methyl cellulose. Polymer bulletin, 69(7), 807-826.

Shuhaimi, N. E. A., Teo, L. P., Woo, H. J., Majid, S. R., & Arof, A. K. (2012). Electrical double-layer capacitors with plasticized polymer electrolyte based on methyl cellulose. Polymer Bulletin, 69(7), 807-826.

Shukur, M., Ithnin, R., & Kadir, M. (2014). Electrical properties of proton conducting solid biopolymer electrolytes based on starch–chitosan blend. Ionics, 20(7), 977-999.

Shukur, M., & Kadir, M. (2015). Hydrogen ion conducting starch-chitosan blend based electrolyte for application in electrochemical devices. Electrochimica Acta, 158, 152-165.

Shukur, M. F., Ithnin, R., Illias, H. A., & Kadir, M. F. Z. (2013). Proton conducting polymer electrolyte based on plasticized chitosan–PEO blend and application in electrochemical devices. Optical Materials, 35(10), 1834-1841.

Shukur, M. F., Ithnin, R., & Kadir, M. F. Z. (2014a). Electrical characterization of corn starch-LiOAc electrolytes and application in electrochemical double layer capacitor. Electrochimica Acta, 136, 204-216.

Shukur, M. F., Ithnin, R., & Kadir, M. F. Z. (2014b). Electrical properties of proton conducting solid biopolymer electrolytes based on starch–chitosan blend. Ionics, 20(7), 977-999.

Shukur, M. F., Ithnin, R., & Kadir, M. F. Z. (2014c). Protonic transport analysis of starch-chitosan blend based electrolytes and application in electrochemical device. Molecular Crystals and Liquid Crystals, 603(1), 52-65.

Shukur, M. F., & Kadir, M. F. Z. (2015). Hydrogen ion conducting starch-chitosan blend based electrolyte for application in electrochemical devices. Electrochimica Acta, 158, 152-165.

Sikkanthar, S., Karthikeyan, S., Selvasekarapandian, S., Pandi, D. V., Nithya, S., & Sanjeeviraja, C. (2015). Electrical conductivity characterization of polyacrylonitrile-ammonium bromide polymer electrolyte system. Journal of Solid State Electrochemistry, 19(4), 987-999.

Sim, L. N., Majid, S. R., & Arof, A. K. (2012). FTIR studies of PEMA/PVdF-HFP blend polymer electrolyte system incorporated with LiCF3SO3 salt. Vibrational Spectroscopy, 58, 57-66.

Singh, R., Baghel, J., Shukla, S., Bhattacharya, B., Rhee, H.-W., & Singh, P. K. (2014). Detailed electrical measurements on sago starch biopolymer solid electrolyte. Phase Transitions, 87(12), 1237-1245.

Singh, R. K., & Singh, A. K. (2013). Optimization of reaction conditions for preparing carboxymethyl cellulose from corn cobic agricultural waste. Waste and Biomass Valorization, 4(1), 129-137.

Sit, Y., Samsudin, A., & Isa, M. (2012). Ionic conductivity study on hydroxyethyl cellulose (HEC) doped with NH4Br based biopolymer electrolytes. Research Journal of Recent Sciences, 2277, 2502.

Sivadevi, S., Selvasekarapandian, S., Karthikeyan, S., Sanjeeviraja, C., Nithya, H., Iwai, Y., & Kawamura, J. (2015). Proton-conducting polymer electrolyte based on PVA-PAN blend doped with ammonium thiocyanate. Ionics, 21(4), 1017-1029.

Siyal, S. H., Li, M., Li, H., Lan, J.-L., Yu, Y., & Yang, X. (2019). Ultraviolet irradiated PEO/LATP composite gel polymer electrolytes for lithium-metallic batteries (LMBs). Applied Surface Science.

Sohaimy, M. I. H., & Isa, M. I. N. (2015). Conductivity and dielectric analysis of cellulose based solid polymer electrolytes doped with ammonium carbonate (NH4CO3). Paper presented at the Applied Mechanics and Materials.

Srivastava, N., & Chandra, S. (2000). Studies on a new proton conducting polymer system: poly (ethylene succinate)+ NH4ClO4. European Polymer Journal, 36(2), 421-433.

Stephan, A. M., & Nahm, K. (2006). Review on composite polymer electrolytes for lithium batteries. Polymer, 47(16), 5952-5964.

Stratmann, R. E., Burant, J. C., Scuseria, G. E., & Frisch, M. J. (1997). Improving harmonic vibrational frequencies calculations in density functional theory. The Journal of chemical physics, 106(24), 10175-10183.

Sudhakar, Y., & Selvakumar, M. (2012). Lithium perchlorate doped plasticized chitosan and starch blend as biodegradable polymer electrolyte for supercapacitors. Electrochimica Acta, 78, 398-405.

Sudhakar, Y., & Selvakumar, M. (2013). Ionic conductivity studies and dielectric studies of poly (styrene sulphonic acid)/starch blend polymer electrolyte containing LiClO 4. Journal of Applied Electrochemistry, 43(1), 21-29.

Sudhamani, S., Prasad, M., & Sankar, K. U. (2003). DSC and FTIR studies on gellan and polyvinyl alcohol (PVA) blend films. Food Hydrocolloids, 17(3), 245-250.

Sukeshini, A. M., Nishimoto, A., & Watanabe, M. (1996). Transport and electrochemical characterization of plasticized poly (vinyl chloride) solid electrolytes. Solid State Ionics, 86, 385-393.

Sundaramahalingam, K., Nallamuthu, N., Manikandan, A., Vanitha, D., & Muthuvinayagam, M. (2018). Studies on sodium nitrate based polyethylene oxide/polyvinyl pyrrolidone polymer blend electrolytes. Physica B: Condensed Matter, 547, 55-63.

Teo, L., Buraidah, M., Nor, A., & Majid, S. (2012). Conductivity and dielectric studies of Li 2 SnO 3. Ionics, 18(7), 655-665.

Teoh, K. H., Lim, C.-S., Liew, C.-W., & Ramesh, S. (2015). Electric double-layer capacitors with corn starch-based biopolymer electrolytes incorporating silica as filler. Ionics, 21(7), 2061-2068.

Tsuchida, Y., Matsumiya, M., & Tsunashima, K. (2019). Preparation of polymer electrolytes using ionic liquids and evaluation of physicochemical properties. Journal of Molecular Liquids, 274, 204-208.

Varnell, D. F., & Coleman, M. M. (1981). FT ir studies of polymer blends: V. Further observations on polyester-poly (vinyl chloride) blends. Polymer, 22(10), 1324-1328.

Varnell, D. F., Runt, J. P., & Coleman, M. M. (1983). FT ir and thermal analysis studies of blends of poly (ε-caprolactone) with homo-and copolymers of poly (vinylidene chloride). Polymer, 24(1), 37-42.

Varzi, A., & Passerini, S. (2015). Enabling high areal capacitance in electrochemical double layer capacitors by means of the environmentally friendly starch binder. Journal of Power Sources, 300, 216-222.

Vashishta, P., Mundy, J. N., & Shenoy, G. (1979). Fast ion transport in solids: electrodes and electrolytes.

Vieira, M. G. A., da Silva, M. A., dos Santos, L. O., & Beppu, M. M. (2011). Natural-based plasticizers and biopolymer films: A review. European Polymer Journal, 47(3), 254-263.

Vijaya, N., Selvasekarapandian, S., Malathi, J., Iwai, Y., Nithya, H., & Kawamura, J. (2013). 1 H NMR study on PVP-NH 4 Cl based-proton conducting polymer electrolyte. Indian J. Appl. Res, 3, 506.

Wang, J., Song, S., Muchakayala, R., Hu, X., & Liu, R. (2017). Structural, electrical, and electrochemical properties of PVA-based biodegradable gel polymer electrolyte membranes for Mg-ion battery applications. Ionics, 23(7), 1759-1769.

Wang, K., Zhang, X., Li, C., Sun, X., Meng, Q., Ma, Y., & Wei, Z. (2015). Chemically crosslinked hydrogel film leads to integrated flexible supercapacitors with superior performance. Advanced Materials, 27(45), 7451-7457.

Wang, S., & Min, K. (2010). Solid polymer electrolytes of blends of polyurethane and polyether modified polysiloxane and their ionic conductivity. Polymer, 51(12), 2621-2628.

Wang, W., Liang, T., Bai, H., Dong, W., & Liu, X. (2018). All cellulose composites based on cellulose diacetate and nanofibrillated cellulose prepared by alkali treatment. Carbohydrate Polymers, 179, 297-304.

Wang, X., Hao, X., Xia, Y., Liang, Y., Xia, X., & Tu, J. (2019). A polyacrylonitrile (PAN)-based double-layer multifunctional gel polymer electrolyte for lithium-sulfur batteries. Journal of Membrane Science, 582, 37-47.

Wang, X., Wang, C., & Zhao, H. (2012). Errors in the Calculation of 27Al Nuclear Magnetic Resonance Chemical Shifts. International journal of molecular sciences, 13(11), 15420-15446.

Wang, X., Yao, C., Wang, F., & Li, Z. (2017). Cellulose- based nanomaterials for energy applications. Small, 13(42), 1702240.

Watanabe, M., & Nishimoto, A. (1995). Effects of network structures and incorporated salt species on electrochemical properties of polyether-based polymer electrolytes. Solid State Ionics, 79, 306-312.

Wei, Q.-B., Fu, F., Zhang, Y.-Q., Wang, Q., & Ren, Y.-X. (2014). pH-responsive CMC/PAM/PVP semi-IPN hydrogels for theophylline drug release. Journal of Polymer Research, 21(6), 453.

Welton, T. (1999). Room-temperature ionic liquids. Solvents for synthesis and catalysis. Chemical Reviews, 99(8), 2071-2084.

Wiers, B. M. (2015). Charge Transport In Metal-Organic Frameworks. UC Berkeley,

Wilkes, J. S. (2002). A short history of ionic liquids—from molten salts to neoteric solvents. Green Chemistry, 4(2), 73-80.

Woo, H., Majid, S., & Arof, A. K. (2013). Effect of ethylene carbonate on proton conducting polymer electrolyte based on poly (ε-caprolactone)(PCL). Solid State Ionics, 252, 102-108.

Woo, H. J., Majid, S. R., & Arof, A. K. (2011). Transference number and structural analysis of proton conducting polymer electrolyte based on poly (ϵ-caprolactone). Materials Research Innovations, 15(sup2), 49-54.

Wright, P. V. (1975). Electrical conductivity in ionic complexes of poly (ethylene oxide). Polymer International, 7(5), 319-327.

Xing, P., Dong, L., Feng, Z., & Feng, H. (1998). Miscibility and specific interactions in poly (β-hydroxybutyrate-co-β-hydroxyvalerate) and poly (p-vinylphenol) blends. European polymer journal, 34(8), 1207-1211.

Y N, S., Kumar, S., & Bhat, d. k. (2018). An introduction of Biopolymer Electrolytes. In (pp. 1-34).

Yahya, M. Z. A., Harun, M. K., Ali, A. M. M., Mohammat, M. F., Hanafiah, M. A. K. M., Ibrahim, S. C., . . . Latif, F. (2006). XRD and surface morphology studies on chitosan-based film electrolytes. Journal of applied sciences, 6(15), 3510-3154.

Yang, C.-C., Lee, Y.-J., & Yang, J. M. (2009). Direct methanol fuel cell (DMFC) based on PVA/MMT composite polymer membranes. Journal of Power Sources, 188(1), 30-37.

Yang, H., Liu, Y., Kong, L., Kang, L., & Ran, F. (2019). Biopolymer-based carboxylated chitosan hydrogel film crosslinked by HCl as gel polymer electrolyte for all-solid-sate supercapacitors. Journal of Power Sources, 426, 47-54.

Yang, J.-M., & Wang, S.-A. (2015). Preparation of graphene-based poly (vinyl alcohol)/chitosan nanocomposites membrane for alkaline solid electrolytes membrane. Journal of Membrane Science, 477, 49-57.

Yong, H., Park, H., Jung, J., & Jung, C. (2019). A fundamental approach to design of injectable high-content gel polymer electrolyte for activated carbon electrode supercapacitors. Journal of Industrial and Engineering Chemistry, 76, 429-436.

Yu, A., Chabot, V., & Zhang, J. (2013). Electrochemical supercapacitors for energy storage and delivery: fundamentals and applications: CRC press.

Yue, Z., McEwen, I., & Cowie, J. (2003). Novel gel polymer electrolytes based on a cellulose ester with PEO side chains. Solid State Ionics, 156(1-2), 155-162.

Yuhanees, M. Y. (2017). Characteristics of corn starch/chitosan blend green polymer electrolytes complexed with ammonium iodide and its application in energy devices/Yuhanees Mohamed Yusof. University of Malaya,

Yusof, Y., Illias, H., & Kadir, M. (2014). Incorporation of NH4Br in PVA-chitosan blend-based polymer electrolyte and its effect on the conductivity and other electrical properties. Ionics, 20(9), 1235-1245.

Yusof, Y., Majid, N., Kasmani, R., Illias, H., & Kadir, M. (2014). The effect of plasticization on conductivity and other properties of starch/chitosan blend biopolymer electrolyte incorporated with ammonium iodide. Molecular Crystals and Liquid Crystals, 603(1), 73-88.

Yusof, Y. M., Illias, H. A., & Kadir, M. F. Z. (2014). Incorporation of NH_4Br in PVA-chitosan blend-based polymer electrolyte and its effect on the conductivity and other electrical properties. Ionics, 20(9), 1235-1245.

Yusuf, S. N. F., Azzahari, A. D., Yahya, R., Majid, S. R., Careem, M. A., & Arof, A. K. (2016). From crab shell to solar cell: a gel polymer electrolyte based on N-phthaloylchitosan and its application in dye-sensitized solar cells. RSC Advances, 6(33), 27714-27724.

Zainuddin, N., Saadiah, M., Abdul Majeed, A., & Samsudin, A. (2018). Characterization on conduction properties of carboxymethyl cellulose/kappa carrageenan blend-based polymer electrolyte system. International Journal of Polymer Analysis and Characterization, 23(4), 321-330.

Zainuddin, N., & Samsudin, A. (2018). Investigation on the Effect of NH4Br at Transport Properties in K–Carrageenan Based Biopolymer Electrolytes via Structural and Electrical Analysis. Materials Today Communications.

Zainuddin, N. K., & Samsudin, A. S. (2018). Investigation on the Effect of NH_4Br at Transport Properties in K–Carrageenan Based Biopolymer Electrolytes via Structural and Electrical Analysis. Materials Today Communications, 14, 199-209.

Zakaria, N., Yahya, S., Isa, M., Nor Sabirin, M., & Subban, R. H. Y. (2010). Conductivity and dynamic mechanical studies of PVC/PEMA blend polymer electrolytes (Vol. 93): Trans Tech Publ.

Zakaria, N. A., Yahya, S. Y. S., Isa, M. I. N., Nor Sabirin, M., & Subban, R. H. Y. (2010). Conductivity and dynamic mechanical studies of PVC/PEMA blend polymer electrolytes (Vol. 93): Trans Tech Publ.

Zeng, J., Li, R., Liu, S., & Zhang, L. (2011). Fiber-like TiO2 nanomaterials with different crystallinity phases fabricated via a green pathway. ACS applied materials & interfaces, 3(6), 2074-2079.

Zhang, P., Yang, L., Li, L., Ding, M., Wu, Y., & Holze, R. (2011). Enhanced electrochemical and mechanical properties of P (VDF-HFP)-based composite polymer electrolytes with SiO2 nanowires. Journal of Membrane Science, 379(1-2), 80-85.

Zhou, D., Shanmukaraj, D., Tkacheva, A., Armand, M., & Wang, G. (2019). Polymer Electrolytes for Lithium-Based Batteries: Advances and Prospects. Chem.

Zhu, M., Wu, J., Wang, Y., Song, M., Long, L., Siyal, S. H., . . . Sui, G. (2018). Recent advances in gel polymer electrolyte for high-performance lithium batteries. Journal of Energy Chemistry.

Zubieta, L., & Bonert, R. (2000). Characterization of double-layer capacitors for power electronics applications. IEEE Transactions on industry applications, 36(1), 199-205.

APPENDICES